

Isotope hydrology and paleohydrology of the
Slave River Delta, NWT

by

Bronwyn Benkert

A thesis
presented to the University of Waterloo
in fulfillment of the
thesis requirement for the degree of
Doctor of Philosophy
in
Earth Sciences

Waterloo, Ontario, Canada, 2010

©Bronwyn Benkert 2010

Author's Declaration

I hereby declare that I am the sole author of this thesis. This is a true copy of the thesis, including any required final revisions, as accepted by my examiners.

I understand that my thesis may be made electronically available to the public.

Abstract

Water isotope tracers and multi-proxy paleolimnological approaches are used to characterize the present and past hydrology of the Slave River Delta (SRD), NWT. This research addresses crucial gaps in knowledge about the role of major hydrological processes on the water balances of northern freshwater lakes, and responds to concerns expressed by local land users about declining flood frequency in the delta following upstream river regulation. Contemporary hydrological studies were conducted using multiple lakewater sampling campaigns from a suite of 41 delta lakes situated in three previously recognized biogeographical zones - outer delta, mid-delta and apex – that were initially sampled in fall 2002, and again immediately following the spring melt, during summer, and in the fall of 2003-2005. Paleolimnological studies aimed at reconstructing flood frequency in the Slave River focus on a sediment core obtained from a flood-susceptible lake in the active delta. Together, contemporary and past studies of SRD hydrology provide a detailed picture of environmental change and variability in an important northern freshwater ecosystem.

The relative importance of major hydrological processes on thaw season 2003 lakewater balances in the SRD is characterized using water isotope tracers and total suspended sediment (TSS) analyses. Oxygen and hydrogen isotope compositions were evaluated in the context of an isotopic framework calculated from 2003 hydroclimatic data. This analysis reveals that flooding from the Slave River and Great Slave Lake dominated early spring lakewater balances in outer and most mid-delta lakes, as also indicated by elevated TSS concentrations ($>0.01 \text{ g L}^{-1}$). In contrast, the input of local snowmelt was strongest on all apex and some mid-delta lakes. After the spring melt, all delta lakes underwent heavy-isotope enrichment due to evaporation, although lakes flooded by the Slave River and Great Slave Lake during the spring freshet continued to be more depleted isotopically than those dominated by snowmelt input. The isotopic signatures of lakes with direct connections to the Slave

River or Great Slave Lake varied throughout the season in response to the nature of the connection. Our findings provide the basis for identifying three groups of lakes based on the major factors that control their water balances: (1) flood-dominated (n = 10), (2) evaporation-dominated (n = 25) and (3) exchange-dominated (n = 6) lakes. Differentiation of the hydrological processes that influence Slave River Delta lakewater balances is essential for ongoing hydroecological and paleohydrological studies, and ultimately, for teasing apart the relative influences of variations in local climate and Slave River hydrology.

Because the spring break-up period has a strong influence on the hydrology of delta lakes, water isotope tracers and total inorganic suspended sediment (TSS) concentrations were measured from lakewater samples collected shortly after the spring melt in 2003-2005. Results are used to characterize the spatial and temporal patterns of spring break-up flooding in the SRD. Strongly contrasting spring melt periods led to a moderate flood in 2003, no flooding in 2004 and widespread flooding in 2005. Flooded lakes have isotopically-depleted $\delta^{18}\text{O}$ ($\delta^2\text{H}$) signatures, ranging between -19.2‰ (-145‰) and -17.1‰ (-146‰) and most have high TSS concentrations (>10 mg/L), while non-flooded lakes have more isotopically-enriched $\delta^{18}\text{O}$ ($\delta^2\text{H}$) signatures, ranging between -18.2‰ (-149‰) and -10.6‰ (-118‰) and low TSS concentrations (<10 mg/L). These results, in conjunction with the isotopic signatures of Slave River water and snowmelt, are used to estimate the proportion of river- or snowmelt-induced dilution in delta lakes during the spring of each study year. Calculations indicate river flooding caused dilution of ~70-100% in delta lakes, while snowmelt dilution in the absence of river flooding ranged from ~0-56%. A positive relationship exists between the spatial extent of spring flooding in the SRD and level and discharge on the Slave River and upstream tributaries, suggesting that upstream flow generation plays a key role in determining the magnitude of spring flooding in the SRD. Parallel variations in the 46-year instrumental record of Slave River discharge and flood stratigraphy in the active delta indicate that there is potential for extending the flood history of the SRD, a development that will contribute to a

more robust understanding of the drivers of historic, contemporary and future flood frequency in the delta.

To investigate the effects of spring flooding on lakewater balances during the subsequent open-water season, and to quantify end-of-thaw-season (fall) lakewater balances in the SRD during 2003-2005, a coupled-isotope tracer model is applied to lakewater isotope results from study lakes. This approach effectively differentiates the relative importance of hydrological processes across the SRD. The model incorporates Great Slave Lake evaporated vapour to the ambient atmospheric vapour pool and is thus tailored to the hydroclimatic setting of the delta, which frequently experiences onshore winds. Results, expressed as evaporation-to-inflow ratios (E/I) for 41 delta lakes, reflect the role of spring break-up flooding and local hydrological setting. Fall E/I ratios for lakes having water balances dominated by exchange with the Slave River or Great Slave Lake are low (0.06-0.53) and do not vary substantially during the three-year monitoring period. E/I ratios for flood-dominated lakes in the active delta are moderate (0.26-0.98) and have low inter-annual variability, even in the absence of spring flooding. This suggests that annual flooding during the spring break-up period is not necessary to maintain positive ($E/I < 1$) water balances in flood-dominated lakes, but multiple years without flooding would clearly lead to greater cumulative evaporation and drawdown. Fall E/I ratios are generally higher and more variable in evaporation-dominated lakes in the relict delta (0.42 to >1), although greater snowmelt runoff tends to occur in sub-sectors with mature spruce forest and offsets open-water vapour loss. These results indicate that spring inputs (river flooding and snowmelt runoff) are key components of the hydrological evolution of SRD lakes during the open-water season, and distinguish regions of the delta where expected declines in river discharge and climate warming will likely cause lake-level drawdown. Such findings have particular relevance for informed ecosystem management in the Peace-Athabasca-Slave watershed, where unprecedented industrial development is imposing substantial additional pressure on freshwater resources.

Recognizing the importance of spring break-up flooding for the water balances of SRD lakes, and to address on-going concerns about declining flood frequency in the SRD, paleolimnological approaches are used to reconstruct variations in the frequency of spring break-up flooding in the SRD during the past ~80 years. This reconstruction is based on multi-proxy analyses (geochemistry, diatoms, plant macrofossils) of a sediment core from a shallow, flood-prone lake in the active delta. Results reveal oscillating decadal-scale intervals of high and low flood frequency. Reconstructed Slave River flood frequency post-1960 parallels variations in measured Slave River discharge and also corresponds to the flood history derived from observations of land users. Notably, the interval of lowest water levels inferred from a peak sedimentary abundance of *Sagittaria cuneata* seeds pre-dates upstream regulation of the Peace River in 1968. In fact, multi-proxy records reveal that the onset of river regulation coincided with a period of increased flood frequency beginning in the early 1960s and ending in the early 1980s. It is therefore unlikely that river regulation has caused a decline in the frequency of spring break-up floods at the study site. Furthermore, the flood record developed here parallels similar changes in flood frequency from an oxbow lake in the northern Peace sector of the upstream Peace-Athabasca Delta. This suggests that climate-driven change in the runoff regime of the upper Mackenzie River Basin is likely the principle driver of variability in flood frequency in both deltas. Continued reductions in snowpacks and headwater runoff are therefore likely to reduce the frequency of flooding in the SRD.

Acknowledgements

I have been financially supported throughout my graduate career by the National Sciences and Engineering Research Council, the Garfield Weston Foundation, the Ontario Graduate Scholarship Program, the University of Waterloo, and the Meteorological Service of Canada. My research activities have been financially supported by the NSERC Northern Research Chair Program, the Polar Continental Shelf Program, the Northern Scientific Training Program, BC Hydro, the Government of Ontario Premier's Research Excellence Award, the Canada Foundation for Innovation and the Ontario Innovation Trust. I am grateful for all of these sources of funding. I am also grateful for the involvement and support of the staff of the University of Waterloo Environmental Isotope Laboratory and Wood Buffalo Helicopters, and for the comments of the anonymous reviewers who reviewed the manuscripts that make up in this thesis.

I have benefited from the support and involvement of a great network of colleagues, family and friends over the course of my program, and I am very thankful for this. Specifically, I would like to express my thanks to the following people, who have made the completion of this thesis possible and have enriched the past several years of my life:

To my co-supervisors Brent Wolfe and Tom Edwards - I am incredibly grateful for the excellent support and supervision I received from you both! You have built a strong research program that I have been proud to be involved with. You are dedicated to your students, to their success, and to fostering a passion for research and northern scholarship in young scientists, and I have benefited from this. You have given me marvelous opportunities of many kinds throughout my graduate career – in some cases, these have been life-changing! Your office doors were always open, your ideas were always flowing, your pencils always sharp, and you were always willing to dedicate your time and attention to guiding me through my research program. You were wonderful co-

advisors, and I truly appreciate everything you have done for me over the past six years!

To Roland Hall and John Johnston - your enthusiasm for research is inspiring, and I have really enjoyed working alongside you both in the field, the office and the lab. Roland, I appreciate your willingness to answer questions and review my writing, despite your very demanding schedule. John, your ideas and guidance during the construction of our vibracorer, our winter coring expedition and our core splitting and analysis were invaluable, and it was really a delight to spend time with you in the field!

To the residents of Fort Resolution - the entire Slave River Delta research program has benefited from the support and participation of the residents of Fort Resolution, the Deninu K'ue First Nation, the Fort Resolution Environmental Working Committee, and the principal, staff and students of Deninu School. Thank you especially to Gaby Lafferty, Lloyd Norn, Paul Boucher and Richard Simon for your participation in, and support of, our research in the Slave River Delta.

To the MBD/NHL team, past and present - I have been fortunate to be a part this active and enthusiastic research group, and I would like to thank its present and past members for sharing knowledge, resources and ideas over the past several years. I've been lucky to spend time in the field with many of you, and it has always been a truly enjoyable experience! Thank you especially to fellow field researchers Maggie Martin and Mike Sokal for all those productive trips out on the delta and the endlessly entertaining ways we passed the time in Fort Resolution, and thank you to my various office-mates for your conversations and distractions.

To Maija Heikkilä and Paige Harms - you two have become fierce friends of mine, and I have learned so much from both of you, in school and in life. Thank you, Paige, for sharing universe moments with me, for laughing with me, for listening to and supporting me, and of course for your starring role

in the Peanut and Button show – you have become a true friend, as you know. Maija, thank you for long conversations, for sharing your passions and enthusiasm for life, for encouraging me, for long runs, lovely coffees, delicious food, chatty emails and cozy house-sharing – you have enriched my life over the last few years, and I hope for many more!

To my family and friends - I am deeply grateful for the constant and unwavering support of all kinds you've given me. You have each been a source of strength and love, and I would not be where I am today without you! Thank you for listening, comforting, encouraging, laughing and relaxing with me during my long university career (and all of the prior years too!). Thank you for all the conversation, drinks, tea, runs and laughs – these have been great distractions from the task of completing this degree!

And finally, but most importantly, thank you to my husband – for all of the reasons you already know.

Table of Contents

Author's Declaration	ii
Abstract.....	iii
Acknowledgements	vii
Table of Contents	x
List of Figures	xiii
List of Tables.....	xxii
Chapter 1: General introduction	1
Introduction	1
Previous research on the upstream Peace-Athabasca Delta and the SRD.....	4
Thesis Objectives.....	8
Research Methods.....	9
Thesis Outline	10
Chapter 2.....	10
Chapter 3	11
Chapter 4.....	11
Chapter 5.....	12
Figures.....	14
Chapter 2: Characterizing the hydrology of shallow floodplain lakes in the Slave River Delta, NWT, using water isotope tracers.....	16
Introduction	16
The Slave River Delta	18
Methodology.....	20
Results and Interpretation	21
An isotopic framework for evaluating lakewater balances.....	21
Hydrological processes in the slave river delta.....	23
Flooding and snowmelt.....	23
Evaporation	26
Great Slave Lake-Slave River exchange.....	27
Thaw season precipitation.....	29
Discussion	31
Summary and Future Directions.....	36
Figures.....	38
Tables.....	50
Appendix A.....	53
Chapter 3: Spatial and temporal perspectives on spring break-up flooding in the Slave River Delta, NWT	56
Introduction	56
The Slave River Delta	58
Methods.....	60
Results and interpretation	62
Isotopic frameworks for the SRD (2003-2005)	62
Slave River Delta spring isotope hydrology and total suspended sediment (2003-2005).....	64

Spatial extent of flooding in the Slave River Delta (2003-2005).....	66
Slave River level and discharge (2003-2005).....	68
Discussion	69
Summary and implications	75
Figures	77
Tables	86
Chapter 4: Multi-year landscape-scale assessment of lakewater balances in the Slave River Delta, NWT, using water isotope tracers	89
Introduction	89
The Slave River Delta and Great Slave Lake	91
Water sample collection and meteorological data	93
Results and discussion	94
Spring and fall 2003-2005 lakewater isotopic compositions.....	94
Quantifying lakewater balances using water isotope tracers.....	95
Resolving isotope-mass-balance calculations using a vapour mixing model	97
The isotopic composition of input water (δ_i).....	97
The isotopic composition of atmospheric moisture (δ_A).....	98
Quantification of E/I ratios for SRD lakes, 2003-2005	101
Conclusions and management recommendations	104
Figures	107
Tables	115
Chapter 5: Flood frequency variability during the past 80 years in the Slave River Delta, NWT, as determined from multi-proxy paleolimnological analysis	118
Introduction	118
The Slave River and its delta	120
Study Site – SD2	122
Field and laboratory methods	123
Core collection and extrusion	123
Slave River sediment collection.....	123
Sediment core chronology.....	123
Physical and geochemical proxies.....	124
Biological proxies	124
Results and interpretation	125
Sediment core chronology.....	125
Physical and geochemical proxies.....	126
Biological proxies	127
Discussion	129
Multi-proxy records of flood frequency in the Slave River Delta.....	129
Measured Slave River discharge and oral history records of flooding	129
Assessing the effects of river regulation and change in distributary flow on flood frequency at SD2.....	131
Past flood frequency in the upper Mackenzie Drainage Basin	132
Concluding comments	133
Figures	136
Chapter 6: Thesis summary and applications	145
Thesis summary	145
Water resource management in the upper Mackenzie River Basin	149

Future research directions and applications.....	152
Figures	159
Permissions.....	160
References.....	162
Appendix A: Slave River Delta study lakes.....	179
Appendix B: Lakewater isotope and total suspended sediment results... 	180

List of Figures

- Figure 1.1. The Mackenzie River Basin, showing the Peace, Athabasca, Slave and Mackenzie Rivers and their associated deltas. (Map produced by Eric Leinberger, University of British Columbia, for the Mackenzie Basin Impact Study.) 14
- Figure 1.2. Conceptual diagram of the interdisciplinary SRD research program (from Wolfe et al., 2007a). The contributions of this thesis to the research program are highlighted in bold. ‘GNWT’ is the Government of the Northwest Territories, ‘DKFN’ is the Deninu Kue First Nation, and ‘FREWC’ is the Fort Resolution Environmental Working Committee..... 15
- Figure 2.1. Location of the Slave River Delta, NWT, including lake and river sampling sites..... 38
- Figure 2.2. Samples collected on 25-Jul-03 from Great Slave Lake (δ_{GSL} , the most isotopically-depleted lake at the time of sample collection) and SD27 (the most isotopically-enriched lake at the time of sample collection) superimposed on the climate normal and 2003 isotopic frameworks, showing the isotopic composition of amount-weighted mean annual (1962-1965) precipitation (δ_{P}) from Fort Smith, NWT (Birks et al., 2004), the isotopic compositions of evaporation-flux-weighted thaw season precipitation (δ_{PS} ; Gibson and Edwards, 2002) and atmospheric moisture (δ_{AS}), the steady state isotopic composition of a terminal basin (δ_{SSL}), the limiting isotopic composition (δ^*), and the isotopic composition of Great Slave Lake vapour ($\delta_{\text{E-GSL}}$). 39
- Figure 2.3. Potential isotopic trajectories of a theoretical SRD lake in response to 1) evaporation, 2) thaw season precipitation (δ_{PS} ; Gibson and Edwards, 2002), 3) Great Slave Lake (δ_{GSL}) exchange, 4) Slave River (δ_{SR}) flooding and 5) snowmelt (δ_{snow}) input, superimposed on the 2003 isotopic framework (see Figure 2). Isotopic framework parameters are shown as open circles. In this

example, the theoretical lake is shown to plot on the Local Evaporation Line (LEL) indicating the lake is fed by water of isotopic composition similar to mean annual precipitation..... 40

Figure 2.4. Results of Slave River Delta (SRD) regional sampling campaigns conducted on a) 23-May-03, b) 23-Jun-03, c) 25-Jul-03 and d) 15-Aug-03. The isotopic compositions of all SRD lakes sampled are superimposed on the 2003 climate isotopic framework (see Figure 2). Lakes identified by name in the text are labeled. Flooded and non-flooded clusters of lakes are circled with a dashed line, and are labeled in b). Isotopic framework parameters are shown as open circles..... 41

Figure 2.5. Total inorganic suspended sediment (TSS), expressed in g L^{-1} , in SRD lakes from water samples collected on 23-May-03. Lakes that have high TSS concentrations were flooded by the Slave River during the spring thaw, while lakes that were not flooded by the Slave River have low TSS concentrations..... 42

Figure 2.6. Depletion trajectories of non-flooded lakes SD12, SD33 and SD35 between Sep-02 and May-03 are towards the isotopic composition of snow (δ_{snow}), in response to an influx of catchment-sourced snowmelt during spring melt period. Isotopic compositions are superimposed on the 2003 climate isotopic framework (see Figure 2). Isotopic framework parameters are shown as open circles..... 43

Figure 2.7. Examples showing dilution percentage estimates for a) SD1, an apex lake flooded by the Slave River (δ_{SR}) in May-03, and b) SD11, a lake in the apex zone of the delta that received exclusively snowmelt input (δ_{snow}) during the spring melt. Snowmelt dilution is calculated using an average snowmelt value ($\delta^{18}\text{O}$, $\delta^2\text{H} = -24.7\text{‰}$, -191‰). Isotopic compositions are superimposed on the 2003 climate isotopic framework (see Figure 2). 44

Figure 2.8. The spatial extent of a) river flooding and snowmelt dilution and b) summer evaporative enrichment in lakes in 2003 interpolated using data from

Figure 4. In a), two-component mixing indicates that flooding occurred in areas adjacent to the main distributary channels of the Slave River in the mid- and outer portions of the active delta (mapped as red areas). Elsewhere, lakes received exclusively snowmelt in the spring (mapped as mainly blue areas). The observed spatial extent of flooding corresponds with the 70% dilution contour, shown as a black contour. Summer isotopic enrichment in b) represents enrichment in ^{18}O (‰) between 23-May-03 and 15-Aug-03..... 45

Figure 2.9. Monthly distribution of total thaw season precipitation, average temperature, average relative humidity and potential evaporation for 2003 in comparison to climate normal values (1971-2000) for Hay River, NWT (Environment Canada, 2002)..... 46

Figure 2.10. Isotopic evolution of four SRD lakes (SD2, SD15, SD29 and SD33) during the 2003 thaw season, showing evaporative enrichment prior to 15-Aug-03 and subsequent isotopic depletion in response to 39 mm of late season precipitation between 15-Aug-03 and 3-Sep-03. Isotopic compositions are superimposed on the 2003 climate isotopic framework (see Figure 2). Isotopic framework parameters are shown as open circles. 47

Figure 2.11. SRD lakes classified based on dominant hydrologic inputs and outputs during the 2003 thaw season. 48

Figure 2.12. Peak Slave River discharge during the spring melt period, measured between 1965-2005 at Fitzgerald, AB (Water Survey of Canada, 2006). The dashed line represents peak discharge measured in the spring of 2003..... 49

Figure 3.1. Location of the Slave River Delta, NWT, including lake and river sampling sites..... 77

Figure 3.2. Daily a) temperature ($^{\circ}\text{C}$), b) rainfall (mm) and c), snow depth (cm) for Hay River, NWT during the spring thaw period for 2003-2005 (Environment Canada, 2005). 78

Figure 3.3. Isotopic frameworks for the SRD during 2003-2005. Parameters include the isotopic composition of amount-weighted mean annual precipitation (δ_P ; $\delta^{18}\text{O}$, $\delta^2\text{H} = -19.0\text{‰}$, -148‰ ; Birks et al., 2004), flux-weighted thaw season precipitation (δ_{PS} ; $\delta^{18}\text{O}$, $\delta^2\text{H} = -17.0\text{‰}$, -132‰ ; Gibson and Edwards, 2002), and the calculated steady state and limiting isotopic compositions (δ_{SSL} and δ^*). The average isotopic composition of snow (δ_{snow}) from samples collected from the SRD in May 2004 is also shown. Open circles show values calculated based on climate normal (1971-2000) conditions (Environment Canada, 2002), while shaded circles show values calculated using flux-weighted thaw season climate conditions for 2003-2005 (Environment Canada, 2005). 79

Figure 3.4. Water isotope and TSS results from regional sampling campaigns on a) 23 May 2003, b) 31 May 2004 and c) 17 May 2005. Isotope results are superimposed on year-specific isotopic frameworks (see Figure 3.3), with framework parameters shown as open circles. Great Slave Lake and the Slave River values are shown as open squares and are labelled. Measured lakewater values are shown as closed circles. 80

Figure 3.5. Percent dilution of lakewater by river flooding and snowmelt on a) 23 May 2003, b) 31 May 2004 and c) 17 May 2005. The observed spatial extent of flooding in 2003 and 2005 corresponds with the 70% dilution isoline, shown as a dashed grey contour in a) and c). 81

Figure 3.6. Slave River discharge and level during the spring melt period (April-May), 2003-2005, measured at Fitzgerald, AB (Water Survey of Canada, 2006). 82

Figure 3.7. Spring discharge on the Slave (Sl), Peace (P) and Smoky (Sm) Rivers, 2003-2005 (Water Survey of Canada, 2006). 83

Figure 3.8. Maximum discharge (m^3/s) measured in a) the Peace River at Peace Point, AB and b) the Slave River at Fitzgerald, AB (Water Survey of Canada, 2006) during the period 14 days prior to and three days after the disappearance of solid and floating ice. Grey bands indicate years in which peak discharge

occurred while river ice cover was intact, while black bands represent years in which peak discharge occurred following the disappearance of river ice cover. Thus, the likelihood of widespread flooding is greatest during years when high levels of peak discharge occur while river ice cover is still intact (e.g., 2005 for the SRD). Peak discharge conditions measured on the Slave River during 2003-2005 monitoring period are indicated by dashed lines on b). Spring ice-jam floods (**) and lower magnitude flood events (*) observed in the PAD (Peters, 2003; Beltaos et al., 2006a; Wolfe et al., 2006) are indicated on a). Plot c) shows weight C/N ratios measured on sediments collected from a flood-dominated SRD lake dated using ^{137}Cs (Mongeon, 2008; see Figure 3.1 for lake location). Peaks in C/N ratios are believed to closely correspond with peaks in Slave River discharge, as indicated by the dotted lines on b) and c). 84

Figure 3.9. Weight C/N ratio sediment records to 1940 from flood-dominated lakes in a) the SRD (Mongeon, 2008; see Figure 3.1 for lake location) and b) the PAD (Wolfe et al., 2006), plotted relative to mean values. Note the PAD15 record has been smoothed by an 11-point running mean to achieve resolution comparable to the SD2 record. 85

Figure 4.1. Location of the Slave River Delta, NWT, including lake and river sampling sites. 107

Figure 4.2. Water isotope results from SRD lakes in the spring of a) 2003, b) 2004 and c) 2005 (Brock et al., 2008; see Chapter 3), and the fall of the same years (d-f). Lakes that were flooded by the Slave River in the spring of each monitoring year are shown in black circles, while lakes that did not flood are shown in grey circles. No flooding occurred in 2004. Isotope results are shown relative to the Local Meteoric Water Line (LMWL: $\delta^2\text{H} = 6.7 \delta^{18}\text{O} - 19.2$; Birks et al., 2004), which approximates the relationship between $\delta^{18}\text{O}$ and $\delta^2\text{H}$ in local precipitation. Great Slave Lake and Slave River values are shown as open triangles and squares, respectively. Lakes identified in the text are labeled. . 108

Figure 4.3. Conceptual diagram showing lake-specific ambient vapour ($\delta_{A-\text{amb}}$) for lake δ_L as a function of mixing between evaporate from Great Slave Lake

(δ_{E-GSL}) and advected vapour (δ_{A-adv}). δ_{E-GSL} is calculated using Equation (3), incorporating δ_{A-adv} . The local meteoric water line (LMWL) approximates the relationship between $\delta^{18}O$ and δ^2H in local precipitation, while a lake (δ_L) with input δ_P undergoing evaporation plots along the local evaporation line (LEL). This conceptual diagram incorporates climate normal (1971-2000) conditions measured at Hay River, NWT (Environment Canada, 2002), and vapour compositions are in equilibrium with amount-weighted (yearly) precipitation (δ_P ; Birks et al., 2004). 109

Figure 4.4. Ambient vapour mixing results (δ_{A-amb}) for fall 2003-2005 calculated using advected vapour (δ_{A-adv}) in equilibrium with a) evaporation-flux-weighted (thaw season) precipitation (δ_{PS} , Gibson and Edwards, 2002) and b) amount-weighted (yearly) precipitation (δ_P , Birks et al., 2004). Also shown are the isotopic compositions of SRD study lakes (δ_L), Great Slave Lake (δ_{GSL}) and Great Slave Lake vapour (δ_{E-GSL}). In a), the definition of δ_{A-adv} in equilibrium with δ_{PS} does not properly characterize atmospheric conditions in the SRD, and δ_{A-amb} results are poorly constrained between δ_{A-adv} and δ_{E-GSL} . Improved characterization of atmospheric conditions is achieved in b), when δ_{A-adv} is defined as being in equilibrium with δ_P 110

Figure 4.5. $\delta^{18}O$ composition of precipitation for northern Canada, reproduced from Gibson and Edwards (2002). Isolines are interpolated from Canadian Network for Isotopes in Precipitation stations, shown as black dots. Similar trends are noted for δ^2H . The black arrow represents the direction of dominant winds affecting the SRD in the fall. 111

Figure 4.6. *E/I* results for SRD lakes in fall 2003-2005. Lakes are grouped according to dominant hydrological processes affecting their water balances (Brock et al., 2007; see Chapter 2) and are sorted in ascending order based on the difference between the minimum and maximum *E/I* ratio at each lake over the 2003-2005 monitoring period. One lake (SD7) in the flood-dominated category that did not flood in 2005 is indicated by a + sign. Lakes in the

evaporation-dominated category that flooded in 2005 (SD8, 18, 19, 29, 32) are indicated by a * sign. Brackets on the x-axis identify lakes more strongly affected by snowmelt versus evaporation. An E/I ratio of 1 represents steady-state hydrological conditions for a terminal basin. Results are modeled based on the assumption that lakes are at “quasi-steady-state” (see the section titled “Quantifying lakewater balances using water isotope tracers”), thus E/I ratios >1 are not physically meaningful, but have comparative value..... 112

Figure 4.7. Percent dilution in SRD lakes by Slave River water or snowmelt in spring of a) 2003, b) 2004 and c) 2005. Percent dilution for each lake was calculated by dividing the difference between a lake’s isotopic composition in the spring and the preceding fall by the difference between the isotopic composition of the diluting sourcewater (Slave River water or snowmelt) and 113

Figure 5.1. Location of the Peace-Athabasca (PAD) and Slave River (SRD) deltas and lake SD2. Inset image shows SD2 and depicts the observed path of floodwater entry in 2003 and 2005..... 136

Figure 5.2. Hydrographs showing average monthly discharge over the period 1960-2005, and for the years 2003-2005, for a) the Slave River, measured at Fitzgerald, AB, and b) the Smoky River, measured at Watino, AB (Water Survey of Canada, 2006)..... 137

Figure 5.3. Aerial photographs showing shifts in distributary channel routing in the active Slave River Delta: a) in 1954, the majority of flow passed through Mid Channel West; b) by 1966, a cleavage bar had developed at the entrance of Mid Channel West; c) by 1973, most distributary flow was diverted via Resdelta Channel; and d) in 1999, the majority Slave River distributary flow continued to pass through Resdelta Channel (see also Hill, 1996; Prowse et al., 2006). Study site SD2 is also shown. Scales are not identical in each photograph. 138

Figure 5.4. a) ^{210}Pb activity versus depth, b) ^{137}Cs activity versus depth and c) the sediment core chronology for SD2. The ^{137}Cs activity peak at 25.0-25.5 cm

depth corresponds to the 1963 above-ground nuclear weapons testing fallout peak (Appleby, 2001), and constrains the sediment core chronology. 139

Figure 5.5. Physical and geochemical proxies for the SD2 sediment sequence, showing a) water content as percent of wet weight, b) $\delta^{13}\text{C}_{\text{org}}$, c) $\delta^{15}\text{N}$, d) organic carbon content as percent of dry mass, e) nitrogen content as percent of dry mass and f) carbon-to-nitrogen ratios. The vertical dashed line on b) – f) represents the composition of Slave River sediment, collected in the catchment of SD2 during the spring flood of 2005. Horizontal grey bars represent inferred periods of high flood frequency..... 140

Figure 5.6. Relative abundance profiles of the dominant diatom taxa (i.e., those with relative abundances of $\geq 5\%$ in at least one sediment interval) from the SD2 sediment sequence. The flood index (right hand panel) is developed from z-scores based on the abundances of taxa indicating high river influence..... 141

Figure 5.7. A stratigraphic plot of the abundance of the eight most abundant macrofossil taxa in the sediment core from SD2. The peak in *S. cuneata* seeds is highlighted with a hatched box, and identifies the period of lowest water level at SD2, as described in the text..... 142

Figure 5.8. Key geochemical and biological geochemical proxies for the SD2 sediment sequence, and measured Slave River discharge (Water Survey of Canada, 2006). The horizontal shaded grey boxes on the proxy records represent periods of high flood frequency, inferred from each proxy. The vertical short-dashed line on a) indicates the C/N value of modern Slave River sediment. The vertical short-dashed line on d) indicates peak spring discharge attained during the 2003 spring break-up flood. Asterisks on d) represent flood events reported in the oral flood history (Wesche, 2009). Horizontal long-dashed boxes outline the main periods of high flood frequency at SD2, inferred from the proxy records..... 143

Figure 5.9. Carbon-to-nitrogen ratios (normalized as z-scores) for SD2 and PAD15, a flood-dominated lake in the upstream Peace-Athabasca Delta (Wolfe et al., 2006). The PAD15 record has been smoothed by an 11-point running

mean to achieve comparable resolution to the SD2 sequence. Periods of high flood frequency inferred from the SD2 sediment record (Figure 8) are outlined with dashed boxes. 144

Figure 6.1. Map of potential SRD monitoring lakes..... 159

List of Tables

Table 2.1. Isotopic framework parameters are derived using flux-weighted thaw season climate data from Hay River (Environment Canada, 2002, 2004) and Equations 6, 7, 9 and 10 in Appendix A.....	50
Table 2.2. Hydrologic inputs and outputs from lakes in the SRD, based on hydrologically-inferred zonation, where R = river inputs during elevated (spring flood) flow conditions (R_F) and normal summer flow conditions (R_N), S = catchment-sourced snowmelt inputs, P = thaw season precipitation, O = surface outflow during elevated (spring flood) flow conditions (O_F) and normal summer flow conditions (O_N), and E = surface water evaporation. Dominant processes are shown in bold. The role of groundwater in lakewater balances is likely minimal, as the SRD is situated in a zone of discontinuous permafrost and lowland drainage is generally poor (Day, 1972).....	51
Table 2.3. All values used for calculations of the isotopic framework for the 2003 thaw season, with references and equation numbers where appropriate...	52
Table 3.1. Flux-weighted thaw season temperature and relative humidity based on climate normal (1971-2000) conditions (Environment Canada, 2002) and conditions measured in 2003, 2004 and 2005 (Environment Canada, 2005) at Hay River, NWT. Data are flux-weighted based on potential evaporation, using methods described by Malmstrom (1969) and Dingman (1993).....	86
Table 3.2. Isotopic framework parameters for 2003-2005.	87
Table 3.3. Peak Slave River discharge and last day of observed ice cover for the 2003-2005 spring melt periods (Water Survey of Canada, 2006) and dates of SRD regional water sampling campaigns.	88
Table 4.1. Evaporation-flux-weighted thaw season temperature and relative humidity for the SRD in 2003, 2004 and 2005, and 1971-2000 Canadian Climate Normals for Hay River (Environment Canada, 2002; 2005).	115

Table 4.2. Isotopic composition of advected atmospheric vapour (δ_{AS-adv} and δ_{A-adv}) in equilibrium with evaporation-flux-weighted (thaw season) precipitation ($\delta^{18}O_{PS}$, $\delta^2H_{PS} = -17.0\text{‰}$; -132‰ ; Gibson and Edwards, 2002) and amount-weighted (yearly) precipitation ($\delta^{18}O_P$, $\delta^2H_P = -19.0\text{‰}$; -148‰ ; measured at the Fort Smith, NWT, CNIP station (Birks et al., 2004)), respectively..... 116

Table 4.3. The percent contribution of recycled or re-evaporated vapour to atmospheric vapour pools in isotope-based studies of atmospheric vapour compositions. 117

Chapter 1: General introduction

Introduction

Water is a vital resource in Canada's North, shaping the northern landscape and influencing human interactions with the land. Almost all Arctic ecosystems are characterized by the presence of lakes, ponds, wetlands and rivers (Schindler and Smol, 2006). The water balances of these features are critical to every aspect of northern hydrology and limnology (Rouse et al., 1997), shaping the structure and function of their associated ecosystems (Wrona et al., 2005) and affecting high-latitude oceanic, atmospheric, cryospheric and biological processes (Woo and Thorne, 2003; Déry and Wood, 2005). The seasonal cycling of water connects the Arctic land mass to the Arctic Ocean (Lammers et al., 2001), linking freshwater and marine ecosystems, and creates highly diverse environments and biota adapted to severe northern conditions (Wrona et al., 2005). Northern wetlands have greater biological diversity than other freshwater ecosystems (Huntington and Weller, 2005), and provide important permanent and transient habitat for a wide range of biota, including diverse vegetation, fish, waterfowl and mammal species (Townsend, 1984; Prowse and Conly, 2002; Wrona et al., 2005).

One ubiquitous feature of northern freshwater ecosystems is the presence of seasonal ice cover, and the spring break-up of river ice and melt of the winter snowpack are among the most significant hydrological events of the year (Rouse et al., 1997; Romolo et al., 2006a). Spring break-up flooding is important for delta and floodplain lakes because it is a key supplier of water (Prowse and Lalonde, 1996; Rouse et al., 1997; Beltaos et al., 2006a; Peters et al., 2006b) and maintains riparian ecosystems and early successional communities along shorelines (English et al., 1997; Prowse et al., 2002a; Schindler and Smol, 2006). The frequency, intensity and duration of flooding affects the physical, chemical and biological properties of lakes (Squires et al.,

2002; Hall et al., 2004; Sokal et al., 2010) and drives primary and secondary production (Wrona et al., 2005). Spring flooding is an important factor that helps maintain the overall vitality of northern floodplains and deltas.

In turn, these ecosystems have supported northern aboriginal communities for millennia (Schindler and Smol, 2006), linking biological and socio-economic systems and contributing to cultural identity (Wesche, 2009). The habitats provided by rivers, lakes, wetlands and floodplains support harvestable species, creating valuable biological resource complexes (Townsend, 1984). Traditional hunting, fishing and trapping practices are carried out by aboriginal land-users, providing important food resources and strengthening the spiritual tie between humans and their environment (Huntington and Weller, 2005). Water also shapes the way the north is settled and traveled. For example, the earliest fur trading in the Northwest Territories began on the south shore of Great Slave Lake, leading to the eventual settlement of the community of Fort Resolution, the oldest documented settlement in the territory (Wesche, 2007). In the early 1800s, all furs in the Great Slave Lake region were traded into Fort Resolution (Smith, 1982), largely due to the town's location at the mouth of the Slave River, a major northern transportation route. The commencement of steamboat operations on the Slave River at the turn of the 20th century positioned Fort Resolution as a central node in the fur trading industry (Wesche, 2009). While the economics of the North have shifted significantly since the early 20th century, northern waterways continue to serve as important year-round transportation routes, and traditional land-use activities play a key role in preserving cultural identity and maintaining knowledge tied to the land (Wesche, 2007).

Despite the crucial role of water for ecosystem integrity and human populations in the North, we lack a comprehensive understanding of the hydrology of northern freshwater ecosystems (Evans, 2000; Kane, 2005). This is compounded by a lack of long-term river and climate data for Canada's North (Rouse et al., 1997; Lammers et al., 2001; Kane, 2005; Rood et al., 2005; Peters

et al., 2006b; Schindler and Donahue, 2006). The critical need to improve our comprehension of northern hydrological processes (Hayashi et al., 2004) is heightened by the effects of natural and anthropogenically-induced climate change. In the North, these effects include shorter snow seasons, warmer lakes and rivers, earlier timing of spring events, later freeze-up dates, declining water storage in glaciers, declining downstream meltwater availability, and strong trends towards warmer summer and winter temperatures (Magnuson et al., 2000; IPCC, 2007a,b). In fact, the Arctic has experienced the greatest warming on Earth in recent decades (Huntington and Weller, 2005). Further, the impacts of climate warming are more severe at high latitudes (Rood et al., 2005), where positive feedback mechanisms have the potential to accelerate northern hydrological change (Overland et al., 2002; Schindler and Smol, 2006). The significance of these changes for northern freshwater ecosystems cannot be understated, as their sensitivity to environmental change means that even small variations in climate have the potential to induce numerous hydroecological changes (Rouse et al., 2005).

Within the context of the rapid and ongoing environmental change described above, this thesis aims to advance our understanding of northern freshwater hydrology. The findings presented herein provide a framework within which to evaluate observations of change at many scales, both on the land and over time. Specifically, this thesis focuses on understanding the role of water in the contemporary and historic Slave River Delta (SRD) and Fort Resolution, NWT, by teasing apart the interrelated factors that cause hydrological change, while taking into account local observations. In the past several decades, observations have been made by land users about changing water dynamics in the SRD. These observations relate primarily to variable flow on the Slave River and a perceived reduction in the frequency of river flooding in the spring, which in turn affect the abundance and quality of traditional food and fur resources, and the safety of travel throughout the year. Local residents suspect increasing water diversion and extraction pressures by upstream river regulation (by the WAC Bennett Dam at the headwaters of the

Peace River) and the development of the tar sands on the Athabasca River, as well as the effects of a shifting climate, are the causes of these changes (Wesche, 2007, 2009; Wolfe et al., 2007a). There is also concern about renewed interest in hydroelectric production on the Slave River near the Alberta-NWT border (see Bell, 2009). Such concerns are not unique to Fort Resolution, and will likely increase as development in the North continues and the effects of climate variability and change become more pronounced.

The findings of this thesis provide a fundamental first step towards better understanding the hydrology of the SRD specifically, and northern ecosystems in general. Because an improved understanding of northern hydroecology can provide a foundation for the sustainable management of water resources (Hannah et al., 2007), this thesis gives northerners the knowledge necessary to frame their observations of change and to build adaptive capacity to prepare for and respond to future variations in water resources and subsequent changes on the land. This thesis demonstrates how quantitative investigations of past and present hydrology in northern environments can complement local and traditional observations of change to develop a holistic picture of ecosystem dynamics – an approach that is collaborative, interdisciplinary, and sensitive to northern priorities.

Previous research on the upstream Peace-Athabasca Delta and the SRD

The SRD is located in the Mackenzie River Basin (MRB), which covers $\sim 1/5^{\text{th}}$ of Canada's land mass and drains 1.8 million km² (Woo and Thorne, 2003). The headwaters of the basin are in the Rocky Mountains of British Columbia and Alberta, where spring meltwater runoff from glaciers and alpine snowcover is a key contributor to discharge in the basin's largest rivers, the Peace, Athabasca, Slave and Mackenzie. At the mouth of the MRB, the Mackenzie River discharges into the Arctic Ocean. It is the largest North American river to do so (Burn, 2008), and its discharge has several important influences on the nearshore Arctic Ocean. These include preserving the integrity of polar sea ice by creating a thermohaline, preventing the intrusion of

saline sea water to the coast, and accelerating spring near-shore ice break-up (Woo and Thorne, 2003).

In addition to the 400 km² SRD, the MRB also contains the Peace-Athabasca Delta (PAD) in northern Alberta and the Mackenzie River Delta (MRD; 13 000 km²) on the coast of the Arctic Ocean near Inuvik, NWT (Figure 1.1). There is a long history of hydroecological research in the PAD, prompted by concerns emanating from the regulation of the Peace River in 1968 by the WAC Bennett Dam. The dam, constructed at the headwaters of the Mackenzie River Basin at Hudson's Hope, BC, has an impoundment capacity of 4.1×10^{10} m³ (Muzik, 1985), and has raised concerns about the impact of river regulation on the frequency of downstream spring flooding. After regulation, local PAD land users reported a decline in flood frequency and drying in the delta, affecting the abundance of wildlife. Several studies were initiated to address these concerns, including the Peace-Athabasca Delta Project Group (PADPG, 1973), the Peace-Athabasca Delta Technical Studies (PADTS, 1996), the Northern River Basins Study (Prowse and Conly, 2002; Prowse et al., 2002) and the Northern Rivers Ecosystem Initiative (Prowse et al., 2006). Many of these studies focused on engineering solutions for restoring flood frequency to the delta, and were hampered by a lack of long term river discharge data necessary to provide adequate temporal context for evaluating perceived changes in flood frequency after impoundment.

To develop a more comprehensive understanding of the contemporary hydrology of the PAD and to establish the temporal context necessary to assess long term changes in flood frequency, Hall et al. (2004) began an extensive research program in the delta. Research focused on characterizing the contemporary hydrology of PAD lakes (Wolfe et al., 2007b; Yi et al., 2008), reconstructing long-term (up to ~1000 year) hydrological records in the northern Peace sector of the PAD (Wolfe et al., 2005, 2006, 2008a; Jarvis, 2008) and in Lake Athabasca during the Little Ice Age (Sinnatamby et al., 2010), and investigating the impacts of changes in river discharge and climate in

the southern Athabasca sector during the 20th century (Wolfe et al., 2008b). Research has revealed that the PAD is a dynamic ecosystem with spatially variable responses to changes in climate and river discharge, reflecting the natural heterogeneity of the landscape. Paleolimnological investigations highlight oscillating multi-decadal periods of high and low flood frequency over the last several centuries (see Figure 3 in Wolfe et al., 2008b), suggesting significant natural variability in flood recurrence intervals. During the Medieval Warm Period, warmer conditions caused early and rapid headwater snowmelt, substantially increasing river discharge and the frequency and magnitude of early spring flooding in the PAD. A transition to colder conditions during the Little Ice Age resulted in reduced and delayed headwater snowmelt, which produced lower downstream discharge during the freshet and less frequent and lower magnitude flooding in the PAD, and higher river discharge during summer. Notably, a further decline in spring river discharge and flooding in the PAD during the 20th century differs from the preceding intervals. This shift is attributed primarily to shrinking headwater glaciers and reduced headwater snowmelt since the termination of the Little Ice Age, and has contributed to a drying trend in many lowland lakes of the PAD over the last ~100 years (Wolfe et al., 2008a). Importantly, research findings indicate that regulation of the Peace River coincided with a period of low flood frequency which began several decades before river impoundment (Jarvis, 2008; Wolfe et al., 2006, 2008a), suggesting impoundment has likely had little effect on the flood hydrology of the delta. Instead, changes in headwater climate (Wolfe et al., 2008a) and local changes in Athabasca River tributary flow (Wolfe et al., 2008b) appear to be the main drivers influencing the frequency and magnitude of river flooding in the PAD.

Until recently, scientific investigations in the SRD have been less extensive than those conducted in the PAD. However, concerns about declining flood frequency in the SRD following Peace River regulation did prompt some examination of the effects of river regulation on SRD geomorphology and spring flood frequency (Hill, 1996; English et al., 1996, 1997). Using aerial

photographs of the delta pre- and post-regulation, these studies documented changes in flow patterns and vegetation assemblages indicative of drying of the delta post-impoundment. However, separating the effects of river regulation from other potential drivers of change (for example, climate variability or natural geomorphological evolution) was hampered by a lack of data about contemporary SRD hydrology and long-term river discharge data.

To address these important knowledge gaps, an extensive, on-going research program was initiated in the SRD in 2002, modeled after the approach taken by Hall et al. (2004) in the PAD. Researchers include ecologists, isotope hydrologists and social scientists. Research directions comprise contemporary hydroecological studies of a suite of delta lakes spanning hydroecological gradients in the delta, and identifying and documenting community perceptions of, and adaptations to, environmental change (Figure 1.2; Wolfe et al., 2007a). The hydrological research presented in this thesis is a major component of this on-going SRD research initiative. It is complemented by theses by Clogg-Wright (2007) and Mongeon (2008), who initiated hydrological research by interpreting preliminary lakewater isotope data and reconstructing water balance conditions over the past ~300 years in selected delta lakes using stable isotope approaches. Adam (2007) and Sokal (2007) used limnological, macrofossil and diatom analysis to examine contemporary relationships between hydrological and limnological conditions in delta lakes (Sokal et al., 2008, 2010) and applied these results to paleolimnological reconstructions of flood frequency from lake sediments. Wesche (2009) conducted a community-based study of environmental change in Fort Resolution, incorporating traditional knowledge and evaluating individual and collective adaptive capacity to present and future change. As this thesis will demonstrate, the SRD research program has been very successful at characterizing contemporary hydroecological conditions in SRD lakes, identifying the relative roles of the drivers of hydroecological change, identifying regions of the delta susceptible to change in the face of the multiple stressors described above, and in reconstructing long-term records of flood frequency from selected delta lakes. Importantly, research in the SRD has

also revealed the key role of headwater discharge and climate variability on the hydrology of the delta, providing valuable insight into the drivers of hydrological change in the upper Mackenzie River Basin.

Thesis Objectives

As described above, this thesis aims to characterize the present and past hydrology of the SRD in order to address concerns about ongoing hydroecological changes in the delta, including recent accounts of declining flood frequency, and in response to widely-held concern in the scientific community about the impacts of current and predicted climate variability on northern water resources. To do this, the research described in the subsequent chapters was designed to fulfill two main objectives:

- 1) to characterize contemporary spatial and seasonal variability in SRD lake hydrology using water isotope tracers, and
- 2) to use a multi-proxy paleolimnological approach to extend our knowledge of the flood history of the Slave River.

This two-pronged approach offers many advantages when investigating the present and past hydrology of the SRD. Studying modern SRD hydrology over the course of several seasons offers insight into hydrological variation at many scales – for example, over the course of a single thaw season in a single lake, or inter-annually at the landscape scale. Understanding individual lake hydrology in conjunction with landscape-scale processes makes it possible to classify delta lakes based on the dominant hydrological processes affecting their water balances, and thus to identify areas of the SRD susceptible to different hydrological stressors and drivers of change. Of equal importance is the insight a comprehensive understanding of contemporary hydrology offers when reconstructing past hydrological conditions. For example, this thesis includes a reconstruction of the flood history of the Slave River, based on lake sediment records. The studies of modern SRD hydrology included in this thesis helped identify a lake for target coring and characterize the relationship between

present-day river discharge and lake flooding, two components necessary for an accurate reconstruction of past flood frequency. Together, the outcomes of this thesis create a comprehensive picture of landscape-scale hydrology in the SRD. This thesis provides the basis for evaluating current hydrological change and establishes important building blocks for anticipating future deltaic evolution in response to natural and anthropogenic stressors on water resources.

Research Methods

Contemporary hydrological studies in the SRD are spearheaded by the use of water isotope tracers (^{18}O and ^2H), which allow for a rapid survey of several lakes at a single point in time. Similar approaches have been used effectively in other studies of hydrology in northern Canada (Gibson, 2001, 2002; Gibson and Edwards, 2002; Wolfe et al., 2007b; Yi et al., 2008). Here, water samples were collected from 41 lakes spanning previously-identified hydroecological gradients of the delta (see English et al., 1997), as well as from the Slave River and Great Slave Lake. Initial sampling was conducted in September 2002, with additional sampling campaigns carried out in the early, mid- and late thaw seasons of 2003-2005. Local climate data (temperature and relative humidity; Environment Canada, 2005) were used to develop season-specific isotopic frameworks for evaluation of lakewater isotope results from each sampling campaign, incorporating subtle variations in ambient conditions over the course of field investigations. In spring, water isotope data were complemented by measurements of total inorganic suspended sediment, which is useful for identifying flooded versus non-flooded lakes following the spring melt period.

Paleohydrological research was carried out using a lake sediment core collected from a flood-susceptible SRD lake, identified based on contemporary hydrological studies. Multiple proxies were analyzed to reconstruct flood history. These included physical and geochemical analyses (water content and elemental and stable carbon and nitrogen isotope analysis) and biological proxies (diatom and macrofossil analysis). An oral history record of past flood

events, compiled based on reports from SRD land users (Wesche, 2009), and a 46-year record of Slave River discharge (Water Survey of Canada, 2006) were also used to identify past flood events.

Thesis Outline

This thesis is composed of four results chapters, each of which has been written as a manuscript and has been published in a peer-reviewed journal. (Chapter 5 was in press at the time this document was written.) Complete references for each chapter are provided below, in addition to a description of the main contributions of each chapter to the thesis. While each data chapter is published independently, all chapters are designed to build on the research findings of the previous work and hence each chapter contributes equally to the thesis as a whole.

Chapter 2

Brock BE, Wolfe BB, Edwards TWD. 2007. Characterizing the hydrology of shallow floodplain lakes in the Slave River Delta, NWT, using water isotope tracers. *Arctic, Antarctic and Alpine Research* 39: 388-401.

This chapter serves as a foundation for subsequent evaluations of SRD hydrology by identifying the major hydrological processes affecting the hydrological evolution of SRD lakes over the 2003 thaw season. It identifies spring flooding by the Slave River, exchange with the Slave River or Great Slave Lake, and snowmelt input as the main water sources for SRD lakes, and open water evaporation during the thaw season as the pathway for water loss. Results are used to classify SRD lakes as flood-dominated, exchange-dominated or evaporation-dominated, based on the relative importance of these processes at each study lake. The spring melt period is identified as a particularly dynamic time for lake hydrology, and that spring conditions have a strong influence over a lake's subsequent hydrological evolution during the thaw season. The dilution by river water or snowmelt in each lake is then quantified. Results distinguish sub-regional landscape units that may be susceptible to

future changes in climate or the hydrological regime of the Slave River, and provide important constraints for ongoing evaluations of modern lakewater data and paleohydrological reconstructions of SRD lakewater balances.

Chapter 3

Brock BE, Wolfe BB, Edwards TWD. 2008. Spatial and temporal perspectives on spring break-up flooding in the Slave River Delta, NWT. *Hydrological Processes* 22: 4058-4072.

This chapter examines the dynamic spring melt period identified in the previous chapter in more detail, using water samples collected from SRD lakes in the springs of 2003-2005. Nature provided an excellent experimental design, with each of the three spring melt periods displaying differing break-up conditions – there was a moderate spring flood in 2003, no flooding in 2004, and a significant spring flood in 2005. Based on the lakewater dilution model developed in the previous chapter, the spatial extent of spring flooding in each year is determined. Importantly, results identify that the magnitude and spatial extent of spring flooding in the SRD is positively correlated with upstream discharge, particularly in the headwater tributaries of the Peace River. Additionally, a 46-year instrumental record of river discharge, with peak discharge attained during the 2005 flood as a benchmark, is used to hindcast flood frequency. This record correlates well with paleolimnological evidence from a flood-dominated lake in the active delta, establishing the foundation for extending records of Slave River flood frequency beyond the period of instrumental records (see Chapter 5).

Chapter 4

Brock BE, Yi Y, Clogg-Wright KP, Edwards TWD, Wolfe BB. 2009. Multi-year landscape-scale assessment of lakewater balances in the Slave River Delta, NWT, using water isotope tracers. *Journal of Hydrology* 379: 81-91.

Building on the semi-quantitative understanding of delta hydrology established in Chapter 2, this chapter focuses on the seasonal evolution of SRD lakewater balances during 2003-2005 following the contrasting spring melt conditions described in Chapter 3. This chapter recognizes the effect of Great Slave Lake on the water balances of delta lakes by incorporating contributions of Great Slave Lake evaporated vapour to the ambient atmospheric vapour pool for the purpose of calculating evaporation-to-inflow ratios over the study period. Results show annual flooding is not necessary to maintain positive water balances in flood-dominated lakes, while snowmelt inputs to evaporation-dominated lakes offset evaporative losses later in the season. These results were used to distinguish regions of the delta that will be most strongly affected by changes in river discharge, winter snowpack depth, and thaw season climate.

Contributions from student co-authors: Y Yi developed the mathematical model applied in this manuscript (see Yi et al., 2008). KP Clogg-Wright developed the original idea of vapour mixing between Great Slave Lake evaporate and ambient SRD vapour (see Clogg-Wright, 2007).

Chapter 5

Brock BE, Martin ME, Mongeon CL, Sokal MA, Wesche SD, Armitage D, Wolfe BB, Hall RI, Edwards TWD. In press. Flood frequency variability in the Slave River Delta, NWT, over the past 80 years from multi-proxy paleolimnological analysis. *Canadian Water Resources Journal*.

Results presented in chapters 2-4 highlighted the strong influence of the spring melt period, in particular spring flooding, on lakewater balances in flood-dominated delta lakes. Local concerns about changing flood frequency reflect the importance of this process to the hydroecology of delta lakes. However, short instrumental records of river discharge hamper the examination of long-term trends in flood frequency and make it difficult to address associated concerns. This chapter presents data to extend the flood frequency record for the active delta, building on preliminary results presented in Chapter 3. Multi-proxy analysis of an ~80-year-long sediment record from a flood-dominated

lake in the active delta reveals multi-decadal periods of high and low flood frequency, identifying intervals of high flood frequency during the late 1930s and 1940s, the early 1960s to 1980s, and the early 1990s to ~2000. Multi-proxy records reveal that the onset of river regulation occurred during a period of increased flood frequency beginning in the early 1960s and ending in the early 1980s, thus demonstrating that river regulation in 1968 did not have a significant negative effect on Slave River flood frequency. Results show parallel variations in flood frequency in both the PAD and the SRD, and suggest that climate-driven changes in runoff in the headwaters of the Mackenzie Basin are the principle drivers of flood frequency variability in both deltas.

Contributions from student co-authors: ME Martin developed the macrofossil record for SD2 (see Adam, 2007). CL Mongeon contributed to the development of the geochemical record for SD2 (see Mongeon, 2008). MA Sokal developed the diatom record for SD2 (see Sokal, 2007). SD Wesche developed the local knowledge record of Slave River flood history for the SRD (see Wesche, 2009).

Figures



Figure 1.1. The Mackenzie River Basin, showing the Peace, Athabasca, Slave and Mackenzie Rivers and their associated deltas. (Map produced by Eric Leinberger, University of British Columbia, for the Mackenzie Basin Impact Study.)

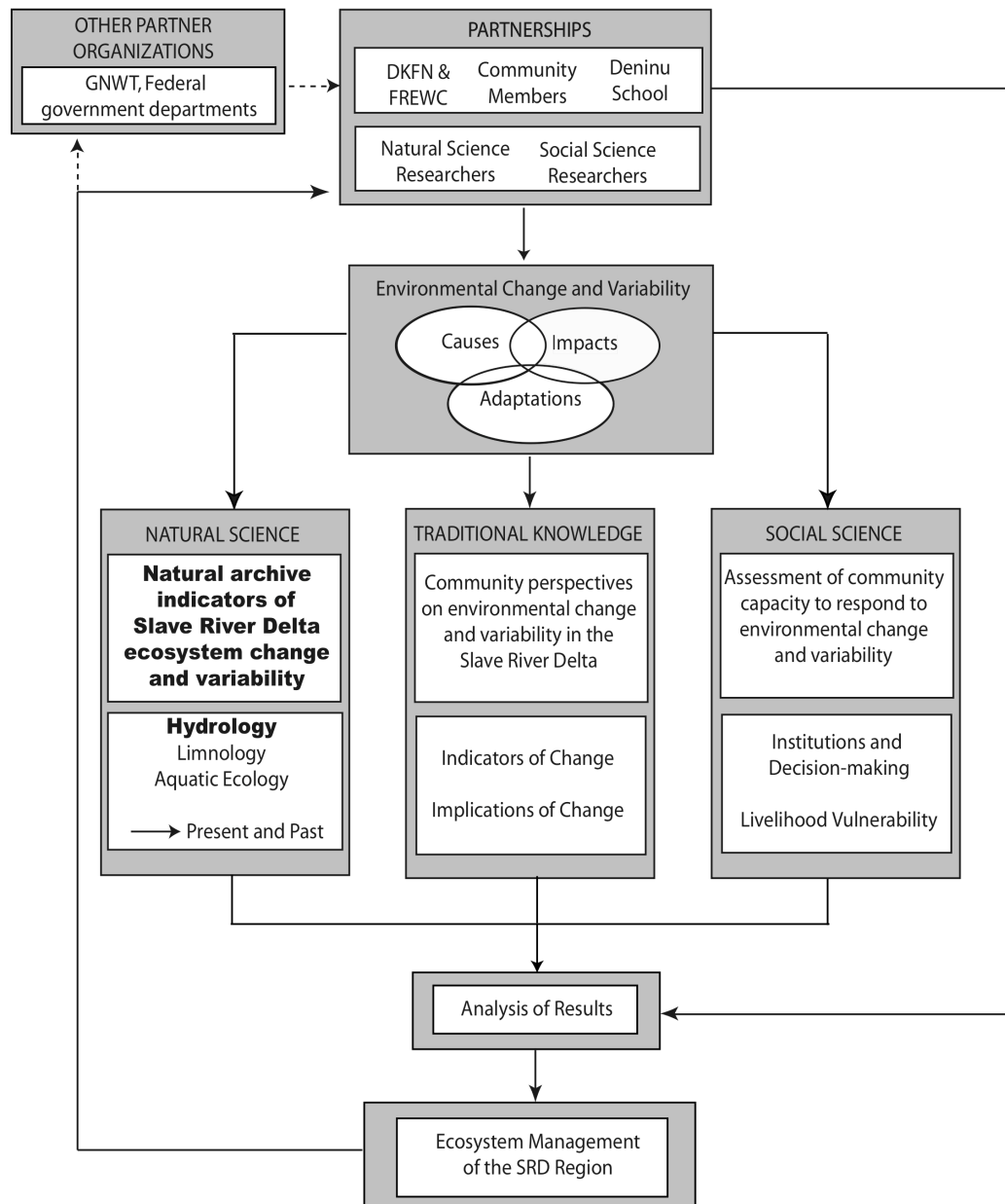


Figure 1.2. Conceptual diagram of the interdisciplinary SRD research program (from Wolfe et al., 2007a). The contributions of this thesis to the research program are highlighted in bold. ‘GNWT’ is the Government of the Northwest Territories, ‘DKFN’ is the Deninu Kue First Nation, and ‘FREWC’ is the Fort Resolution Environmental Working Committee.

Chapter 2: Characterizing the hydrology of shallow floodplain lakes in the Slave River Delta, NWT, using water isotope tracers

Complete citation: Brock BE, Wolfe BB, Edwards TWD. 2007. Characterizing the hydrology of shallow floodplain lakes in the Slave River Delta, NWT, using water isotope tracers. *Arctic, Antarctic and Alpine Research* 39: 388-401.

Introduction

The Slave River Delta (SRD) is a highly productive ecosystem located on the south shore of Great Slave Lake, NWT, Canada. Flood events from the Slave River supply water and nutrient-rich sediment to delta lakes, which is believed to be important for maintaining extensive shoreline habitat and overall vitality of this northern ecosystem (English et al., 1997; Prowse et al., 2002a). In recent years, increased recognition of the potential impacts of multiple stressors on SRD hydroecology, including climate variability and regulation of the Peace River upstream for hydroelectric production by the WAC Bennett Dam (Figure 2.1), have raised concerns regarding the current state of the ecosystem. These concerns have implications for management of the delta and for residents of the nearby community of Fort Resolution, who utilize the delta's natural resources. However, there is limited scientific knowledge of the hydroecology of the delta and of the potential impacts of changes in climate and river discharge. Further complications arise because hydrometric and climatic records are insufficient in duration to clearly explore relationships between apparent drying of the delta over the past few decades (Bill et al., 1996; English et al., 1997) and potential causes (e.g., lower river discharge, reduced flood frequency, natural deltaic evolution, and climate variability and change). Thus, the relative roles of various driving forces on hydroecological conditions of the SRD remain largely uncertain (Prowse et al., 2002a).

At a more fundamental level, key questions exist regarding the basic functioning of the SRD ecosystem. For example, no previous studies have been

conducted on the water balances of the hundreds of lakes and wetlands that populate the delta, yet the maintenance of water in these basins provides habitat for significant wildlife populations. Variation of lakewater balances over seasonal and longer time-scales is essentially unknown, as is the relative importance of various hydrological processes. These processes include precipitation, snowmelt runoff, river flooding, Great Slave Lake seiche events and evaporation.

As part of ongoing multidisciplinary research to assess contemporary and past hydroecological conditions in the SRD (Wolfe et al., 2007a), we are using water isotope tracers (^{18}O , ^2H) to examine the roles of major hydrological processes on lakewater balances. Here we interpret results from lake and river sampling conducted during the 2003 ice-free (thaw) season. Stable isotope tracers offer an effective method to assess controls on lakewater balances because isotopic partitioning in the hydrological cycle is well understood and a rapid survey of many basins at a single point in time can be acquired without the need for field-intensive, site-specific investigations (see Edwards et al., 2004). This technique has been used extensively in hydrological studies to characterize spatial and temporal variability in the water balances of lakes in other remote regions of northern Canada (e.g., Gibson, 2001, 2002b; Gibson and Edwards, 2002), including the Peace-Athabasca Delta, a similar riparian ecosystem upstream of the SRD (Wolfe et al., 2007b).

As discussed in detail below, the main sources of water for SRD lakes – snowmelt, rain, the Slave River, and Great Slave Lake – each possess characteristic isotopic signatures. This feature, in addition to subsequent heavy-isotope enrichment during evaporation, is used to characterize the relative importance of key hydrological processes on SRD lakewater balances against the backdrop of an isotope framework developed from hydroclimatic conditions that prevailed during 2003. Furthermore, spatial mapping offers insight into the relative importances of these hydrological processes across local landscapes of the SRD. Such knowledge is critical for constraining

reconstructions of past hydrological conditions and predicting hydrological responses of the SRD ecosystem to natural and anthropogenic changes in climate and river discharge characteristics.

The Slave River Delta

The SRD (61°15' N, 113°30' W) began to form during the retreat of the Keewatin Sector of the Laurentide Ice Sheet and the drainage of Glacial Lake McConnell at ~8070 ¹⁴C yr BP (Vanderburgh and Smith, 1988). Relict deltaic and alluvial sediments cover approximately 8300 km² (Vanderburgh and Smith, 1988) and extend along the Slave River 180 km downstream from Fort Smith, NWT, to the active delta. Currently, the active portion of the SRD spans approximately 400 km² (English et al., 1997), and occurs downstream of the point where the Slave River fans into distributaries.

Climate in the SRD is strongly seasonal, with cold winters (mean January temperature = -23.1°C) and cool summers (mean July temperature = 15.9°C) (Environment Canada, 2002). The SRD receives approximately 320 mm of precipitation annually, half of which falls as rain during the thaw season. Average thaw season temperature and relative humidity, flux-weighted based on potential evapotranspiration (Malmstrom, 1969; Dingman, 1993), are 11.4°C and 69.2%, respectively, using 1971-2000 normals measured at Hay River, NWT, located 150 km west of the SRD (Environment Canada, 2002).

The Slave River begins its 420 km course north to Great Slave Lake at the confluence of the Peace River and Rivière des Rochers, at the northern edge of the Peace-Athabasca Delta in northern Alberta (Figure 2.1). The Slave River receives ~66% of its annual flow from the Peace River (English et al., 1996), with the remaining flow mainly supplied by Lake Athabasca and the Athabasca River via the Rivière des Rochers, as well as other northward-flowing tributaries upstream of the Peace-Rochers confluence. The Slave River drains 15100 km² (Prowse et al., 2002a) and its discharge contributes 74% of all inflow to Great Slave Lake (Gibson et al., 2006b), the primary source of water

for the Mackenzie River. Additional water sources for Great Slave Lake are its bordering catchments, contributing 21% of the lake's inputs, and direct precipitation, contributing 5%, based on water budget modeling (Gibson et al., 2006b).

Wind-forced seiche events from Great Slave Lake can inundate the delta front, and affect water levels in the Slave River and outer delta lakes (Gardner et al., 2006). Southwest winds force the majority of seiche set-up events, predominantly in the late summer and early autumn when the hydraulic resistance of the Slave River is low. The majority of seiche events are low in magnitude, with water level increases of 0.05-0.09 m. Levee heights along the lower distributaries of the Slave River are in the range of most seiche events, resulting in the potential for flooding along the delta front.

English et al. (1997) identified three distinct biogeographical zones in the active part of the SRD: the outer, youngest portion of the delta, which supports aquatic and emergent vegetation and where lakes are susceptible to annual floods during the spring freshet due to low levee heights, at or within 0.1 m of low summer Great Slave Lake levels; the oldest apex portion of the delta, where levee heights are 2.5-3 m above low summer Great Slave Lake water levels, flooding is infrequent and climax forest communities of white spruce (*Picea glauca*) dominate; and the mid-delta zone, an ecological transition zone between the outer and apex portions of the delta, where alder-willow vegetation complexes dominate, levee heights are 0.5-2.5 m above low summer Great Slave Lake water levels and widespread flooding is thought to occur every five to seven years (Prowse et al., 2002a). Lakes from each of these delta zones have been selected for this study. Maximum lake depths range between 0.15 and 4 m, with the exception of SD30 (Ring Lake, a partially cut-off meander of the Slave River), which has a maximum depth of 10 m.

Methodology

Forty lakes spanning all three biogeographical zones in the SRD and extending well upstream, plus Great Slave Lake, SD30 (Ring Lake) and the Slave River, were sampled with the aid of a helicopter between 22-Sep-02 and 24-Sep-02, and on 23-May-03, 23-Jun-03, 25-Jul-03 and 05-Aug-03 (Figure 2.1). A subset of six lakes was also sampled on 15-Aug-03 and 03-Sep-03. Water samples were collected from ~10 cm below the water surface at the centre of each study lake in 30 mL high density polyethylene bottles and sealed tightly before transportation to the University of Waterloo Environmental Isotope Laboratory. The $^{18}\text{O}/^{16}\text{O}$ and $^2\text{H}/^1\text{H}$ ratios were measured using standard methods (Epstein and Mayeda, 1953; Coleman et al., 1982). Results are reported as δ values, representing deviations in per mil (‰) from the V-SMOW standard, such that $\delta^{18}\text{O}_{\text{sample}}$ or $\delta^2\text{H}_{\text{sample}} = 10^3[(R_{\text{sample}}/R_{\text{V-SMOW}})-1]$ where R is the ratio of $^{18}\text{O}/^{16}\text{O}$ or $^2\text{H}/^1\text{H}$ in sample and standard, normalized to $\delta^{18}\text{O}$ and $\delta^2\text{H}$ values for Standard Light Antarctic Precipitation of -55.5‰ and -428‰ (Coplen, 1996). Analytical uncertainties for $\delta^{18}\text{O}$ and $\delta^2\text{H}$ are $\pm 0.2\text{‰}$ and $\pm 2\text{‰}$ respectively, based on replicate field samples.

Total inorganic suspended sediment (TSS) analysis was also conducted on water samples collected during the 23-May-03 sampling campaign. A known volume of water was agitated and filtered through a 1.2 μm glass microfibre filter of a known weight. Filters were ashed at 550°C for four hours and reweighed to determine the mineral matter content of the filtered sample (Dean, 1974). TSS results are reported in g L^{-1} . Analytical uncertainty for TSS is $\pm 0.002 \text{ g L}^{-1}$, based on replicate field samples.

Meteorological data for 2003 were obtained for Hay River, NWT (Environment Canada, 2004; Figure 2.1). The isotopic composition of amount-weighted mean annual (1962-1965) precipitation (δ_{p}) was obtained from Fort Smith, NWT (Birks et al., 2004). The isotopic composition of evaporation flux-weighted thaw season precipitation (δ_{PS}) is taken from Gibson and Edwards (2002). The reported isotopic composition of snow (δ_{snow}) is given as a range,

based on snow samples collected from SD2, 15, 20, 28, 29, 33 and 39 during an early May 2004 field campaign, prior to ice break-up.

Total precipitation amounts reported were measured at Environment Canada's Hay River, NWT, meteorological station. Snowfall was converted to snow water equivalent and summed with total rainfall.

Results and Interpretation

An isotopic framework for evaluating lakewater balances

Natural isotope labeling of precipitation is typically manifested by the existence of prominent trends in $\delta^{18}\text{O}$ - $\delta^2\text{H}$ space, reflecting systematic mass-dependent partitioning of water molecules in the hydrologic cycle (Edwards et al., 2004). The isotopic composition of precipitation at a site generally clusters along a Local Meteoric Water Line (LMWL) lying near the Global Meteoric Water Line (GMWL) of Craig (1961). The GMWL, given by $\delta^2\text{H} = 8\delta^{18}\text{O} + 10$, closely describes the observed relationship between $\delta^{18}\text{O}$ and $\delta^2\text{H}$ for amount-weighted annual precipitation worldwide. Based on analysis of weighted monthly precipitation collected at Fort Smith (1962-65), the LMWL for the SRD can be approximated by $\delta^2\text{H} = 6.7\delta^{18}\text{O} - 19.2$ (Birks et al., 2004). Local surface waters that have undergone subsequent evaporation are offset from the LMWL in proportion to their individual water balances, often forming a variably well-defined linear trend (Local Evaporation Line or LEL) having a slope in the range 4-6.

The LEL can also be predicted using the linear resistance model of Craig and Gordon (1965), which accounts for ^{18}O and ^2H build-up in evaporating water bodies, by incorporating appropriate local isotopic and hydroclimatic information (Barnes and Allison, 1983; Gibson and Edwards, 2002; Edwards et al., 2004; Wolfe et al., 2007b). These include the respective $\delta^{18}\text{O}$ and $\delta^2\text{H}$ values of local precipitation and ambient atmospheric moisture, as well as relative humidity and air temperature prevailing during the open-water season. Key reference points along the LEL include the steady-state isotopic

composition for a terminal basin (δ_{SSL}), which represents the special case of a lake at hydrologic and isotopic steady state in which evaporation exactly equals inflow, and the limiting non-steady-state isotopic composition (δ^*), which indicates the maximum potential transient isotopic enrichment of a lake as it approaches complete desiccation (see Appendix A).

As shown in Figure 2.2, the isotopic framework for the SRD includes two alternative LELs to aid in the evaluation of the isotopic evolution of lakewaters during summer 2003. Both LELs are anchored by the estimated amount-weighted mean annual isotopic composition of precipitation (δ_p) and assume the isotopic composition of ambient atmospheric moisture (δ_{AS}) is in approximate isotopic equilibrium with evaporation-flux-weighted summer precipitation (δ_{PS} ; see Gibson and Edwards, 2002). The predicted LEL prevailing under average thaw-season conditions, based on 1971-2000 climate normals measured at Hay River, is described by $\delta^2H = 4.5\delta^{18}O - 63.5$, whereas the predicted LEL for the 2003 thaw season ($\delta^2H = 4.1\delta^{18}O - 69.7$) has a slightly lower slope and more enriched δ_{SSL} and δ^* values because of lower-than-normal relative humidity and higher-than-normal temperature (Table 2.1).

Although the predicted "climate normal" LEL is probably a good indicator of average thaw-season conditions in the SRD, it is clear from the behaviour of several lakes in 2003 that the season-specific LEL provides a more appropriate metric for assessing the isotope hydroclimatology of this particular season. For example, in mid-summer, SD27 is one of a cluster of lakes that plot close to the climate normal δ^* (Figure 2.2), but was not near desiccation when observed in the field. This deviation from the climate normal isotopic framework suggests that SD27, and all other SRD study lakes, evolved isotopically under hydrometeorological conditions that differed from climate normals.

As expected, the isotopic composition of Great Slave Lake ($\delta^{18}O$, $\delta^2H = -17.9\text{‰}$, -142‰) lies close to the reported δ_p value from Fort Smith (Figure

2.2). Because Great Slave Lake is a large, deep lake (surface area = 28400 km², maximum depth = 614 m) (CNCIHD, 1978) with a long residence time, it is probable that its isotopic composition will closely approximate the regional composition of long-term average precipitation and river inputs. Figure 2.2 also identifies predicted vapour forming from Great Slave Lake ($\delta_E - \text{GSL}$), which has a distinct depleted isotopic signature and represents a potential source of atmospheric moisture for the SRD.

Hydrological processes in the slave river delta

The major sources of water for SRD lakes - the Slave River, Great Slave Lake (via seiche events), snowmelt, and summer precipitation - each possess characteristic isotopic signatures (Figure 2.3). This key feature, along with the enrichment effects of evaporation, can be used to identify the hydrological processes that drive changes in SRD lakewater isotope compositions. The relative roles of these hydrological processes on SRD lakes during the 2003 thaw season are described below in the context of expected isotopic trajectories (Figure 2.3). As Figure 2.3 illustrates, a lake's position relative to the reference LEL will vary depending on the relative importance of the various input sources and evaporation.

Flooding and snowmelt

Lakewater samples were collected from SRD lakes on 23-May-03 to evaluate the role of river flooding and snowmelt. Prior to sampling, daily average temperature exceeded 0°C on 15 days in May (Environment Canada, 2004) and the Slave River at Fitzgerald, Alberta, had been ice-free for approximately 11 days (Water Survey of Canada, 2006). These data suggest that the majority of snow- and ice-melt in the SRD occurred within two weeks of sample collection, and minimal isotopic evaporative enrichment of delta lakes took place prior to sampling. Instead, strong flooding and snowmelt signals are evident in several lakes in the 23-May-03 sample set (Figure 2.4a). The $\delta^{18}\text{O}-\delta^2\text{H}$ plot of this dataset clearly shows two clusters of samples – those

that were strongly influenced by river flooding, and those that only received catchment-sourced snowmelt. Flooded sites are more isotopically-depleted than non-flooded sites, and cluster around the Slave River isotopic composition ($\delta^{18}\text{O}$, $\delta^2\text{H} = -19.2\text{‰}$, -152‰), with $\delta^{18}\text{O}$ and $\delta^2\text{H}$ values ranging between -19.2‰ and -17.1‰ and -155‰ and -146‰ , respectively. In contrast, non-flooded sites are more isotopically-enriched than flooded sites and are less strongly clustered ($\delta^{18}\text{O}$ and $\delta^2\text{H} = -16.2\text{‰}$ and -139‰ to -10.6‰ and -122‰), suggesting snowmelt influences on individual lakes were variable. Total inorganic suspended sediment (TSS) data support the interpretation of isotopically-distinct flooded and non-flooded lakes. Flooded lakes with lower $\delta^{18}\text{O}$ signatures contain higher concentrations of TSS, delivered by Slave River floodwaters, compared to non-flooded lakes with higher $\delta^{18}\text{O}$ values (Figure 2.5). Slave River sediment is also discharged in high quantities into Great Slave Lake during the spring melt, resulting in the elevated TSS concentration measured in Great Slave Lake (TSS = 0.016 g L^{-1}).

While river flooding clearly influences early-season isotopic signatures in several SRD lakes, the impact of snowmelt (δ_{snow}) can also be observed in lakewater isotopic compositions. Three SRD lakes (SD2, SD10 and SD38), which all received early spring floodwaters, are equally or more depleted than Slave River water (Figure 2.4a). For example, the $\delta^{18}\text{O}$ ($\delta^2\text{H}$) values of SD2 and the Slave River are -19.2‰ (-155‰) and -19.2‰ (-152‰), respectively. While it is clear from TSS data that SD2 did receive Slave River floodwater (SD2 TSS = 0.1 g L^{-1} ; Figure 2.5), the lake's depleted isotopic signature indicates it was also influenced to a lesser degree by snowmelt ($\delta^{18}\text{O}$ and $\delta^2\text{H}$ range of snow = -21.1‰ to -27.7‰ and -165‰ to -211‰).

Snowmelt influence is also evident in lakes that are more isotopically-enriched than Slave River water. For example, lakes that did not receive Slave River floodwater were drawn below the predicted LEL towards the isotopic composition of snow. Even the most isotopically-enriched lakes sampled on 23-May-03 (SD12, SD33 and SD35) were influenced by snowmelt. During a

September 2002 reconnaissance sampling campaign, those three lakes had the highest isotopic compositions, with $\delta^{18}\text{O}$ ($\delta^2\text{H}$) values of -9.9‰ (-108‰), -10.2‰ (-108‰) and -9.4‰ (-106‰), respectively. On 23-May-03, the $\delta^{18}\text{O}$ ($\delta^2\text{H}$) values of the same three lakes were lowered to -12.2‰ (-123‰), -12.4‰ (-121‰) and -10.6‰ (-112‰) respectively. Plotting of these results in $\delta^{18}\text{O}$ - $\delta^2\text{H}$ space reveals that the trajectory of isotopic depletion between September 2002 and May 2003 was towards the isotopic composition of snow (Figure 2.6; see also Figure 2.3).

The magnitude of river floodwater and snowmelt dilution on May lakewater balances can be estimated using a two-component mixing model incorporating end-of-thaw-season lakewater isotopic composition from 2002, early thaw-season lakewater isotopic composition from 2003 (Figure 2.4a), Slave River or snowmelt isotopic composition (Figure 2.4a), and identification of basins that received river water (Figure 2.4a, Figure 2.5). For example, river floodwater dilution of SD1 (Figure 2.7a) was determined by:

$$1) \text{ \% floodwater dilution} = [(\delta_{\text{SD1 May-03}} - \delta_{\text{SD1 Sep-02}}) / (\delta_{\text{Slave River May-03}} - \delta_{\text{SD1 Sep-02}})] \times 100$$

Similar calculations were performed for lakes that only received snowmelt, such as SD 11 (Figure 2.7b):

$$2) \text{ \% snowmelt dilution} = [(\delta_{\text{SD11 May-03}} - \delta_{\text{SD11 Sep-02}}) / (\delta_{\text{snow}} - \delta_{\text{SD11 Sep-02}})] \times 100$$

Calculations were performed for both $\delta^{18}\text{O}$ and $\delta^2\text{H}$ and average percent dilution values were obtained for each basin. These first-order mass-balance calculations indicate that these flooded basins were diluted from ~70% to as much as 100% by river water. While these estimates do not account for changes in volume nor the added effect of snowmelt input, spatial interpolation suggests that flooding occurred adjacent to the main distributary channels of the Slave River in the active mid- and outer delta zones, with the exception of SD8 (Willow Lake) (Figure 2.8a). The spatial distribution of floodwater, estimated

by the 70% dilution contour, is consistent with field observations and elevated TSS concentrations in lakes situated in the active delta. In this part of the delta, natural levee heights are 0.1-1.5 m above Great Slave Lake water levels (English et al., 1997) and lakes are susceptible to inundation by Slave River floodwaters. Snowmelt dilutions of between ~7 and 35% were calculated for non-flooded sites, located in the older part of the delta where bank levees are greater than 2.5 m in relief (English et al., 1997).

Evaporation

By mid-summer (Figure 2.4c), evaporative isotopic enrichment of every lake as well as the Slave River had occurred. The dominant effect of evaporation was also expressed by increased clustering of lakes along the LEL in the absence of dilution from summer precipitation (Figure 2.4b, c, d; see also Figure 2.3). In fact, seven lakes are shown to exceed δ_{SSL} by 15-Aug-03 indicating non-steady state evaporation (Figure 2.4d), consistent with field observations of lake level drawdown. The four most isotopically enriched lakes, SD12, SD27, SD33 and SD35, were among the shallowest of apex lakes and were not affected by spring flooding.

Increases in lakewater $\delta^{18}\text{O}$ between May and August range from 0.9‰ to 8.4‰ ($\delta^2\text{H} = 5‰$ to 41‰) (Figure 2.8b). The greatest isotopic enrichment occurred in lakes in the apex zone of the delta that lack channel connections to the Slave River and were not affected by spring flooding. In contrast, minimal isotopic enrichment is evident in lakes with direct connections to the Slave River or Great Slave Lake, and in those lakes that were inundated by Slave River floodwaters during the spring melt (Figure 2.8a).

In both the June and July datasets, lakes continue to be separated in $\delta^{18}\text{O}$ - $\delta^2\text{H}$ space, depending on whether they were flooded by the Slave River in the spring (Figure 2.4b, c). Lakes that did not receive Slave River floodwater continue to be more isotopically enriched due to evaporation compared to lakes that were flooded (although some non-flooded lakes still plot below the LEL,

reflecting strong early season snowmelt signals). Direct connections between the Slave River or Great Slave Lake also limit possible evaporative enrichment in delta lakes. For example, in June, July and August, six lakes capable of exchanging water with the Slave River or Great Slave Lake (SD10, SD17, SD28, SD30, SD39 and SD41) generally have lower isotopic signatures than unconnected lakes. The influence of both connectivity and thaw season precipitation on delta lakes will be discussed in more detail in the following sections.

Great Slave Lake-Slave River exchange

Of the six of the lakes sampled in the SRD that can readily exchange water with the Slave River or Great Slave Lake, SD10, SD17, SD28 and SD30 have direct channel connections to the Slave River. SD39 and SD41 are situated on the outer delta, where dominant emergent and aquatic vegetation communities and low levee heights, at or within 0.1 m of low summer Great Slave Lake levels (English et al., 1997), allow mixing of lakewater with that of Great Slave Lake, particularly during high spring water levels and late summer seiche events. All of the six connected lakes behave differently isotopically compared with other delta lakes, reflecting the effects of Slave River or Great Slave Lake exchange on their water budgets.

Spring flooding was mainly concentrated in the mid- and outer delta (Figure 2.8a). Samples from 23-May-03 show that connected lakes in this area of the delta (SD10, $\delta^{18}\text{O}$ and $\delta^2\text{H} = -18.9\text{‰}$ and -154‰ ; SD39, $\delta^{18}\text{O}$ and $\delta^2\text{H} = -18.7\text{‰}$ and -152‰) are isotopically similar to the Slave River ($\delta^{18}\text{O}$ and $\delta^2\text{H} = -19.2\text{‰}$ and -152‰) and Great Slave Lake ($\delta^{18}\text{O}$ and $\delta^2\text{H} = -17.5\text{‰}$ and -144‰) (Figure 2.4a). SD41, a third connected lake in the active delta, was submerged under Great Slave Lake during the spring of 2003 and no water sample was collected. Its isotopic signature is assumed to be identical to that of Great Slave Lake. SD30 (Ring Lake), a partially cut-off meander of the Slave River located in the apex zone of the delta, is isotopically similar to outer delta lakes, with an isotopic signature of -18.4‰ for $\delta^{18}\text{O}$ and -151‰ for $\delta^2\text{H}$. The persistent

channel connection between SD30 and the Slave River allows ample mixing between the two. SD17 and SD28 are also both situated in the apex zone of the SRD, but have longer, narrower channel connections to the Slave River than SD30. Despite their channel connections, these two lakes are more isotopically-enriched than the Slave River during the spring melt, with $\delta^{18}\text{O}$ and $\delta^2\text{H}$ values of -17.4‰ and -145‰ and -17.0‰ and -141‰, respectively. The isotopic signatures of SD17 and SD28 indicate that penetration by Slave River floodwater was less significant than in other connected lakes, a likely consequence of both the length and depth of the connecting channel and the spatial distribution of flooding.

Later in the thaw season, evaporative isotopic enrichment is severely suppressed in lakes capable of exchange with Slave River or Great Slave Lake water (Figure 2.4c). On 25-Jul-03, the Slave River had a $\delta^{18}\text{O}$ ($\delta^2\text{H}$) value of -18.1‰ (-145‰), while that of SD30 was -17.7‰ (-144‰). SD30 maintains its channel connection with the Slave River throughout the thaw season and receives a continual input of Slave River water. SD10, SD39, and SD41, lakes in the active delta with very low isotopic signatures during the spring thaw, continue to be more isotopically-depleted than all other lakes ($\delta^{18}\text{O}$ and $\delta^2\text{H}$ = -16.6‰ and -142‰, -16.4‰ and -138‰, and -16.6‰ and -139‰, respectively), indicating periodic input of isotopically-depleted Slave River or Great Slave Lake water, possibly through seiche events during the summer. On 25-Jul-03, apex lakes SD17 and SD28 have $\delta^{18}\text{O}$ ($\delta^2\text{H}$) values of -15.1‰ (-136‰) and -14.6‰ (-130‰), similar to non-connected, flooded lakes in the outer delta (Figure 2.4c). The isotopic compositions of SD17 and SD28 indicate inputs of Slave River water have been restricted since the spring flood, possibly by declining water levels in the Slave River following the flood peak. Field observations also indicate that emergent vegetation was growing in the channels of SD17 and SD28 at the time of sampling, further impeding Slave River inflow. Consequently, while these lakes continue to be more isotopically-

depleted than nearby, unconnected apex zone lakes, SD17 and SD28 undergo more evaporative enrichment than other connected lakes in the SRD.

By 15-Aug-03, a strong distinction exists between lakes that have a direct connection with the Slave River or Great Slave Lake and those that do not (Figure 2.4d). Outer delta lakes SD39 and SD41 are among the most isotopically-depleted water bodies sampled, with $\delta^{18}\text{O}$ ($\delta^2\text{H}$) values of -17.4‰ (-140‰) and -16.5‰ (-137‰), respectively. It is probable that seiche events, which occur most frequently during the late summer and early autumn (Gardner et al., 2006), facilitate water exchange between Great Slave Lake ($\delta^{18}\text{O}$ and $\delta^2\text{H}$ = -17.4‰ and -141‰) and SD39 and SD41. SD30 and SD10 also continue to receive river water during the late summer. Because of its river connection, SD30 maintains low $\delta^{18}\text{O}$ ($\delta^2\text{H}$) values of -17.5‰ (-145‰), similar to those of the Slave River ($\delta^{18}\text{O}$ and $\delta^2\text{H}$ = -17.6‰ and -142‰). SD10 ($\delta^{18}\text{O}$ and $\delta^2\text{H}$ = -15.9‰ and -138‰) has a narrower direct connection to a major distributary channel in the active delta, limiting its evaporative enrichment. Because of their open hydrologic status, evaporative isotopic enrichment in SD10, SD30, SD39 and SD41 has been minimal. Consequently, these lakes are separated in $\delta^{18}\text{O}$ - $\delta^2\text{H}$ space from lakes that are not directly connected to the distributary channel network and for which evaporative enrichment over the course of the thaw season is significant. SD17 and SD28 continue to undergo evaporative enrichment as restrictions in channel connections persist and limit the influence of Slave River inflow on the water balances of these two lakes. As a result, their isotopic signatures ($\delta^{18}\text{O}$ and $\delta^2\text{H}$ = -14.2‰ and -131‰ and -14.6‰ and -128‰, respectively) are similar to those of the most isotopically-depleted, non-connected, flooded lakes in the active outer and mid-delta (Figure 2.4d).

Thaw season precipitation

The regional sampling campaigns carried out in the SRD offer no strong evidence of lakewater isotopic depletion due to thaw season precipitation, in the form of the expected trajectory of a delta lake towards summer precipitation composition (δ_{PS} ; Figure 2.3). This observation is consistent with below normal

precipitation during the first three months of the thaw season (Figure 2.9) and 15-Aug-03 results, which indicate that all lakes incapable of exchanging water with the Slave River or Great Slave Lake were more isotopically-enriched than δ_{PS} ($\delta^{18}O$, $\delta^2H = -17.0\text{‰}$, -132‰ ; see Figure 2.3). While precipitation during the month of August exceeded climate normal conditions, the majority of August rain fell after the 15-Aug-03 sampling campaign (59.6 mm).

However, the results of samples collected from four lakes (SD2, SD15, SD29 and SD33) after 15-Aug-03 illustrate the isotopic responses of delta lakes to thaw season precipitation. Sampling conducted between May and August demonstrates that these four lakes became progressively more evaporatively enriched over the course of the summer. Samples collected on 03-Sep-03, however, show a strong reduction in lakewater isotopic signatures in response to late season precipitation (Figure 2.10). Precipitation-induced isotopic depletion at SD2, SD15, SD29 and SD33 between 15-Aug-03 and 03-Sep-03 ranges from -2.5‰ to -9.8‰ for $\delta^{18}O$ and -9‰ to -40‰ for δ^2H .

Between 15-Aug-03 and 03-Sep-03, 39 mm of rain were recorded at Hay River (Environment Canada, 2002), although an unusual snow event was reported by residents of Fort Resolution on 01-Sep-03. A lake effect storm, with precipitation derived from Great Slave Lake vapour ($\delta_E -_{GSL}$; see Figure 2.2), would produce snow that is more isotopically depleted than typical SRD summer precipitation (δ_{PS} ; $\delta^{18}O$, $\delta^2H = -17.0\text{‰}$, -132‰). For example, snow sampled during a lake effect storm in the SRD in September 2002 had an isotopic composition that plotted above the LMWL (Figure 2.10). Because SD15 is a relatively deep (~ 4 m), sinuous lake, a sample collected from the margin of the lake could reflect the isotopic composition of the storm's snow, rather than the average isotopic composition of the lake itself. Such a storm would be capable of producing the depletion trajectories observed in the other three sampled lakes (Figure 2.10). Assuming the lakewater sample from SD15 reflects the isotopic composition of the storm's precipitation, it is possible to estimate the maximum amount of storm-sourced water in each lake at the time

of sampling. For example, at SD33, up to 20% of the lake may have been made up of precipitation from the storm at the time of sampling, encompassing both precipitation falling directly on the lake and runoff from the catchment. At SD29, snowfall may have made up 10% of the lake's water at the time of sampling. Comparably, isotopic depletion at shallow SD33 ($\delta^{18}\text{O}$, $\delta^2\text{H} = -16.7\text{‰}$, -138‰) is more significant than that of deeper SD29 ($\delta^{18}\text{O}$, $\delta^2\text{H} = -11.2\text{‰}$, -118‰). A wide grass fringe may have captured some of the catchment-sourced runoff at SD29 and prevented it from mixing completely with lakewater. In contrast, a terrestrial meadow surrounding SD33 may have promoted runoff into the lake, where no emergent vegetation fringe prevented mixing between runoff and lakewater. At SD2, Slave River influences may have contributed to the lake's late season water balance, and drawn the isotopic composition of that lake below the LEL. While the degree of depletion in response to this late season precipitation varies between lakes and is related to lake surface area and volume, catchment characteristics, and likely also spatial variations in the intensity, duration and isotopic composition of rainfall and snowfall, their isotopic responses are comparable. As these lakes span both the mid- and apex zones of the delta, it is likely that other unconnected lakes across the delta responded isotopically in a similar manner.

Discussion

The isotopic evolution of lakes in the SRD has been evaluated against an isotopic framework based on flux-weighted climate data from the 2003 thaw season. The isotopic framework used in this study is based on climate data specific to the year of sampling, thus the hydroclimatic conditions under which lakes evolved are inherently included in the framework. In 2003, average thaw season temperature and relative humidity differed from climate normals, particularly during the months of July and August when potential evaporation is greatest (Figure 2.9). The results of these deviations were a decrease of 6.4% in flux-weighted relative humidity and an increase of 2°C in flux-weighted temperature during the thaw season as compared to climate normal conditions.

Accordingly, δ_{SSL} and δ^* values were higher in $\delta^{18}O$ by 1.5‰ ($\delta^2H = 5‰$) and 3.6‰ ($\delta^2H = 14‰$) compared to calculations using climate normal values (Table 2.1). Consequently, in 2003 SRD lakes had the potential to become more isotopically enriched than they would under climate normal conditions. Assuming climate normal conditions appropriately represent the hydroclimatic conditions under which a lake evolves over the course of a thaw season may thus under- or over-estimate potential evaporative enrichment and result in the calculation of inappropriate δ_{SSL} and δ^* values. In this case, using a year-specific isotopic framework significantly improves semi-quantitative assessments of lakewater balance conditions. The 2003-specific framework is strongly supported by the isotopic compositions of Great Slave Lake and the most isotopically-enriched lakewater sample (SD27; Figure 2.2). The tight clustering of mid-summer lakewater isotopic compositions along the predicted LEL, when thaw season precipitation was minimal, provides further support for the framework, including the estimated value for δ_{AS} (Figure 2.4c, d; Figure 2.10).

Using an isotopic framework based on summer 2003 climate data, evaluations of SRD lakewater isotopic compositions during the 2003 thaw season reveal that the relative influence of hydrological processes in the delta varied spatially and over time. River flooding during the spring ice break-up was the dominant input into mid- and outer delta lakes, while apex lakes were not affected by spring flooding. In contrast, catchment-sourced snowmelt affected all delta lakes. While snowmelt input varied with lake catchment size and presumably with spatial variations in snowpack depth and density, it was the dominant input to apex lakes during the spring. Snowmelt input played a less important role in lakes affected by river flooding, probably because a greater volume of floodwater versus snowmelt entered each flooded lake.

As the thaw season progressed, evaporation became the dominant factor controlling lakewater isotopic signatures across the delta. However, the degree of evaporative enrichment in SRD lakes varied. Evaporative enrichment was

greater in lakes that were not flooded by the Slave River during the spring melt compared to lakes that were. Lakes capable of exchange with the Slave River or Great Slave Lake were minimally affected by evaporation. Evaporative enrichment following ice break-up was therefore partially controlled by the nature and spatial distribution of spring flooding, the degree of snowmelt influence on each lake, and the strength of connections with the distributary channel network and Great Slave Lake. By late in the thaw season, evaporative enrichment blurred the distinction between flooded and non-flooded lakes, and was the dominant process controlling most lakewater balances. However, in lakes that are connected, exchange with Great Slave Lake or the Slave River governed lakewater isotopic signatures. While results from the 2003 sampling campaigns were not capable of showing SRD-wide effects of thaw season precipitation on delta lakes, evidence from selected lakes suggests that during a very wet season precipitation in the SRD would have the capacity to significantly affect lakewater isotopic signatures and play a potentially significant role in maintaining lakewater balances across the entire delta.

A lake's geographic position in the delta is a major determinant of the relative roles of river flooding, snowmelt, evaporation and Slave River or Great Slave Lake exchange on lakewater balances. Isotopic evolution of lakes in the active part of the delta was most strongly controlled by spring flooding until late in the thaw season, when evaporative enrichment dominated. Lakes in the apex zone of the SRD were affected by spring snowmelt, and by early summer, in the absence of significant summer precipitation, the dominant process controlling their lakewater balances was evaporation. For lakes in direct communication with the Slave River or Great Slave Lake, exchange between the lake basin and external water dominated its water balance conditions throughout the thaw season.

While biogeographical zones developed for the SRD by English et al. (1997) do reflect the variability observed in the isotopic evolution of SRD study lakes, a hydrologically-based classification scheme for delta lakes is a more

appropriate frame of reference from which to describe SRD hydrology. This study has revealed that levee height, and consequently flood susceptibility, is not the only factor governing SRD lakewater balances. Based on the data presented here, three hydrologic classes of lakes can be identified in the SRD based on dominant hydrologic inputs and outputs in 2003 (Table 2.2): 1) flood-dominated lakes in the active part of the delta; 2) evaporation-dominated lakes in the apex zone of delta; and 3) Great Slave Lake and Slave River-exchange dominated lakes in the active delta and along the Slave River (Figure 2.11). Late-season isotope data also indicate that precipitation inputs to evaporation-dominated lakes have the potential to significantly affect lakewater balances, and thus in very wet summers, precipitation inputs could dominate lakewater balances in many delta lakes. Redefining the classification of SRD lakes based on the three categories described above incorporates the strongest influences on lakewater balances observed during the 2003 thaw season and emphasizes that local snowmelt input is an important contributor to maintaining lakewater balances in the older delta.

SD8 (Willow Lake) provides an excellent example of the appropriateness of this improved classification scheme. SD8 falls in the mid-delta biogeographical zone, and consequently would be expected to flood every five to seven years (Prowse et al., 2002a). However, unlike other mid-delta lakes, SD8 was not flooded in the spring of 2003 (Figure 4a). Based on the hydrologically-based classification scheme developed here, SD8 is considered an evaporation-dominated lake, rather than a flood-susceptible mid-delta lake. The channel next to SD8 was historically a major distributary channel in the delta, before shifts in flow patterns reduced its discharge. As a result of former high flows in the channel adjacent to SD8, levees were built up to heights that now impede flooding. As flow in the channel adjacent to SD8 declined, possibly in association with a major eastward shift in flow to the ResDelta channel beginning in 1966 (Gibson et al., 2006a), the susceptibility of SD8 to Slave River distributary flooding has been greatly reduced. Currently, SD8 is evaporation-dominated (Figure 2.11), and flooding no longer plays a prominent

role in its water balance, as was suggested by the former biogeographical classification.

Using this new hydrologically-based classification scheme, preliminary assessments and predictions of hydrological change in response to variations in climate or alterations of the river regime can be made. For example, a change in the magnitude or frequency of spring flooding will have the greatest effect on flood-dominated lakes. Increases or decreases in relative humidity or temperature will have the most significant effects on evaporation-dominated lakes. In very wet summers, precipitation inputs may dominate the water balances of lakes classed here as evaporation-dominated. Exchange-dominated lakes will be most affected by increases or decreases in Slave River flows during the thaw season or by changes in the frequency or magnitude of Great Slave Lake seiche events. Warmer, drier climate conditions and reduced flood frequency may cause flood-dominated lakes to behave hydrologically like evaporation-dominated lakes, while the latter may desiccate.

It is important to note that the classification scheme described above is based on one season of sampling and the intensity of spring flooding, snowpack depth and density, and thaw season relative humidity, temperature and precipitation will vary from year to year. For example, a 46-year discharge record for the Slave River (Figure 2.12) shows peak discharge during spring 2003 ($5370 \text{ m}^3 \text{ s}^{-1}$) is equivalent to average peak discharge ($5391 \text{ m}^3 \text{ s}^{-1}$) measured over the period of record (Water Survey of Canada, 2006). Discharge conditions measured in 2003 were met or exceeded during 24 of the spring seasons monitored, while discharge was less than that of 2003 on 22 occasions. During years in which discharge is low, spring flooding is reduced or absent, and climatic conditions are similar to those that prevailed during 2003, isotopic enrichment from evaporation would dominate the water balances of all unconnected SRD lakes, including those classed here as flood-dominated. In years with large ice jams, spring flooding may be more widespread than that of 2003. Winters with deep snowpacks or rapid spring melting may increase the

influence of catchment-sourced snowmelt on delta lakes. Variations in relative humidity and temperature during the thaw season may also affect the amount of evaporative enrichment a lake may undergo over the course of the thaw season. Alternatively, wet summers may suppress potential evaporation in delta lakes.

Summary and Future Directions

Analysis of water isotope tracers, supplemented by measurement of total inorganic suspended sediment, provides insight into hydrological processes that controlled SRD lakewater balances during the 2003 thaw season. Results differentiate the relative roles of flooding from the Slave River, exchange with Great Slave Lake, snowmelt, and thaw season precipitation as input sources, as well as evaporative loss. Distinguishing hydrological characteristics in our survey are used to identify three lake types in the SRD. The water balances of *flood-dominated lakes* in the active delta were strongly influenced by floodwater derived from the Slave River during the spring melt. The hydrological impact of spring flooding in these lakes persisted well into mid-summer, off-setting the isotopic effects of evaporation. *Evaporation-dominated lakes* in the apex zone of the delta received snowmelt input in the spring, but evaporation rapidly became the over-riding process controlling lakewater balances by early summer. Late season precipitation also played a strong role in the water balances of selected evaporation-dominated lakes. *Exchange-dominated lakes* along the fringes of the outer delta and adjacent to the upstream reaches of the Slave River possessed variable water balances throughout the thaw season, determined mainly by the strength of connection arising from Great Slave Lake seiche events or Slave River inflow. Notably, while our results confirm that flooding from the Slave River is an important supplier of water to the active delta (English et al., 1997; Prowse et al., 2002a), this study has revealed that snowmelt input is a key contributor to maintaining lakewater balances in the older apex zone of the delta, and is also likely a key water source to lakes in the active delta during years in which no flooding occurs.

Results from this initial survey highlight the utility of water isotope tracers as an efficient, semi-quantitative approach for examining the behaviour of lakewater balances with respect to a range of hydrological processes over a broad fluvial-deltaic landscape. Thus, a solid foundation has been developed to characterize inter-annual variability in lakewater balances from isotopic measurements obtained over multiple years, and to assess the impact of variable hydroclimatic conditions. These subsequent analyses will also have implications for contemporary hydroecological studies in the SRD, and will provide important constraints for ongoing multi-proxy paleolimnological investigations. Collectively, insights gained will contribute to understanding both contemporary water balance conditions and the evolution of hydroecological conditions in the SRD, necessary for anticipating future hydroecological trajectories in the context of hydroclimatic variability and change.

Figures

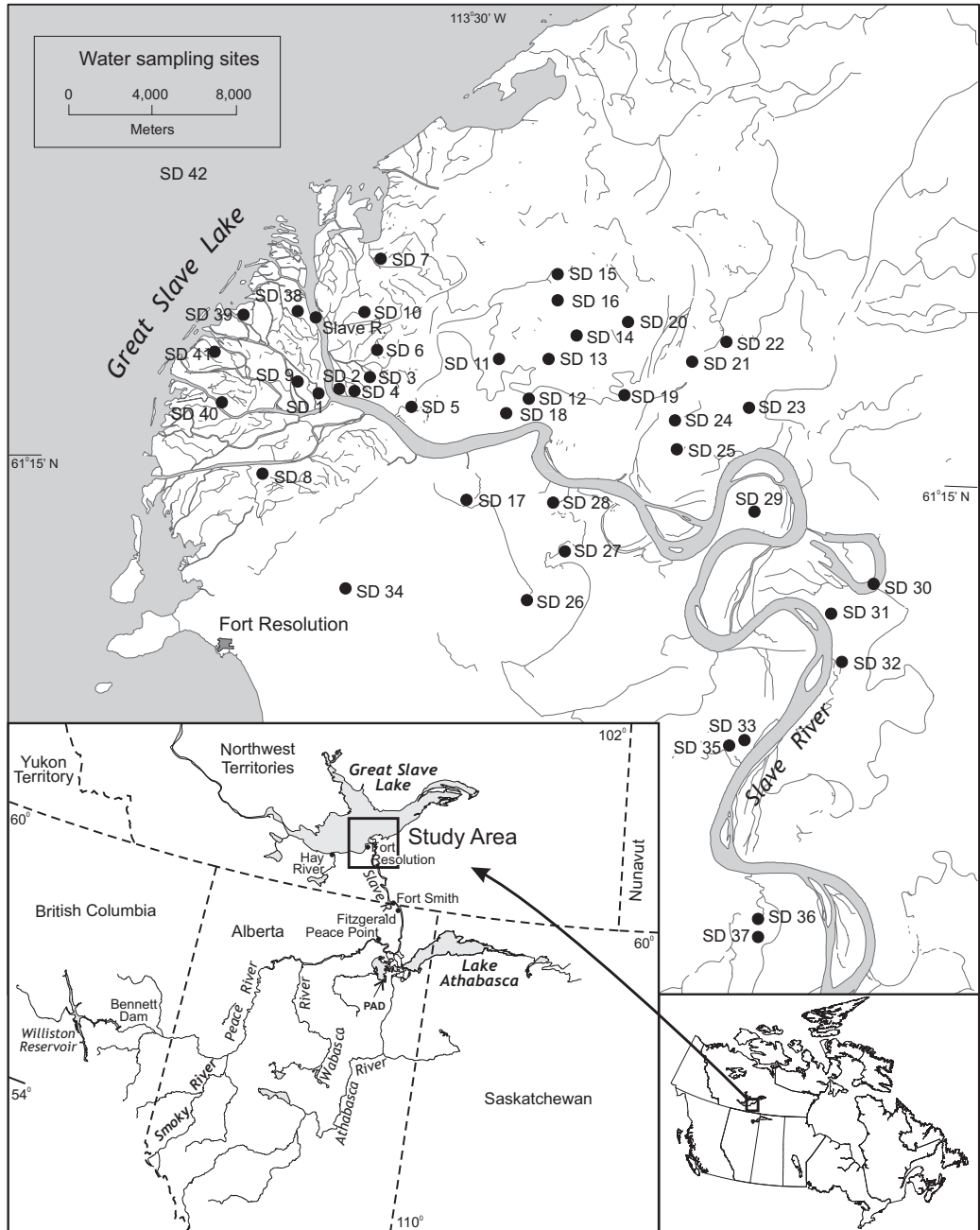


Figure 2.1. Location of the Slave River Delta, NWT, including lake and river sampling sites.

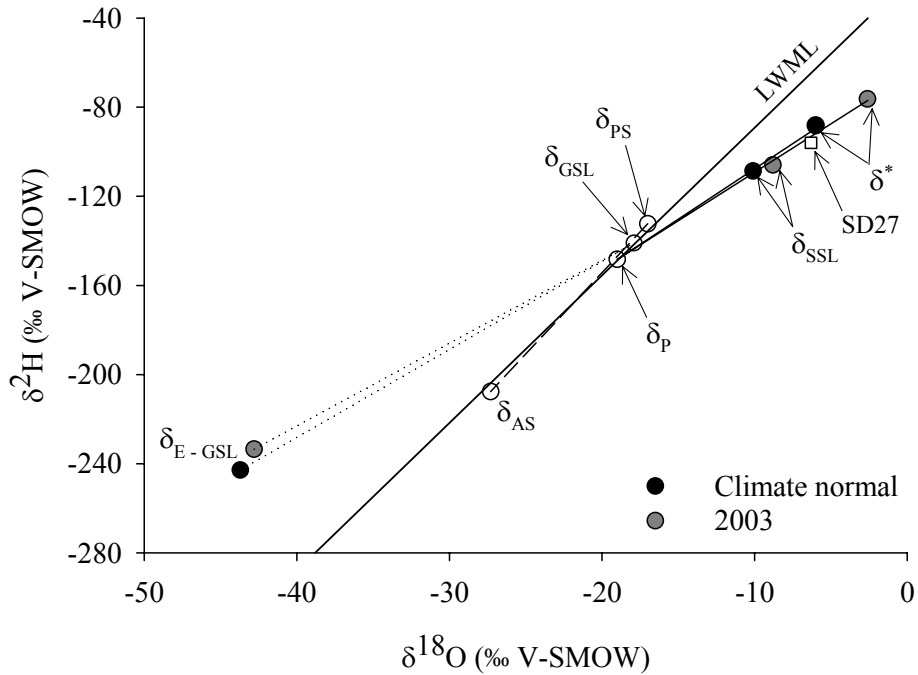


Figure 2.2. Samples collected on 25-Jul-03 from Great Slave Lake (δ_{GSL} , the most isotopically-depleted lake at the time of sample collection) and SD27 (the most isotopically-enriched lake at the time of sample collection) superimposed on the climate normal and 2003 isotopic frameworks, showing the isotopic composition of amount-weighted mean annual (1962-1965) precipitation (δ_{P}) from Fort Smith, NWT (Birks et al., 2004), the isotopic compositions of evaporation-flux-weighted thaw season precipitation (δ_{PS} ; Gibson and Edwards, 2002) and atmospheric moisture (δ_{AS}), the steady state isotopic composition of a terminal basin (δ_{SSL}), the limiting isotopic composition (δ^*), and the isotopic composition of Great Slave Lake vapour ($\delta_{\text{E-GSL}}$).

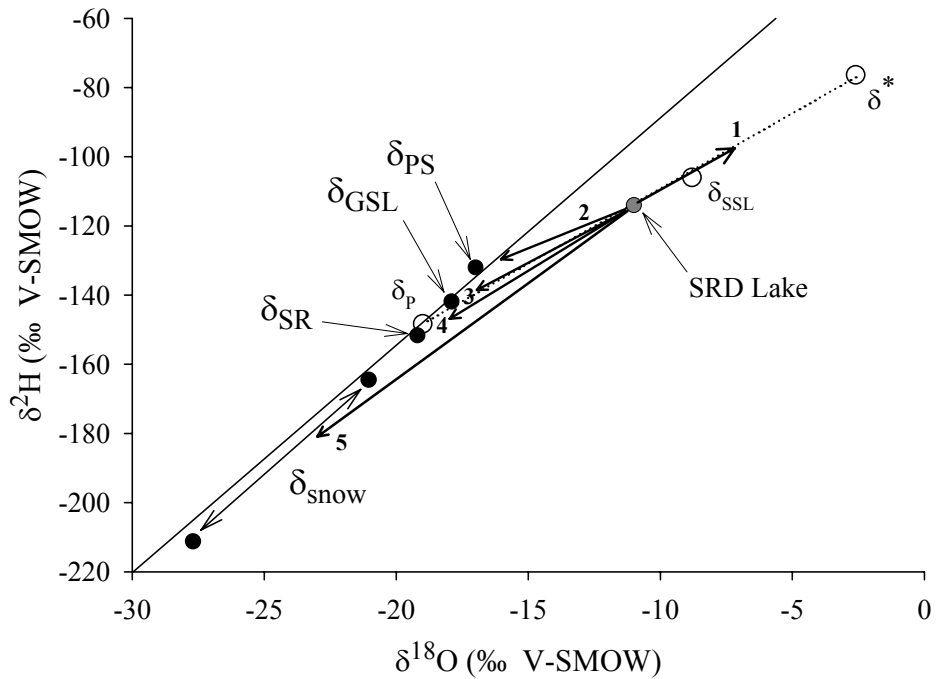


Figure 2.3. Potential isotopic trajectories of a theoretical SRD lake in response to 1) evaporation, 2) thaw season precipitation (δ_{PS} ; Gibson and Edwards, 2002), 3) Great Slave Lake (δ_{GSL}) exchange, 4) Slave River (δ_{SR}) flooding and 5) snowmelt (δ_{snow}) input, superimposed on the 2003 isotopic framework (see Figure 2). Isotopic framework parameters are shown as open circles. In this example, the theoretical lake is shown to plot on the Local Evaporation Line (LEL) indicating the lake is fed by water of isotopic composition similar to mean annual precipitation.

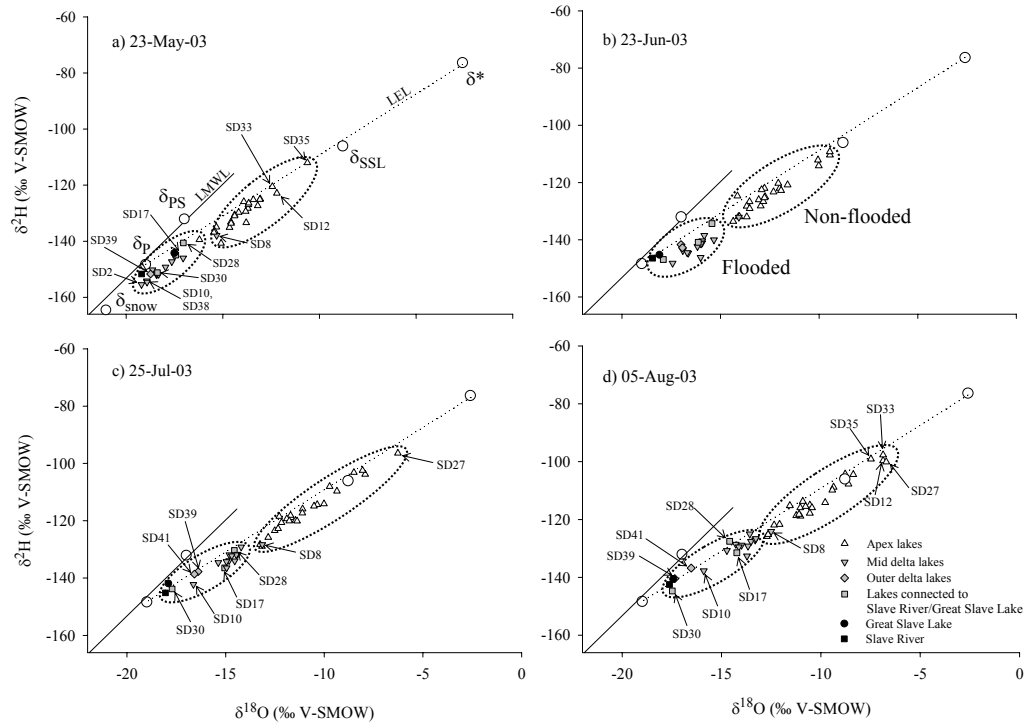


Figure 2.4. Results of Slave River Delta (SRD) regional sampling campaigns conducted on a) 23-May-03, b) 23-Jun-03, c) 25-Jul-03 and d) 15-Aug-03. The isotopic compositions of all SRD lakes sampled are superimposed on the 2003 climate isotopic framework (see Figure 2). Lakes identified by name in the text are labeled. Flooded and non-flooded clusters of lakes are circled with a dashed line, and are labeled in b). Isotopic framework parameters are shown as open circles.

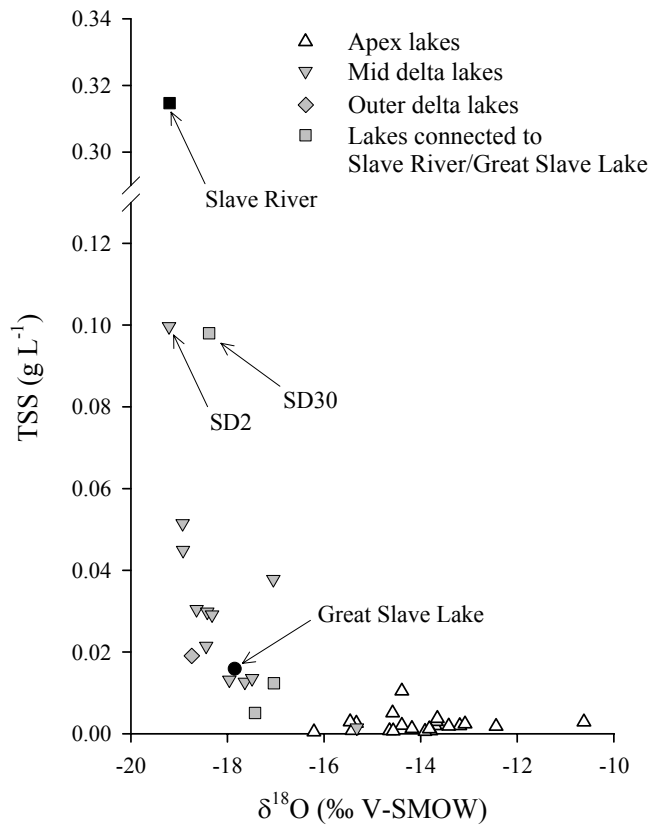


Figure 2.5. Total inorganic suspended sediment (TSS), expressed in g L^{-1} , in SRD lakes from water samples collected on 23-May-03. Lakes that have high TSS concentrations were flooded by the Slave River during the spring thaw, while lakes that were not flooded by the Slave River have low TSS concentrations.

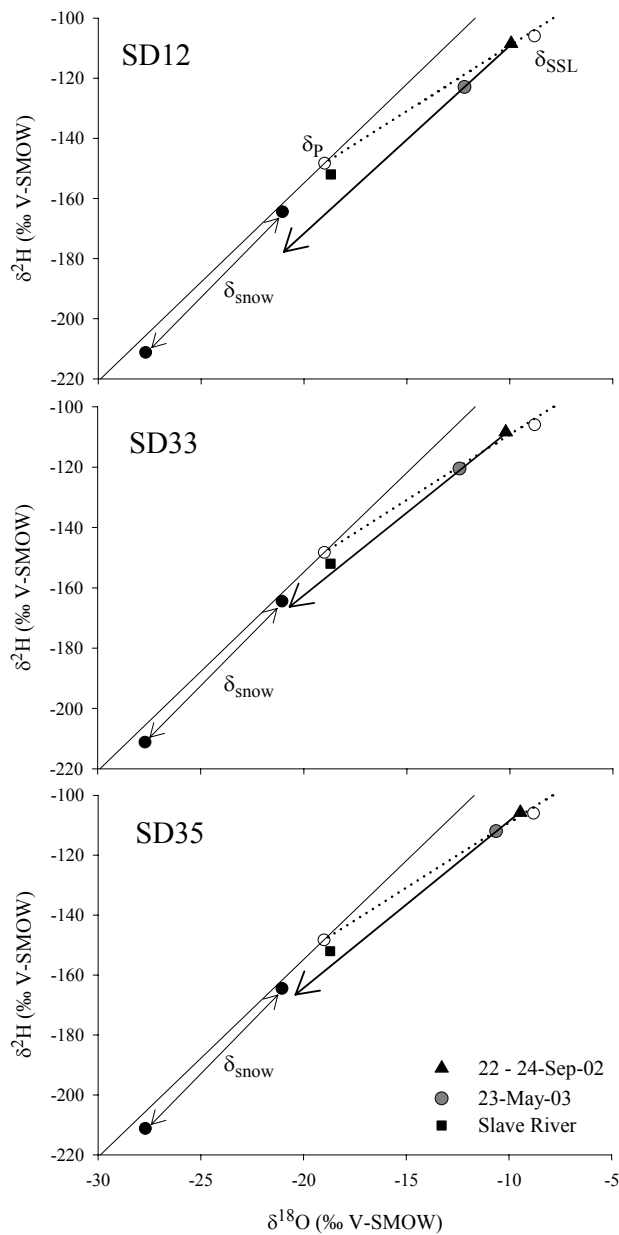


Figure 2.6. Depletion trajectories of non-flooded lakes SD12, SD33 and SD35 between Sep-02 and May-03 are towards the isotopic composition of snow (δ_{snow}), in response to an influx of catchment-sourced snowmelt during spring melt period. Isotopic compositions are superimposed on the 2003 climate isotopic framework (see Figure 2). Isotopic framework parameters are shown as open circles.

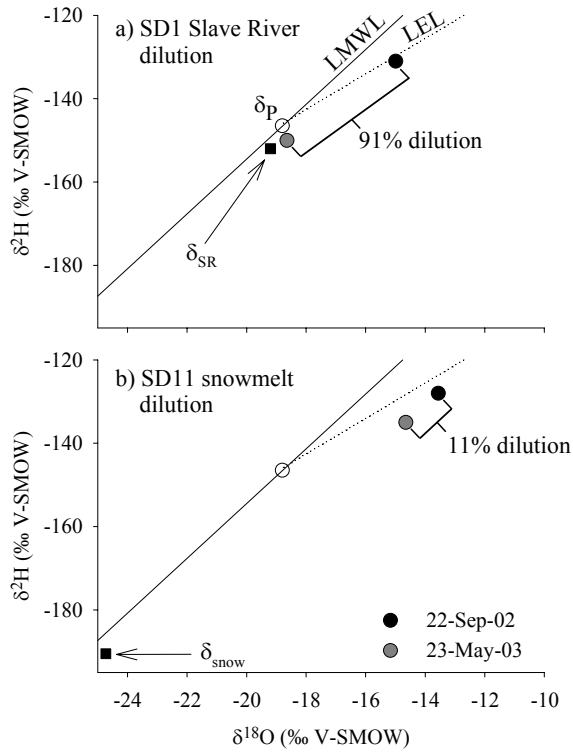


Figure 2.7. Examples showing dilution percentage estimates for a) SD1, an apex lake flooded by the Slave River (δ_{SR}) in May-03, and b) SD11, a lake in the apex zone of the delta that received exclusively snowmelt input (δ_{snow}) during the spring melt. Snowmelt dilution is calculated using an average snowmelt value ($\delta^{18}\text{O}$, $\delta^2\text{H}$ = -24.7‰, -191‰). Isotopic compositions are superimposed on the 2003 climate isotopic framework (see Figure 2).

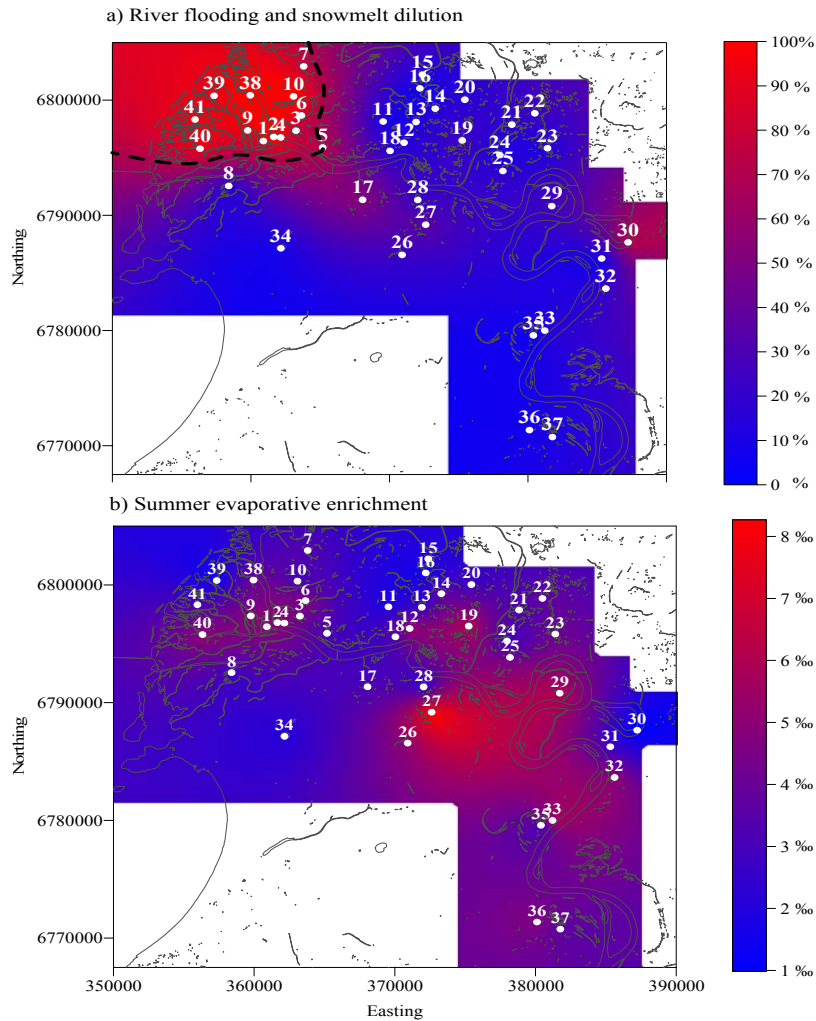


Figure 2.8. The spatial extent of a) river flooding and snowmelt dilution and b) summer evaporative enrichment in lakes in 2003 interpolated using data from Figure 4. In a), two-component mixing indicates that flooding occurred in areas adjacent to the main distributary channels of the Slave River in the mid- and outer portions of the active delta (mapped as red areas). Elsewhere, lakes received exclusively snowmelt in the spring (mapped as mainly blue areas). The observed spatial extent of flooding corresponds with the 70% dilution contour, shown as a black contour. Summer isotopic enrichment in b) represents enrichment in ^{18}O (‰) between 23-May-03 and 15-Aug-03.

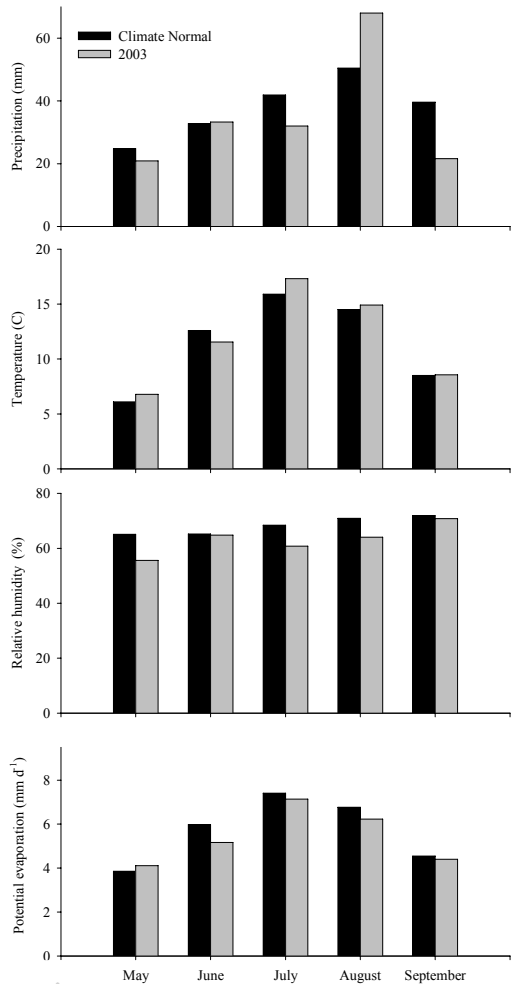


Figure 2.9. Monthly distribution of total thaw season precipitation, average temperature, average relative humidity and potential evaporation for 2003 in comparison to climate normal values (1971-2000) for Hay River, NWT (Environment Canada, 2002).

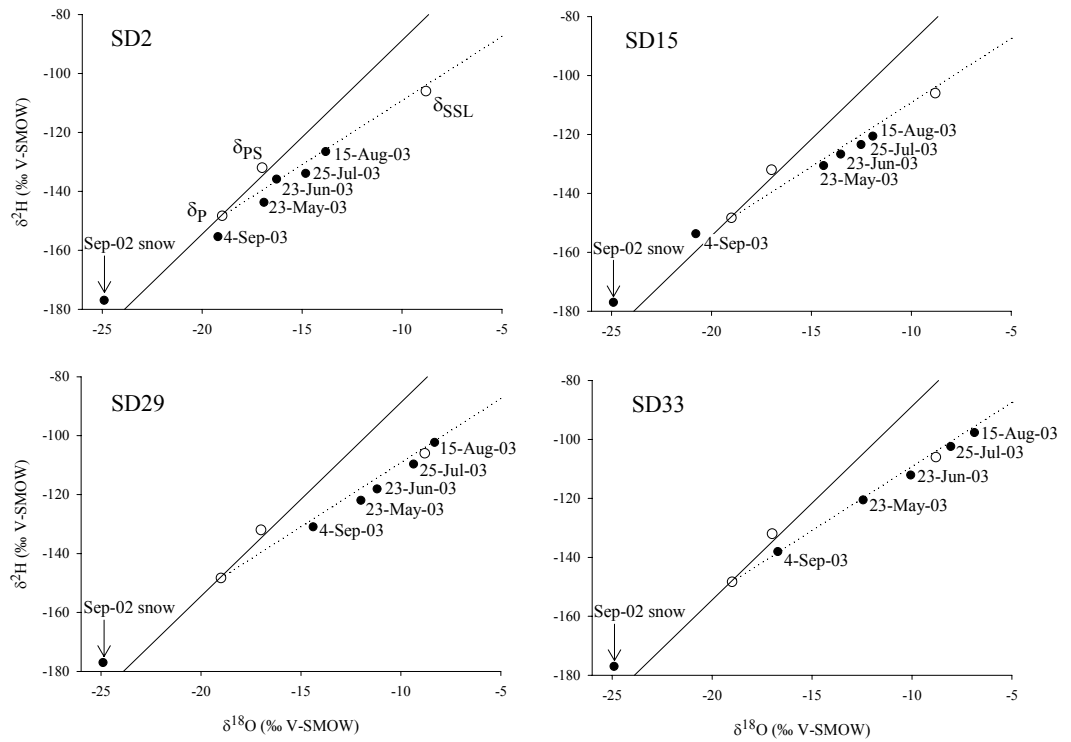


Figure 2.10. Isotopic evolution of four SRD lakes (SD2, SD15, SD29 and SD33) during the 2003 thaw season, showing evaporative enrichment prior to 15-Aug-03 and subsequent isotopic depletion in response to 39 mm of late season precipitation between 15-Aug-03 and 3-Sep-03. Isotopic compositions are superimposed on the 2003 climate isotopic framework (see Figure 2). Isotopic framework parameters are shown as open circles.

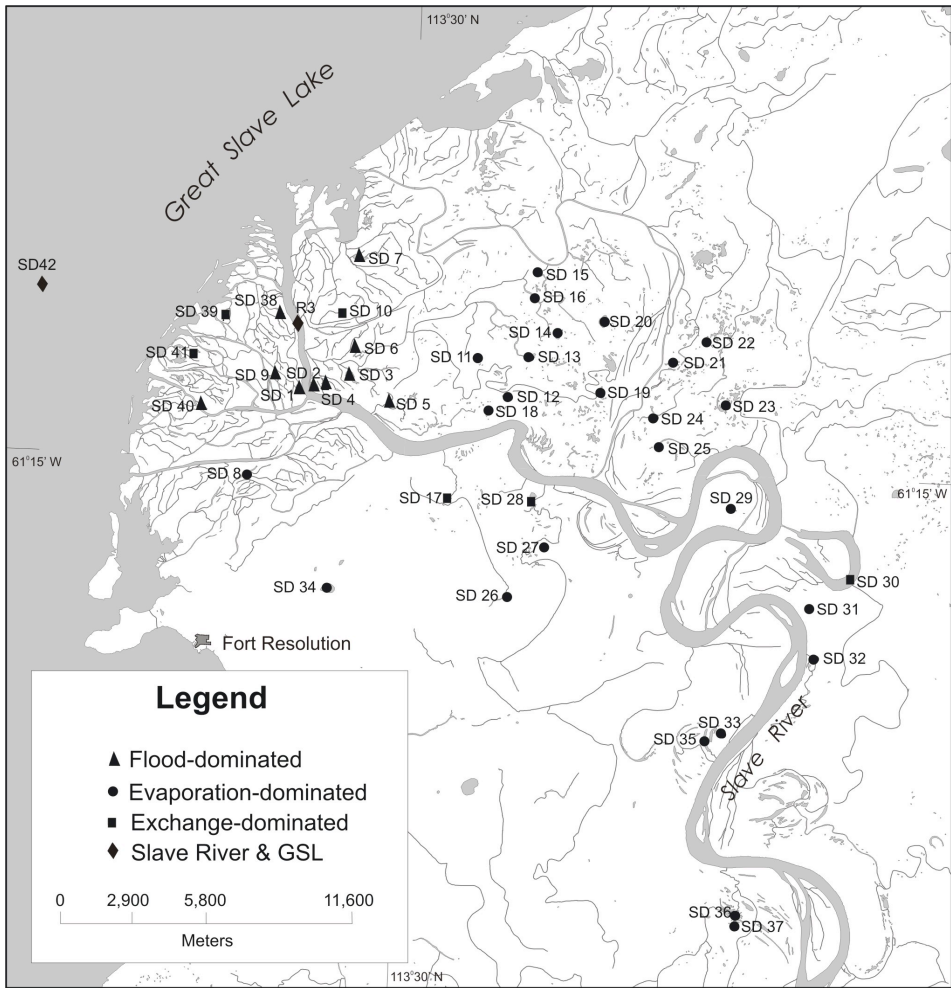


Figure 2.11. SRD lakes classified based on dominant hydrologic inputs and outputs during the 2003 thaw season.

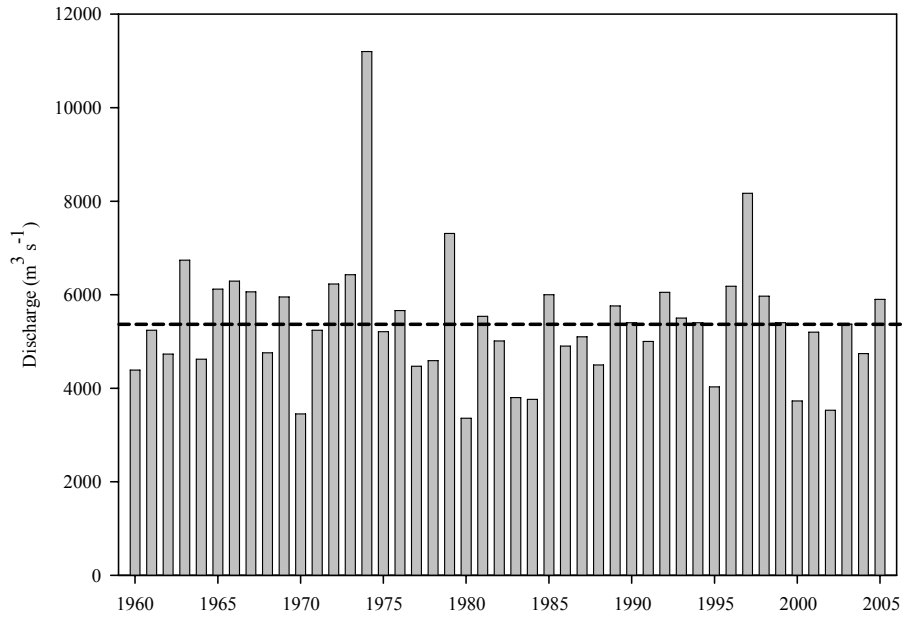


Figure 2.12. Peak Slave River discharge during the spring melt period, measured between 1965-2005 at Fitzgerald, AB (Water Survey of Canada, 2006). The dashed line represents peak discharge measured in the spring of 2003.

Tables

Table 2.1. Isotopic framework parameters are derived using flux-weighted thaw season climate data from Hay River (Environment Canada, 2002, 2004) and Equations 6, 7, 9 and 10 in Appendix A.

	Climate normal	2003
$\delta^{18}\text{O}_{\text{SSL}}, \delta^2\text{H}_{\text{SSL}} (\text{‰})$	-10.1, -109	-8.8, -106
$\delta^{18}\text{O}^*, \delta^2\text{H}^* (\text{‰})$	-6.0, -88	-2.6, -76
$\delta^{18}\text{O}_{\text{E-GSL}}, \delta^2\text{H}_{\text{E-GSL}} (\text{‰})$	-43.7, -243	-42.8, -234
LEL	4.5 $\delta^{18}\text{O}$ - 63.5	4.1 $\delta^{18}\text{O}$ - 69.7
h (%)	69.2	62.8
T (°)	11.4	13.4

Table 2.2. Hydrologic inputs and outputs from lakes in the SRD, based on hydrologically-inferred zonation, where R = river inputs during elevated (spring flood) flow conditions (R_F) and normal summer flow conditions (R_N), S = catchment-sourced snowmelt inputs, P = thaw season precipitation, O = surface outflow during elevated (spring flood) flow conditions (O_F) and normal summer flow conditions (O_N), and E = surface water evaporation. Dominant processes are shown in bold. The role of groundwater in lakewater balances is likely minimal, as the SRD is situated in a zone of discontinuous permafrost and lowland drainage is generally poor (Day, 1972).

	SRD ZONE		
	Flood-dominated	Evaporation-dominated	Exchange-dominated
Inputs	$R_F + S + P$	$S + P$	$R_F + R_N + S + P$
Outputs	$O_F + \mathbf{E}$	E	$O_F + O_N + E$

Table 2.3. All values used for calculations of the isotopic framework for the 2003 thaw season, with references and equation numbers where appropriate.

	Value	Data Source	Equation
h (%)	62.8	Environment Canada (2002)	
T (°C)	13.4		
$\alpha^*_{L-V} (^{18}\text{O}, ^2\text{H})$	1.0104, 1.0925		1, 2
$\varepsilon^*_{L-V} (^{18}\text{O}, ^2\text{H}) (\text{‰})$	10.4, 92.5		3
$\varepsilon_K (^{18}\text{O}, ^2\text{H}) (\text{‰})$	5.3, 4.7		4, 5
S	4.1		6
d	-69.7		7
$\delta^{18}\text{O}_{AS}, \delta^2\text{H}_{AS} (\text{‰})$	-27.3, -208		8
$\delta^{18}\text{O}^*, \delta^2\text{H}^* (\text{‰})$	-2.6, -76		9
$\delta^{18}\text{O}_{E-GSL}, \delta^2\text{H}_{E-GSL} (\text{‰})$	-42.8, -234		10
$\delta^{18}\text{O}_{SSL}, \delta^2\text{H}_{SSL} (\text{‰})$	-8.8, -106		
$\delta^{18}\text{O}_P, \delta^2\text{H}_P (\text{‰})$	-19.0, -148	Fort Smith CNIP Station	
$\delta^{18}\text{O}_{PS}, \delta^2\text{H}_{PS} (\text{‰})$	-17.0, -132	Gibson and Edwards (2002)	

Appendix A

Isotopic framework parameters are calculated using approaches described in detail in Edwards et al. (2004b), Gibson and Edwards (2002), Gonfiantini (1986) and Barnes and Allison (1983), and are based on the linear resistance model of Craig and Gordon (1965). Values for 2003 are summarized in Table A1.

Equilibrium liquid-vapour isotopic fractionation (α^*) is calculated from equations given by Horita and Wesolowski (1994), where

$$1000\ln\alpha^* = -7.685 + 6.7123(10^3/T) - 1.6664(10^6/T^2) + 0.35041(10^9/T^3) \quad (1)$$

for $\delta^{18}\text{O}$ and

$$1000\ln\alpha^* = 1158.8 (T^3/10^9) - 1620.1(T^2/10^6) + 794.84(T/10^3) - 161.04 + 2.9992(10^9/T^3) \quad (2)$$

for $\delta^2\text{H}$, where T represents the interface temperature in degrees Kelvin. Equilibrium separation between the liquid and vapour phases (ϵ^*) is expressed in decimal notation by

$$\epsilon^* = (\alpha^* - 1). \quad (3)$$

Kinetic separation (ϵ_K) is given in decimal notation by

$$\epsilon_K = 0.0142 (1 - h) \quad (4)$$

for $\delta^{18}\text{O}$ and

$$\epsilon_K = 0.0125 (1 - h) \quad (5)$$

for $\delta^2\text{H}$, where h is relative humidity in decimal notation (Gonfiantini, 1986).

The slope (S) and intercept (d) of the local evaporation line can be calculated using the approach of Barnes and Allison (1983), formulated for δ , ε and h values in decimal notation as

$$S = \frac{\alpha^{*2} [(\varepsilon_K^2 + \varepsilon^{*2} / \alpha^{*2})(1 + \delta_P^2) - h(\delta_P^2 - \delta_{AS}^2)]}{\alpha^{*18} [(\varepsilon_K^{18} + \varepsilon^{*18} / \alpha^{*18})(1 + \delta_P^{18}) - h(\delta_P^{18} - \delta_{AS}^{18})]} \quad (6)$$

and

$$d = \delta_P^2 - S \delta_P^{18} \quad (7)$$

where δ_P and δ_{AS} are the respective isotopic compositions of input water and ambient atmospheric moisture. The latter is assumed to be in equilibrium with evaporation-flux-weighted (~summer) precipitation, as given by

$$\delta_{AS} = \frac{\delta_{PS} - \varepsilon^*}{\alpha^*} \quad (8)$$

(Gibson and Edwards, 2002).

The LEL extends from δ_P to the limiting non-steady-state composition (δ^*) of a water body approaching complete desiccation, calculated from

$$\delta^* = \frac{h\delta_{AS} + \varepsilon_K + \varepsilon_{L-V}^* / \alpha_{L-V}^*}{h - \varepsilon_K - \varepsilon_{L-V}^* / \alpha_{L-V}^*} \quad (9)$$

for δ , ε and h values in decimal notation (Gonfiantini, 1986).

The calculated limiting steady-state isotopic composition (δ_{SSL}) also provides a key datum on the LEL, representing the isotopic signature of a terminal lake in which evaporation exactly balances inflow. This can be obtained readily from the Craig-Gordon equation for the isotopic composition (δ_E) of the evaporating flux from a lake (δ_L) undergoing steady-state evaporation (also for δ , ε and h values in decimal notation)

$$\delta_E = \frac{(\delta_L - \varepsilon^*) / \alpha^* - h\delta_{AS} - \varepsilon_K}{1 - h + \varepsilon_K} \quad (10)$$

for the special case in which $\delta_E = \delta_P$.

As noted in the text, δ values are conventionally multiplied by 1000 and expressed in per mil (‰).

Chapter 3: Spatial and temporal perspectives on spring break-up flooding in the Slave River Delta, NWT

Complete citation: Brock BE, Wolfe BB, Edwards TWD. 2008. Spatial and temporal perspectives on spring break-up flooding in the Slave River Delta, NWT. *Hydrological Processes* 22: 4058-4072.

Introduction

Rivers are an integral part of Canada's northern landscape, draining three-quarters of Canada's land mass to the Arctic Ocean and North Atlantic and affecting high latitude oceanic, atmospheric, cryospheric and biological processes (Déry and Wood, 2005). Because high latitudes are especially sensitive to climate warming as a result of positive feedback mechanisms (Overland et al., 2002; Schindler and Smol, 2006) that accelerate hydrological fluxes (Kane, 2005), the effects of a changing climate, coupled with anthropogenic stressors like flow regulation and water diversion and extraction, have the potential to significantly alter northern river flow patterns, including the timing and volume of discharge. Interrelationships between northern rivers and their associated landscapes are poorly understood (Rouse et al., 1997), and thus the effects of changing river dynamics on riparian ecosystems remain largely uncertain. Our ability to predict the future evolution of northern rivers and their catchments is further confounded by a lack of long-term river and climate data for Canada's North (Rouse et al., 1997; Lammers et al., 2001; Kane, 2005; Rood et al., 2005; Peters et al., 2006b; Schindler and Donahue, 2006).

In northern river deltas, which are often highly productive nodes in the northern landscape, seasonal variations in river discharge have long been thought to be critical to their hydroecology. Flooding during spring break-up is a key supplier of water to delta lakes (Prowse and Lalonde, 1996; Rouse et al., 1997; Beltaos et al., 2006a; Peters et al., 2006b), maintaining riparian ecosystems and early successional communities (English et al., 1997; Schindler

and Smol, 2006), driving primary and secondary production, and affecting mesoscale climate conditions (Wrona et al., 2005). Decreasing river discharge (Lammers et al., 2001; Déry and Wood, 2005; Rood et al., 2005) and earlier spring snowmelt (Lammers et al., 2001; Overland et al., 2002; Beltaos et al., 2006a; Romolo et al., 2006b) have the potential to significantly alter spring break-up conditions, the frequency and extent of spring ice-jam flooding (Beltaos et al., 2006a; Schindler and Smol, 2006) and delta ecosystems (Schindler and Donahue, 2006).

To investigate the crucial role of water in major northern freshwater ecosystems, multidisciplinary research has been initiated in the Slave River Delta, NWT (SRD; Figure 3.1). The SRD is one of three major river deltas in the Mackenzie Drainage Basin, northern Canada. The lakes and wetlands that make up the SRD provide extensive shoreline habitat and support diverse populations of migratory fish and waterfowl, large and small mammals and terrestrial and aquatic vegetation communities. Residents of nearby Fort Resolution participate in traditional lifestyle occupations, including hunting, trapping and fishing on the delta, and maintain strong socio-cultural ties to the delta ecosystem (Wesche, 2007). Multidisciplinary research in the SRD aims to address concerns about the impacts of natural and anthropogenic variations in climate and river discharge on the hydroecology of this important northern ecosystem (Wolfe et al., 2007).

Recent hydrological studies have focused on characterizing the major processes affecting the water balances of SRD lakes (Brock et al., 2007; see Chapter 2). Using water isotope tracers (^{18}O , ^2H) and total inorganic suspended sediment data collected during the 2003 thaw season, a year with a moderate spring break-up flood in the active portion of the delta, three types of SRD lakes have been identified. These are: 1) flood-dominated lakes in the active, outer portion of the SRD; 2) evaporation-dominated lakes in the older, relict delta; and 3) Great Slave Lake and Slave River exchange-dominated lakes along the outer edge of the active delta and along the Slave River. Continued monitoring

in 2004 and 2005 has provided data from a range of spring melt conditions in the SRD. In 2004, spring flooding was almost entirely absent. Ice-induced tree scars and large blocks of river ice were observed by field researchers along the banks of the Slave River and its distributaries during the spring of 2005, remnants of an ice-jam flood observed by local residents that caused extensive flooding in the SRD. Although some flooding can result from high discharge on the Slave River during the open-water season and seiche events on Great Slave Lake, spring ice-jam-induced backwater events have the greatest potential to flood the landscape.

Here we focus on hydrological aspects of varying spring melt conditions in lakes on the delta over these three consecutive years. Water isotope tracers and total suspended sediment analysis are used to identify flooded versus non-flooded lakes, estimate floodwater- or snowmelt-induced dilution in delta lakes, and to estimate the spatial extent of river flooding during 2003-2005. Slave River level and discharge are examined to explore for relationships between river hydrology and the observed variability in spring flooding in the SRD during 2003-2005. The potential roles of key trigger tributaries upstream of the Slave River are also considered. The understanding of spring melt conditions developed here will be used to interpret historical Slave River discharge and lake sediment records, and to hindcast flood frequency and its relationship with hydroecological evolution of the delta. Collectively, this information is critical for evaluating potential consequences of changes in river discharge on delta hydroecology.

The Slave River Delta

The Slave River begins its course to Great Slave Lake on the northern edge of the Peace-Athabasca Delta (PAD), at the confluence of the Peace River and Rivière des Rochers (Figure 3.1). The Peace River contributes approximately 66% of the annual flow of the Slave River (English et al., 1997). Additional water sources to the Slave River include the Athabasca River and Lake Athabasca. Smaller watercourses downstream from the PAD also

contribute to Slave River flow. The Slave River's 420 km route north passes through relict deltaic and alluvial sediments, laid down during the drainage of Glacial Lake McConnell at the time of the retreat of the Keewatin Ice Sheet around 8070 ¹⁴C yr BP (Vanderburgh and Smith, 1988). Between the Peace-Rochers confluence and Great Slave Lake, the Slave River drains 15 100 km² (Prowse et al., 2002a) and delivers 74% of inflow to Great Slave Lake (Gibson et al., 2006b), the primary water source for the Mackenzie River.

For most of its upper reaches, the Slave River is relatively straight. However, as it approaches Great Slave Lake, meander bends and island and bar complexes become more common (Figure 3.1). These features are prime locations for the development of ice-jams (Beltaos and Prowse, 2001). Further downstream, the active delta is approximately 400 km² (English et al., 1997) and has been prograding into Great Slave Lake at a rate of approximately 10 m per year since 1180 ¹⁴C yr BP (Vanderburgh and Smith, 1988), infilling the southern arm of Great Slave Lake and becoming increasingly exposed to the lake's wave, wind and ice action (Prowse et al., 2006). Currently, the active delta begins where the Slave River bifurcates into several distributary channels (Figure 3.1), while the rest of the delta is considered relict.

The SRD is populated by hundreds of small, shallow lakes. SRD study lakes span a range of biogeographical and hydrological zones in the delta, and have been classified based on the dominant process affecting their water balances during the 2003 thaw season (Brock et al., 2007; see Chapter 2). Flood-dominated lakes are typically found in the active delta, where levee heights are moderate (0.5-2.5 m above Great Slave Lake low summer water levels; Prowse et al., 2002) and flooding is the dominant process controlling lake water balances. Lakes in this hydrological class have high alkalinities and high concentrations of nutrients and ions (Sokal et al., 2008). Evaporation-dominated lakes are typically found in the relict delta, where levees are higher (2.5-3 m above Great Slave Lake low summer water levels; Prowse et al., 2002). These lakes have low concentrations of most nutrients and ions and low

alkalinity (Sokal et al., 2008). Exchange-dominated lakes lie along the Slave River and the delta front. Lakes with direct channel connections to the Slave River and its distributaries receive water from the river, while seiche events on Great Slave Lake promote exchange with lakes along the delta's outer fringes (Gardner et al., 2006). These lakes have a range of limnological conditions that vary relative to the strength of their connections to other surface waters (Sokal et al., 2008). SRD study lakes have maximum depths of 0.15 to 4 m, with the exception of SD30 (Ring Lake), a partially cut-off meander of the Slave River that has a maximum depth of 10 m.

The climate of the SRD is highly seasonal, characterized by long, cold winters and short, warm summers. Based on 1971-2000 Canadian climate normals for Hay River, NWT (Environment Canada, 2002), mean yearly temperature is -2.9°C , with mean January and July temperature of -23.1°C and 15.9°C , respectively. A total of 320 mm of precipitation falls annually, half as rain during the May to September thaw (ice-free) season. Temperature, rainfall and snow depth for the 2003-2005 spring melt period are shown in Figure 3.2. Temperature was variable in all three years, although 2004 was cooler overall than 2003 and 2005, with several prolonged periods below 0°C during the melt period. Rainfall was low in all three years, while in 2004, snow depth prior to melting exceeded that of 2003 and 2005 by ~ 20 cm (Environment Canada, 2005).

Methods

Water samples for analysis of stable isotopes and total inorganic suspended sediment (TSS) were collected from Great Slave Lake, the Slave River, SD30 (Ring Lake, a partially cut-off meander of the Slave River) and 40 small (<0.2 ha) delta lakes (Figure 3.1) spanning all hydrologic classifications (Brock et al., 2007; see Chapter 2). Samples were collected on several occasions between September 2002 and September 2005. Here we focus on results from water sampling campaigns conducted on 23 May 2003, 31 May 2004, and 17 May 2005 to assess the inter-annual effects of river flooding and

snowmelt on spring water balances of lakes in the delta. Water samples were collected from 10 cm below the surface at the approximate centre of each study lake in 30 mL high density polyethylene bottles and transported to the University of Waterloo Environmental Isotope Laboratory. Snow samples were collected in heavy-gauge polyethylene sample bags from seven geographically dispersed SRD lakes (SD2, 15, 20, 28, 29, 33, 39; Figure 3.1) on 03 May 2004. Snow samples were melted and the meltwater was transferred to 30 mL bottles for analysis.

Water isotope ratios ($^{18}\text{O}/^{16}\text{O}$, $^2\text{H}/^1\text{H}$) were measured on each sample using standard methods (Epstein and Mayeda, 1953; Coleman et al., 1982) at the University of Waterloo Environmental Isotope Laboratory. Results are expressed in δ values, representing per mil (‰) deviations of the measured sample from the V-SMOW standard such that $\delta^{18}\text{O}_{\text{sample}}$ or $\delta^2\text{H}_{\text{sample}} = 10^3 [(R_{\text{sample}}/R_{\text{V-SMOW}})-1]$, where R is the ratio of $^{18}\text{O}/^{16}\text{O}$ or $^2\text{H}/^1\text{H}$ in the sample and standard, respectively. $\delta^{18}\text{O}$ and $\delta^2\text{H}$ results are normalized using Standard Light Antarctic Precipitation ($\delta^{18}\text{O} = -55.5\text{‰}$, $\delta^2\text{H} = -428\text{‰}$; Coplen, 1996), with maximum analytical uncertainties for $\delta^{18}\text{O}$ and $\delta^2\text{H}$ of $\pm 0.2\text{‰}$ and $\pm 2\text{‰}$, respectively.

Water samples were collected for measurement of TSS concentrations to identify lakes that received turbid river water. Agitated water samples of known volume were passed through a 1.2 μm glass microfibre filter of a known weight. Samples were dried at 95°C for twenty-four hours and weighed. Weight loss after burning at 550°C was used to calculate the mineral matter content of each sample. Inorganic TSS concentrations are reported in mg/L.

Climate data from Hay River, NWT (Environment Canada, 2005) were used to aid the interpretation of water isotope results because these records are more complete than at Fort Resolution Airport. Slave River level and discharge data were collected from Fitzgerald, AB (Station ID 07NB001), the closest river gauge station to the SRD, and are used in conjunction with upstream discharge

data from Alberta's Peace (Station ID 07KC001) and Smoky (Station ID 07GJ001) rivers (Water Survey of Canada, 2006) to explore potential factors responsible for observed hydrological variability in the SRD during spring 2003-2005 and to identify possible major flood events since 1960. Estimated values for river level and discharge or results based on a partial day of record account for <6%, 8% and 5% of data for the Slave, Peace and Smoky rivers, respectively, during the break-up period (01 April – 01 June).

Results and interpretation

Isotopic frameworks for the SRD (2003-2005)

Water isotope results are evaluated in conventional $\delta^{18}\text{O}$ - $\delta^2\text{H}$ space and with respect to two prominent reference lines: (1) the Local Meteoric Water Line (LMWL), which is based on local amount-weighted monthly mean precipitation ($\delta^2\text{H} = 6.7\delta^{18}\text{O}-19.2$; (Birks et al., 2004)); and (2) the Local Evaporation Line (LEL), which falls to the right of the LMWL and typically has a slope of 4-6. While the LMWL is a consequence of the isotopic labeling of precipitation, the LEL reflects secondary alteration in isotopic compositions due to heavy-isotope (^{18}O , ^2H) build-up in surface waters because of evaporation. As a result, the LEL varies with changes in thaw season relative humidity and temperature, as well as the isotopic composition of summer (thaw season) ambient atmospheric moisture (δ_{AS}). Because climate conditions in 2003-2005 differ from climate normal (1971-2000) values, season-specific LELs are calculated for each sampling year as described below, utilizing yearly flux-weighted thaw season relative humidity and temperature (Table 3.1) measured at Hay River, NWT (Environment Canada, 2005; Figure 3.3).

The slope (S) and intercept (d) of the LELs (Table 3.2) are derived from the linear resistance model of Craig and Gordon (1965) using equations (for h , ϵ and δ values expressed in decimal notation) defined by Barnes and Allison (1983), where

$$S = \frac{\alpha^{*2} [(\epsilon_K^2 + \epsilon^{*2} / \alpha^{*2})(1 + \delta_p^2) - h(\delta_p^2 - \delta_{AS}^2)]}{\alpha^{*18} [(\epsilon_K^{18} + \epsilon^{*18} / \alpha^{*18})(1 + \delta_p^{18}) - h(\delta_p^{18} - \delta_{AS}^{18})]} \quad (1)$$

and

$$d = \delta_p^2 - S \delta_p^{18} \quad (2)$$

Equilibrium liquid-vapour fractionation (α^*_{L-V}) values (Table 3.2) are derived from Horita and Wesolowski (1994) as $1000 \ln \alpha^*_{L-V} = -7.685 + 6.7123(10^3/T) - 1.6664(10^6/T^2) + 0.35041(10^9/T^3)$ and $1000 \ln \alpha^*_{L-V} = 1158.8 (T^3/10^9) - 1620.1(T^2/10^6) + 794.84(T/10^3) - 161.04 + 2.9992(10^9/T^3)$, where T is the water-atmosphere interface temperature in degrees K. Liquid-vapour equilibrium separation (ϵ^*_{L-V}) is expressed in decimal notation and is defined as $\epsilon^*_{L-V} = (\alpha^*_{L-V} - 1)$ (Table 3.2). Kinetic separation ($\epsilon_{K L-V}$), also expressed in decimal notation, is a function of the humidity (h) deficit, and is defined as $\epsilon_{K L-V} = 0.0142(1-h)$ and $\epsilon_{K L-V}^2 = 0.0125(1-h)$ (Table 3.2). The isotopic composition of δ_{AS} is assumed to be in approximate isotopic equilibrium with summer amount-weighted precipitation (δ_{PS}), and is expressed in decimal notation such that $\delta_{AS} = (\delta_{PS} - \epsilon^*_{L-V}) / \alpha^*_{L-V}$ (Table 3.2).

The LELs are anchored at their depleted ends by the isotopic composition of yearly amount-weighted precipitation (δ_p), using samples collected at Fort Smith, NWT (Birks et al., 2004) (Figure 3.3). Conceptually, the limiting isotopic composition (δ^*) constrains the enriched end of the LELs, and is calculated in decimal notation as

$$\delta^* = \frac{h\delta_{AS} + \epsilon_K + \epsilon^* / \alpha^*}{h - \epsilon_K - \epsilon^* / \alpha^*} \quad (3)$$

(Gonfiantini, 1986; Table 3.2). A key datum along each LEL is the composition of a terminal basin at isotopic and hydrologic steady state (δ_{SSL} ; Table 3.2), which occurs as a special case when the evaporative flux (δ_E) is equal to δ_p . δ_E can be calculated in decimal notation from Craig and Gordon (1965) as

$$\delta_E = \frac{(\delta_L - \varepsilon^*) / \alpha^* - h\delta_A - \varepsilon_K}{1 - h + \varepsilon_K} \quad (4)$$

Isotopic framework parameters outlined briefly here are described in detail in Gonfiantini (1986), Gibson and Edwards (2002) and Edwards et al. (2004), and framework parameters for each sampling year are given in Table 3.2. Note that delta values are conventionally multiplied by 1000 and expressed in per mil (‰). Results from these calculations, as shown in Figure 3.3, indicate that very similar LELs characterize the 2003-05 thaw seasons, although they differ measurably from the LEL calculated using climate normals.

Slave River Delta spring isotope hydrology and total suspended sediment (2003-2005)

Most lakewater isotopic compositions measured from water samples collected in the springs of 2003-2005 plot below the LEL and all are more depleted than δ_{SSL} (Figure 3.4), signifying the importance of river water and snowmelt in generating positive water balances in delta lakes during the spring. These two input sources have distinct isotopic compositions. The spring $\delta^{18}\text{O}$ ($\delta^2\text{H}$) composition of the Slave River was -19.2‰ (-151‰) in 2003, -17.7‰ (-144‰) in 2004 and -18.6‰ (-148‰) in 2005 (Figure 3.4). In contrast, $\delta^{18}\text{O}$ ($\delta^2\text{H}$) values of snow range from -27.7‰ to -21.2‰ (-211‰ to -165‰) (average $\delta^{18}\text{O}$, $\delta^2\text{H}$ = -24.7‰, -191‰), based on snow samples collected in the spring of 2004. By examining spring lakewater compositions relative to these two key input sources, in addition to total inorganic suspended sediment (TSS) measurements, we identify which lakes were flooded and which received exclusively snowmelt during the spring melt, as described below.

As described by Brock et al. (2007; see Chapter 2), isotope results from lakes sampled on 23 May 2003 form two distinct clusters in $\delta^{18}\text{O}$ - $\delta^2\text{H}$ space (Figure 3.4a). The more isotopically-depleted lakes cluster around the isotopic composition of the Slave River, suggesting these lakes were flooded by the river during the spring melt. A more isotopically-enriched group of lakes, where

catchment-sourced snowmelt was the main input, is less strongly clustered, suggesting variable snowmelt influences at each lake. TSS concentrations in SRD lakes sampled on 23 May 2003 support the interpretation that lakes in the isotopically-depleted cluster were flooded by the Slave River. Most lakes in this group contain relatively high TSS concentrations (TSS >10 mg/L), as turbid Slave River water (TSS = 315 mg/L) introduced suspended sediment to the lakes during the spring flood. In contrast, the more isotopically-enriched, non-flooded lakes, where snowmelt was a major contributor, have low TSS values (TSS <10 mg/L), consistent with the absence of Slave River flooding.

In contrast to the 2003 dataset, water samples collected on 31 May 2004 do not show distinct flooded and non-flooded clusters, but are instead distributed uniformly along and generally below the calculated LEL in the absence of widespread spring flooding (Figure 3.4b). Although a flood did not occur, measured isotopic values from this sampling campaign are similar to those measured in the springs of 2003 (and 2005; Figures 3.4a and c), ranging between -18.2‰ and -10.9‰ in $\delta^{18}\text{O}$, and -149‰ and -116‰ in $\delta^2\text{H}$. Generally, lakes in the active delta, where flooding occurred in 2003, fall along the more depleted end of the spectrum, while lakes in the relict zone of the delta fall along the more enriched end. TSS concentrations also cluster at or below 10 mg/L (Figure 3.4b), consistent with the absence of substantial river flooding in 2004. The TSS concentration of the Slave River in the spring of 2004 (TSS = 40 mg/L) is also much lower than the concentrations measured in the river in 2003 and 2005 (TSS = 310 and 260 mg/L, respectively). In the absence of river flooding, catchment-sourced snowmelt was the dominant input to most delta lakes during the spring of 2004.

Isotopic results from 17 May 2005 (Figure 3.4c) reveal comparable conditions to those of the spring of 2003 (Figure 3.4a). As in 2003, SRD lakes sampled in the spring of 2005 form two distinct clusters in $\delta^{18}\text{O}$ - $\delta^2\text{H}$ space, indicating Slave River floodwater likely entered several lakes during the spring melt. Flooded lakes cluster tightly around the isotopic composition of the Slave

River, with values ranging between -19.0‰ and -17.1‰ in $\delta^{18}\text{O}$ and -154‰ and -146‰ in $\delta^2\text{H}$. Measured isotopic values for non-flooded lakes ($\delta^{18}\text{O}$, $\delta^2\text{H}$ ranges = -14.6‰ and -10.6‰, -140‰ and -118‰) are also similar to those measured in non-flooded lakes in 2003. In this case, however, five lakes that were not flooded during the spring of 2003 were flooded in 2005 (SD8, 18, 19, 29 and 32), while one lake that was flooded in 2003 did not receive river floodwaters in 2005 (SD7). These data suggest that Slave River flooding was more widespread in 2005 than in 2003, although some areas that were flooded in 2003 were not flooded in 2005. As in 2003, TSS concentrations also distinguish flooded and non-flooded lakes, with most flooded lakes having values >10 mg/L (Figure 3.4c). Low TSS values in several of the isotopically-identified flooded lakes may be due to a variety of factors, including snowmelt influence, sediment settling after flooding, timing of sample collection, and filtering of suspended sediment by catchment wetlands or surrounding vegetation.

Spatial extent of flooding in the Slave River Delta (2003-2005)

To determine the spatial extent of spring flooding in the SRD over the study period, the magnitude of lakewater replenishment by spring flooding or snowmelt input in delta lakes is estimated using a two-component mixing model. Lakewater isotopic signatures and TSS concentrations are used to identify the dominant spring input (catchment-sourced snowmelt or river floodwater) for each sampled lake (Figure 3.4). Percent dilution by the dominant input source during the spring melt period is calculated by incorporating the isotopic composition of the diluting source water, the end-of-thaw-season lake water isotopic composition, and the lakewater isotopic composition of each lake the following spring (Brock et al., 2007; see Chapter 2). Specifically, percent dilution is calculated by

$$\% \text{ dilution} = \frac{(\delta_{L-\text{spring}} - \delta_{L-\text{fall}})}{(\delta_{\text{source}} - \delta_{L-\text{fall}})} \times 100 \quad (5)$$

where $\delta_{L-spring}$ and δ_{L-fall} are the lakewater compositions in the spring and the fall, respectively, and δ_{source} is the isotopic composition of sourcewater, either snowmelt or river water. Percent dilution is based on an average of results obtained for both $\delta^{18}\text{O}$ and $\delta^2\text{H}$. While these estimates do not account for changes in lake volume, or the added influence of catchment-sourced snowmelt on flooded delta lakes, they effectively illustrate the significant differences in the spatial distribution of river floodwaters in the SRD in the springs of 2003-2005 and are supported by field observations made during each of the sampling campaigns.

In 2003, flooded lakes in the active, outer SRD were diluted by between ~70 and 100% by Slave River floodwater during the spring melt (Figure 3.5a) (Brock et al., 2007; see Chapter 2). Natural levees in this area of the delta are only 0.1-1.5 m above Great Slave Lake low summer water levels (English et al., 1997), thus outer delta lakes are susceptible to flooding by the Slave River. In contrast, non-flooded lakes in the relict delta, where levee heights are typically greater than 2.5 m above Great Slave Lake low summer levels (English et al., 1997), were diluted up to ~35% by snowmelt.

Very different hydrological conditions characterized delta lakes during the spring melt of 2004 (Figure 3.5b), a year in which water isotope tracers, TSS data and field observations indicate no spring flooding occurred. Dilution in delta lakes, exclusively by snowmelt, ranges between ~0 and 40%.

Significant flooding during the spring of 2005 affected a number of lakes in both the active and relict portions of the delta (Figure 3.5c). The spatial extent of flooding in the spring of 2005 exceeds that of 2003 (Figure 3.5a), and includes several lakes that were not flooded in 2003 (SD8, 18, 19, 29, 32). Dilution in lakes in the active delta and along the Slave River approached 100%. The development and location of ice-jams on the Slave River likely accounts for much of the spatial distribution of flooding during the 2005 spring season. For example, ice blocks, observed on the banks of the Slave River downstream of SD30 (Ring Lake), are likely the remnant of a mechanical-type

break-up (Gray and Prowse, 1993), which under specific hydraulic conditions, can result in an ice-jamming event and associated flooding (Beltaos, 1995). Flooding in SD8 (TSS = 12 mg/L), a lake on the southern edge of the active delta that was not flooded in 2003, and the absence of flooding in SD7 (TSS = 3 mg/L), a lake on the northern edge of the active delta where flooding did occur in 2003, also suggests that the location of spring ice-jams on the Slave River differed between 2003 and 2005. Greater dilution in lakes along the Slave River in 2005 indicates that water levels in the river upstream of the active delta were likely higher than in the preceding two years. High water marks observed on willows surrounding SD28, a lake with a direct channel connection to the Slave River (Figure 3.1), confirm water levels peaked ~2 m above those observed at the time of sampling. Estimated snowmelt dilution in non-flooded lakes in the relict delta ranges between ~0 and 56%.

Slave River level and discharge (2003-2005)

To explore potential factors responsible for variability in the extent of spring flooding of the SRD during the years 2003-2005, Slave River discharge was examined, as recorded at Fitzgerald, AB, ~200 km upstream of the SRD (Figure 3.1). Substantial differences in the magnitude and timing of Slave River spring discharge peaks are evident in 2003-2005 (Figure 3.6; Table 3.3). In 2003, Slave River discharge peaked on 4 May at 5370 m³/s, with smaller subsequent peaks on 11 May (4900 m³/s) and 23 May (4860 m³/s). River levels were highest on 4 May, at 4.46 m above the Water Survey Canada's (2006) assumed datum, followed by subsequent peaks of 4.29 m and 3.98 m on 11 May and 23 May. The Water Survey of Canada (2006) reports that May 11 was the last day of ice conditions (solid or floating ice) observed on the Slave River. In 2004, ice break-up occurred on 15 May. Peak discharge and level in 2004 were lower than 2003, with a maximum discharge of 4740 m³/s and river level of 4.03 m, both attained on 15 May. In 2005, river discharge and level peaked twice. On 22 April, river discharge peaked at 3970 m³/s, while level peaked at 4.07 m on 23 April. Higher discharge and level crests occurred 1 May, at 5900 m³/s and

4.64 m, respectively. The last day of ice conditions on the Slave River was 1 May (Water Survey of Canada, 2006).

Discussion

The break-up of river ice is a brief but influential period in the seasonal evolution of a northern riverine ecosystem (Beltaos, 1997; Beltaos and Prowse, 2001; Romolo et al., 2006), particularly when associated with ice-jam-induced flooding. Ice-induced backwater has been identified as the historic source of high water levels in the Peace-Athabasca Delta (PAD) (Prowse and Lalonde, 1996; Prowse et al., 2002b; Peters et al., 2006b), upstream of the SRD, as well as in the Mackenzie Delta (Marsh and Hey, 1989). The nature of the break-up and jamming process and ensuing flooding is governed by a number of driving and resisting forces, including the thickness and strength of river ice cover, attachment of ice cover to the river bed or banks, overall river morphology, the rate of river discharge, and general climatological and antecedent moisture conditions (Beltaos, 1998; Prowse and Conly, 1998; Beltaos and Prowse, 2001; Beltaos et al., 2006). The initiation of river ice break-up is triggered by mild weather, which begins melting river ice cover. Increases in rainfall and snowmelt contribute to rising rates of river discharge. Rapid increases in water level and discharge can cause a mechanical break-up of ice cover and can create ice blocks that can be arrested against river banks, along meander bends or by other intact ice cover. Subsequent backwater flooding behind the break-up front can occur, with surges resulting from the release of the ice-jam. The magnitude of backwater flooding produced after ice movement is arrested is a function of spring river discharge (Prowse and Conly, 1998). On the other hand, extensive decay of ice thickness and strength as the result of a protracted melt results in a remnant ice cover that is susceptible to displacement by low river flows and modest discharge, leading to minor increases in water level during the spring melt period (Prowse and Conly, 1998; Beltaos and Prowse, 2001).

In spite of the recognized complexity in the numerous factors that can potentially contribute to a mechanical break-up, an apparently straightforward

positive relationship exists between Slave River level and discharge and the magnitude of flooding in the SRD during the three years of observation. Specifically, a moderate flood in 2003 (Figures 3.4a, 3.5a) corresponds with a moderate peak in Slave River discharge and level (Figure 3.6a). There was no flooding in the SRD in 2004 (Figures 3.4b, 3.5b), when Slave River discharge and level were both low (Figure 3.6b). In 2005, high Slave River discharge and level (Figure 3.6c) are associated with extensive flooding in both the active and relict areas of the SRD (Figure 3.4c, 3.5c).

The timing and magnitude of measured river level and discharge also afford insight about the nature of the spring break-up. In 2003, level and discharge on the Slave River peaked nine days before the river was free of solid or floating ice (Figure 3.6a, Table 3.3). A second increase in discharge on the same day the Slave River became ice-free suggests that flooding during this period may have occurred behind an ice-jam along the Slave River.

The lowest peaks in Slave River level and discharge were measured in 2004 (Figure 3.6b, Table 3.3) and correspond with a spring in which no flooding occurred (Figures 3.4b, 3.5b). The rate of rise of the river was muted and fluctuated over the course of the melt period, peaking around the same time the river became free of ice (Water Survey of Canada, 2006). A slow decay of the ice cover on the Slave River, observed during attempted spring sampling in early May, prevented the formation of mechanical ice-jams and eliminated the potential for ice-jam-induced spring flooding. A protracted melt resulting in an over-mature decay of ice cover may have been the result of mean daily temperatures fluctuating around 0°C during the month of May (Figure 3.2). Many other factors are likely associated with the slow decay of ice cover, including ice thickness, but these data are not available.

Widespread flooding of the SRD during the spring of 2005 (Figures 3.4c, 3.5c) is consistent with the highest measured Slave River discharge values of the three years studied (Figure 3.6c, Table 3.3). As in 2003, two peaks in level and discharge were measured during the spring melt period. The first

discharge and level peaks occurred 10 and 9 days, respectively, before ice cover on the Slave River disappeared (Water Survey of Canada, 2006), suggesting flooding may have occurred behind an ice-jam, consistent with field observations of tree scars and remnant ice blocks on the banks of the Slave River during the spring of 2005. The second, larger peak in both parameters occurred on the same day as the disappearance of Slave River ice cover. In the four days prior to this second peak, the daily mean rate of increase in river discharge was very high, and may therefore have contributed to the development of ice-jams along the Slave River and the release of an associated flood pulse on May 1.

Interannual variability in Slave River level and discharge evidently has a strong impact on the nature of the spring break-up and the spatial extent of flooding in the SRD, which is likely driven by variability in the contributions of major upstream water sources. Not surprisingly, spring discharge on the Slave River mimics that of the Peace River (Figure 3.7), which provides 66% of all seasonal flow to the Slave River (English et al., 1997). During the three-year monitoring period, similar variations in discharge on the Slave and Peace rivers are particularly clear in the period leading up to discharge maxima on both rivers, although this is especially evident in 2003 and 2005 when spring discharge on both rivers was high. In 2003, peak discharge measured on the Peace River was 5770 m³/s, while that of the Slave River was 5370 m³/s. It is interesting to note that in 2003, Slave River peak discharge preceded peak discharge on the Peace River by one day, indicating that other drivers of river discharge, such as drainage basin snowmelt, may be important for Slave River flow in some years. This also indicates that Peace River flow may not be used as a surrogate for Slave River flow in some years, although values in both rivers follow similar trends. Lower peak discharge in the Slave River in 2004 (4740 m³/s) also mimics a decrease in peak discharge in the Peace River (3880 m³/s), while in 2005, discharge in both rivers is high (Slave River peak discharge = 5900 m³/s; Peace River peak discharge = 4700 m³/s).

In 2004 and 2005, peak discharge on the Slave River followed peak Peace River discharge. In turn, the likelihood of a mechanical break-up on the Peace River is thought to be driven in part by the nature of spring discharge on upstream trigger tributaries. Prowse and Conly (1998) concluded that the Wapiti-Smoky drainage basin contains key trigger tributaries to the Peace River and is the source of flows generating major spring flood events in the PAD. Higher discharge on the Smoky River (Figures 3.1 and 3.8) in 2003 ($1400 \text{ m}^3/\text{s}$) and 2005 ($1180 \text{ m}^3/\text{s}$) corresponds with higher discharge on both the Peace and Slave rivers and flooding of the SRD, while very low early spring discharge ($672 \text{ m}^3/\text{s}$) on the Smoky River in 2004 corresponds with low downstream discharge and an absence of flooding in the SRD (Figure 3.5b). Likewise, major historic break-up events in the PAD have all occurred when spring snowpack snow-water equivalents in the Smoky River basin were high (Romolo et al., 2006a). An observed shift to lower snowpacks in the basin since the mid-1970s may therefore be a crucial factor in perceived declines in major break-up events and flood frequency in the PAD (Prowse and Conly, 1998; Romolo et al., 2006a) and subsequently, the SRD.

Evidence presented based on the 2003-2005 monitoring period indicates spring break-up flooding in the SRD is strongly controlled by Slave River discharge, derived principally from upstream tributary flow. Therefore, examining historical discharge records for the Slave River can be used to identify years in which spring break-up flooding may have occurred in the SRD. Complete year-long records of Slave River discharge measured at Fitzgerald, AB, date back to 1960 (Water Survey of Canada, 2006) and include the last date of observed ice conditions for each year. Yearly rates of discharge were compiled, based on data collected 14 days prior to, and three days after, the disappearance of ice cover on the Slave River. These data encompass the period in which high flows in the SRD were identified in 2003 and 2005, when ice-induced backwater or possible ice-jam-release flooding occurred. By comparing discharge levels measured in this period in 2003-2005 to historical

flow records, other years that may have had similar spring melt conditions to those measured in the SRD can be identified (Figure 3.8b).

Historical peak Slave River discharge from the 46-year (1960-2005) discharge record reveal that, during the identified melt period, discharge from the Slave River exceeded that measured in 2005 in 14 years. Nine of these events occurred prior to ice disappearance, perhaps as a result of ice-induced backwater, while five events occurred following the disappearance of ice, possibly the result of a flood pulse released by a breaking ice-jam. In contrast, discharge measured during 13 years since 1960 was lower than discharge measured in 2004, when there was no flooding of the SRD, identifying years in which a thermal melt likely characterized the decay of ice cover. Six of these events were measured while ice remained intact on the river, while seven events occurred after the disappearance of ice cover. Discharge during the remaining 16 years fell between 2004 and 2005 Slave River discharge levels, with discharge during 12 of these years occurring before the disappearance of ice cover. From this analysis, it appears that high-magnitude discharge events on the Slave River were more frequent in the earlier part of the measured record – nine high-discharge events (>2005) were measured pre-1980 (~ once every two years), of which five occurred after river ice cover disappearance (~ once every five years). In contrast, five high-discharge events were measured post-1980 (~ once every five years), and all occurred while ice conditions were still present on the Slave River. This apparent decline in flood frequency is consistent with evidence of drier conditions in the delta over the past few decades (English et al., 1997; Wesche 2007).

Striking correspondences also exist between historical discharge records for the Peace and Slave rivers (Figure 3.8a, b), which is consistent with contemporary spring discharge patterns (Figure 3.7). One particularly large discharge peak occurred in 1974, when peak discharge on the Slave River reached $11200 \text{ m}^3/\text{s}$. An extreme ice-jam flood was also observed in the PAD during the spring of 1974 (Peters et al., 2006b), when peak discharge on the

Peace River reached 8700 m³/s. During this spring thaw, local residents reported ice-jams on the Peace River extended down the Slave River and overland sheet flow flooded virtually the entire PAD (Peters et al., 2006b). Interestingly, this is also the year in which snow-water equivalent at Grand Prairie in the Smoky River basin reached its measured historical maximum (Prowse and Conly, 1998). Other flood events known to have occurred in the PAD include spring ice-jam floods in 1963, 1965, 1967, 1972, 1979, 1994, 1996 and 1997, as well as lower magnitude events in 1973, 1976, 1977 and 1981 (Peters, 2003; Beltaos et al., 2006a; Wolfe et al., 2006). Discharge peaks associated with spring ice-jam floods in the PAD are also evident in the Slave River discharge record, with discharge in the Slave River exceeding 2005 discharge in all but the 1994 PAD spring flood event. Most lower magnitude events have discharge amounts similar to those measured on the Slave River in 2003, with the exception of the 1973 event, which exceeded 2005 discharge, and the 1987 event, in which discharge was lower than that measured during the lower-flow conditions of 2004.

These data can be used to speculate about past flood frequency and intensity in the SRD – the 14 >2005 discharge events may have caused extensive flooding in the SRD, while the 13 <2004 discharge events may be associated with years of limited or non-existent flooding in the delta. Importantly, this information can assist in the interpretation of sediment core records collected from ponds in the SRD for paleohydrological and paleolimnological reconstructions (Figure 3.8c). A 49-cm sediment core was collected from SD2 (Figure 3.1), a lake adjacent to the Slave River in the active delta that was flooded during the 2003 and 2005 spring flood events (Figure 3.4a, c), to reconstruct SRD flood history. Visual interpretation shows spikes in C/N ratios, indicative of inputs of allochthonous material to the lake bed, correspond with peaks in Slave River discharge, consistent with the introduction of riverine sediment to the lake during floods (Mongeon, 2008). Fluctuations in the C/N record collected from a similar flood-dominated lake in the PAD (Figure 3.9; Wolfe et al., 2006) highlight broadly parallel variations in decadal

flood frequency in both deltas over the last ~65 years likely as a result of common upstream drivers of river discharge. These results offer much promise to extend the record of Slave River flood frequency using longer sediment cores from the SRD to more fully examine relationships among climate variability, Slave River discharge and delta hydroecology.

Summary and implications

Results from measurements of lake water isotope compositions and total inorganic suspended sediment concentrations over three years illustrate a straightforward relationship between the spatial extent of spring flooding in the Slave River Delta (SRD) and recorded peak Slave River discharge upstream of the delta. Flooding was widespread in 2005, spanning the active delta and extending well upstream, and corresponded to peak Slave River discharge 9% above the long-term mean. Conversely, river flow was confined to the main channel and its distributaries in 2004, a year in which peak river discharge was 12% below the long-term mean. Maximum discharge on the Slave River in 2003 was comparable to the long-term mean and corresponded with moderate flooding in the active portion of the SRD. Parallel hydrographs during the three-year monitoring period for the Slave River, Peace River and the Wapiti-Smoky tributary system, the latter previously identified as a key upstream trigger tributary for generating ice-jam floods along the Peace River in the vicinity of the Peace-Athabasca Delta (Prowse and Conly, 1998), strongly suggest that driving forces (i.e., snow accumulation, rate of melt) several hundred kilometres upstream are also largely responsible for determining the magnitude of spring flooding of the SRD. Furthermore, there is close correspondence between major discharge events in the instrumental record for the Slave and Peace rivers, several of which can be linked to known flood events and deposits in lake sediments in both the Peace-Athabasca and Slave River deltas.

Ongoing analysis of extended sediment records from SRD lakes will be used to reconstruct the delta's flood history beyond the instrumental discharge

record. Identification of past periods of reduced flooding from a longer temporal perspective, for instance, will foster greater understanding of hydroecological responses under such conditions (e.g., Wolfe et al. 2006), thereby addressing mounting concerns about the consequences of declining discharge in northern Canadian rivers (Lammers et al., 2001, Déry and Wood, 2005; Rood et al., 2005; Schindler and Donahue, 2006), and ultimately contributing to anticipating future deltaic evolution and effective ecosystem management of the SRD.

Figures

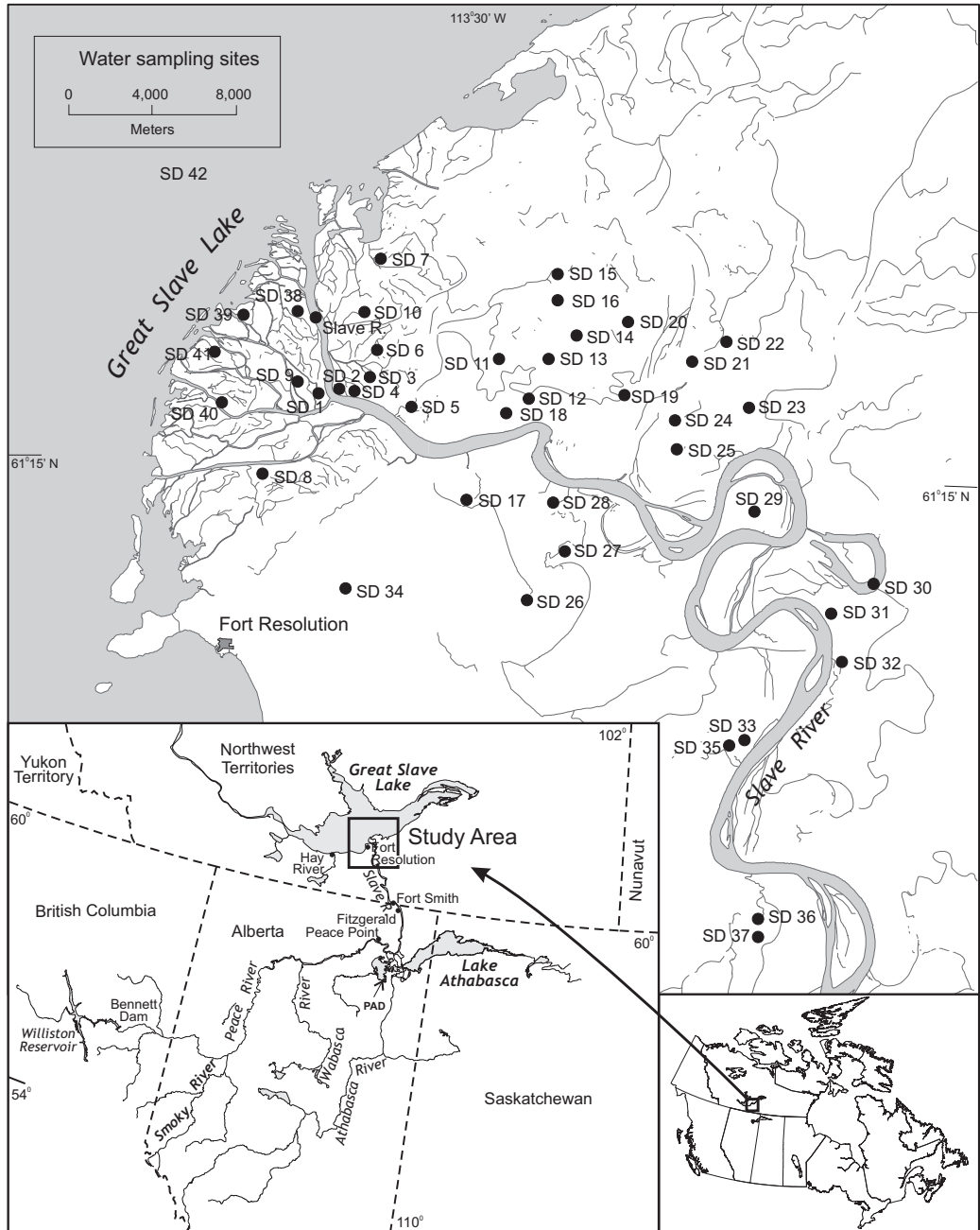


Figure 3.1. Location of the Slave River Delta, NWT, including lake and river sampling sites.

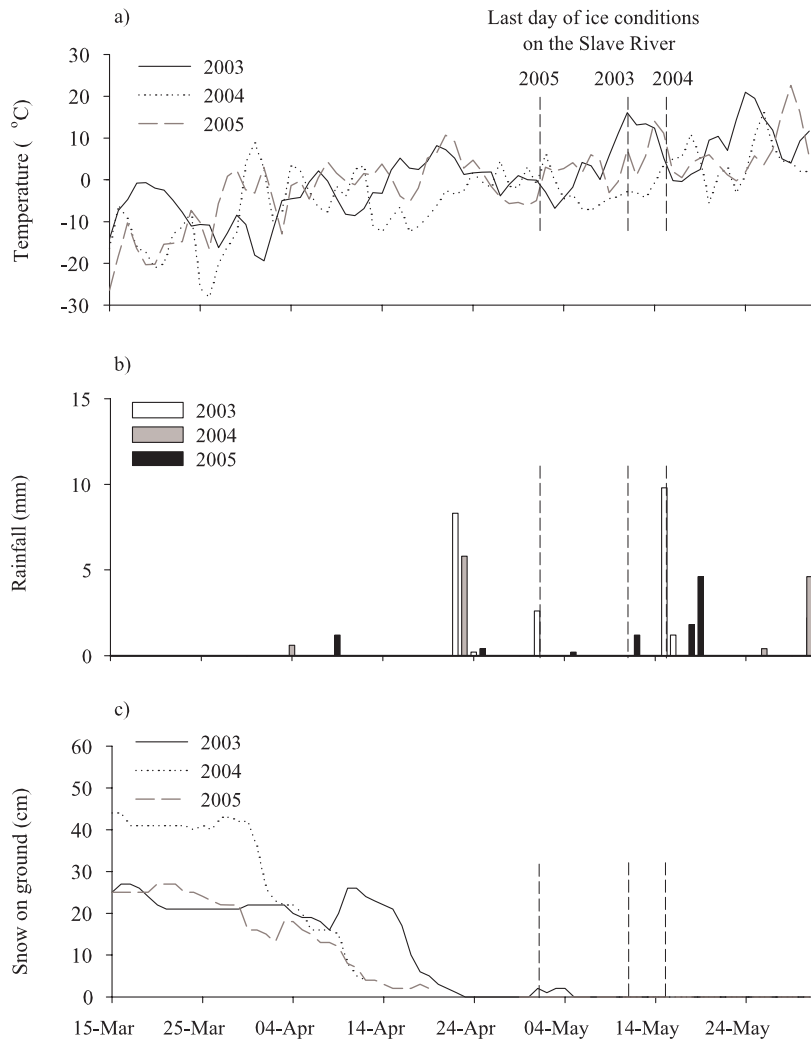


Figure 3.2. Daily a) temperature (°C), b) rainfall (mm) and c), snow depth (cm) for Hay River, NWT during the spring thaw period for 2003-2005 (Environment Canada, 2005).

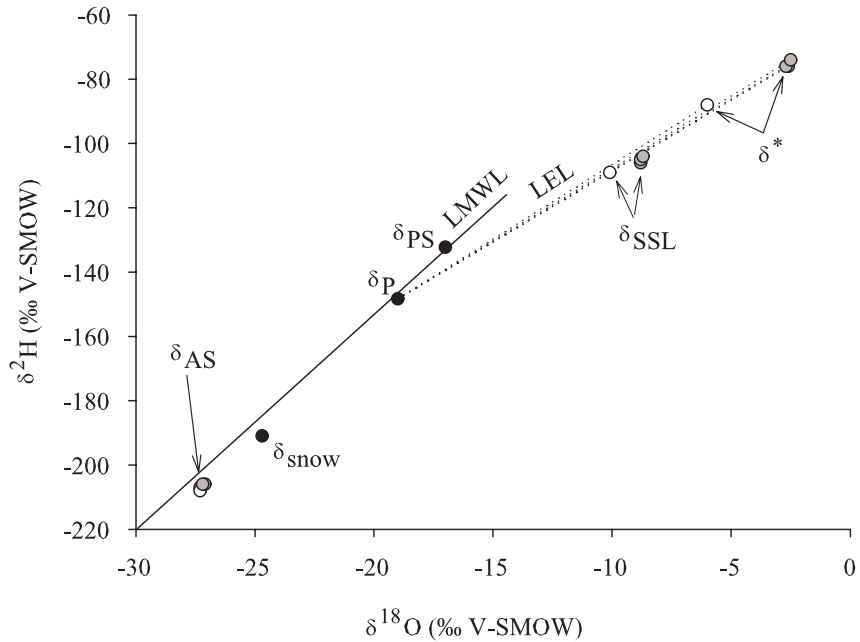


Figure 3.3. Isotopic frameworks for the SRD during 2003-2005. Parameters include the isotopic composition of amount-weighted mean annual precipitation (δ_P ; $\delta^{18}\text{O}$, $\delta^2\text{H} = -19.0\text{‰}$, -148‰ ; Birks et al., 2004), flux-weighted thaw season precipitation (δ_{PS} ; $\delta^{18}\text{O}$, $\delta^2\text{H} = -17.0\text{‰}$, -132‰ ; Gibson and Edwards, 2002), and the calculated steady state and limiting isotopic compositions (δ_{SSL} and δ^*). The average isotopic composition of snow (δ_{snow}) from samples collected from the SRD in May 2004 is also shown. Open circles show values calculated based on climate normal (1971-2000) conditions (Environment Canada, 2002), while shaded circles show values calculated using flux-weighted thaw season climate conditions for 2003-2005 (Environment Canada, 2005).

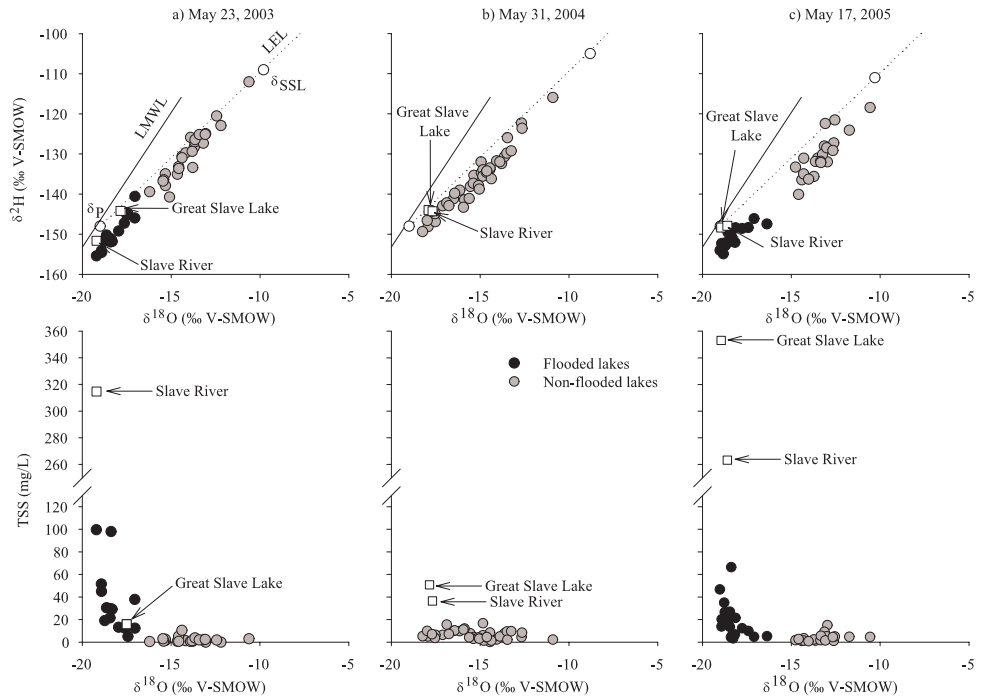


Figure 3.4. Water isotope and TSS results from regional sampling campaigns on a) 23 May 2003, b) 31 May 2004 and c) 17 May 2005. Isotope results are superimposed on year-specific isotopic frameworks (see Figure 3.3), with framework parameters shown as open circles. Great Slave Lake and the Slave River values are shown as open squares and are labelled. Measured lakewater values are shown as closed circles.

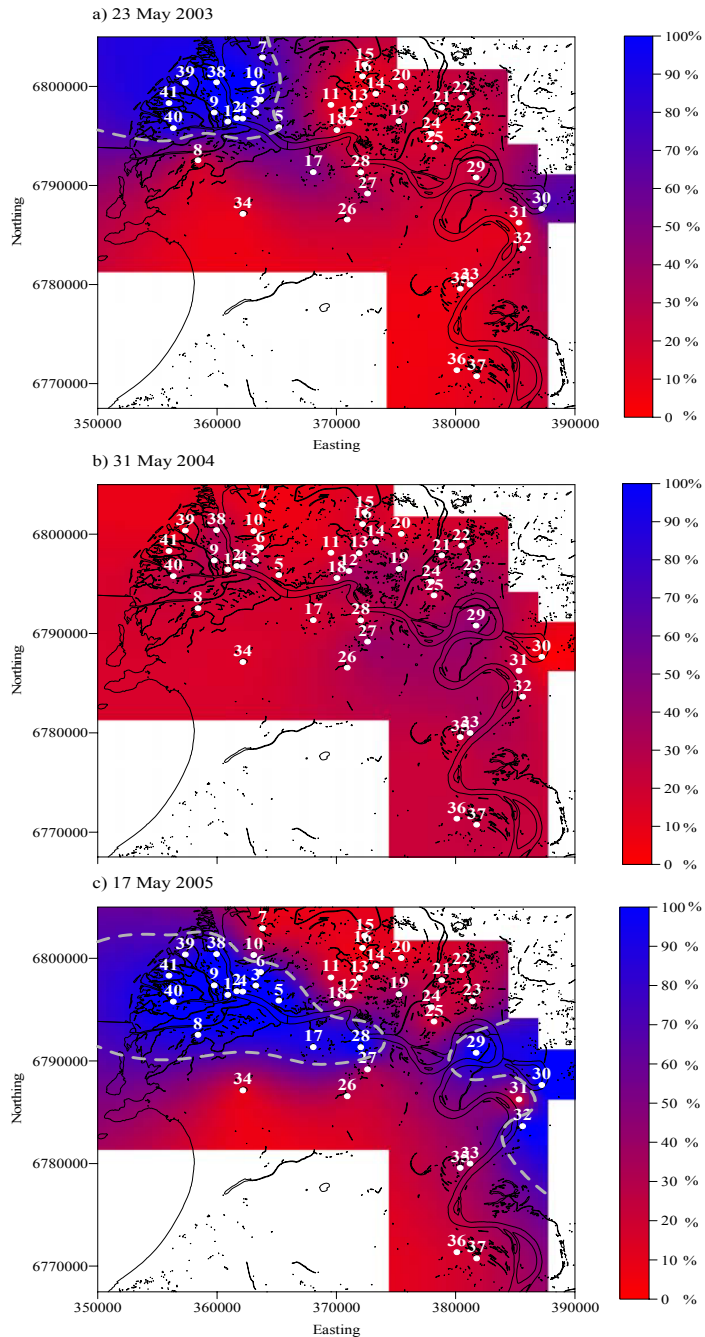


Figure 3.5. Percent dilution of lakewater by river flooding and snowmelt on a) 23 May 2003, b) 31 May 2004 and c) 17 May 2005. The observed spatial extent of flooding in 2003 and 2005 corresponds with the 70% dilution isoline, shown as a dashed grey contour in a) and c).

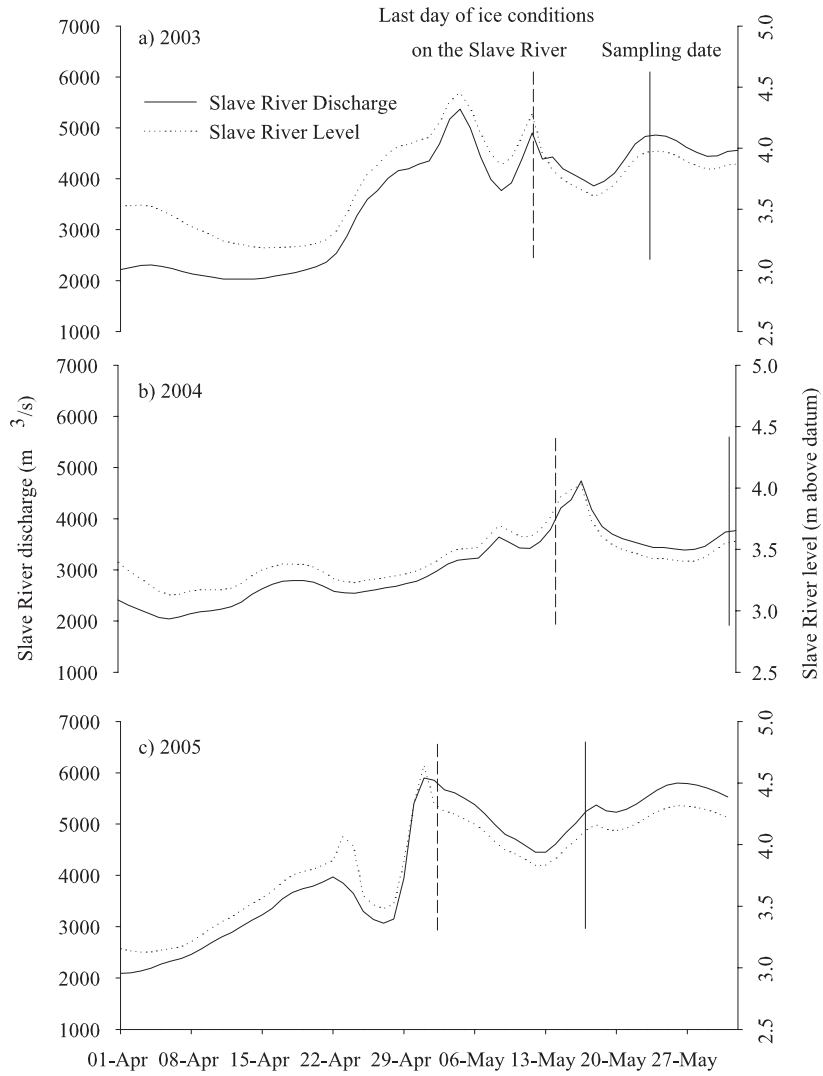


Figure 3.6. Slave River discharge and level during the spring melt period (April-May), 2003-2005, measured at Fitzgerald, AB (Water Survey of Canada, 2006).

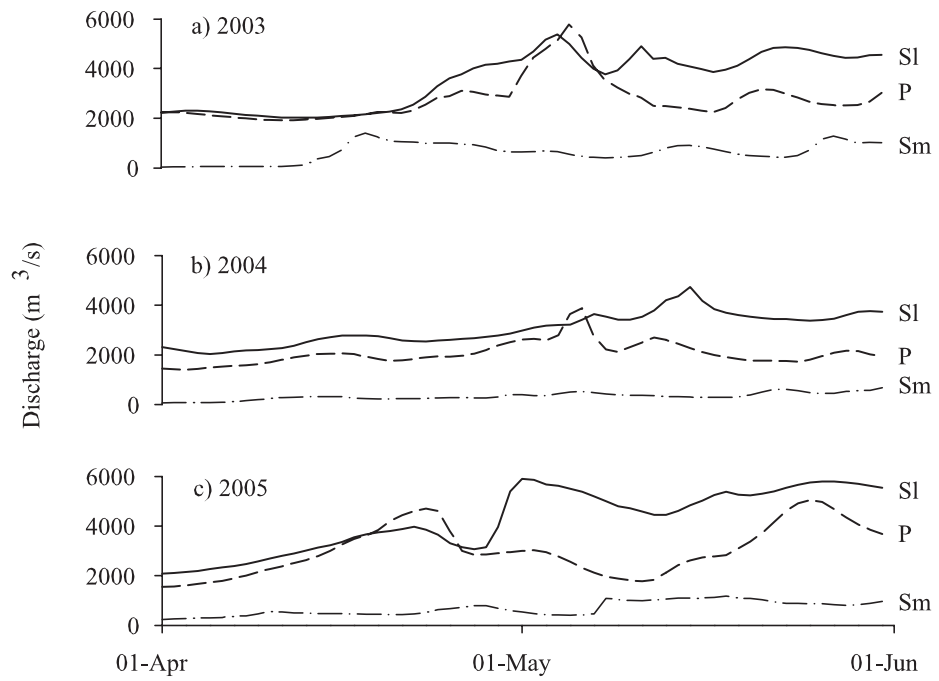


Figure 3.7. Spring discharge on the Slave (SI), Peace (P) and Smoky (Sm) Rivers, 2003-2005 (Water Survey of Canada, 2006).

Figure 8 TOP

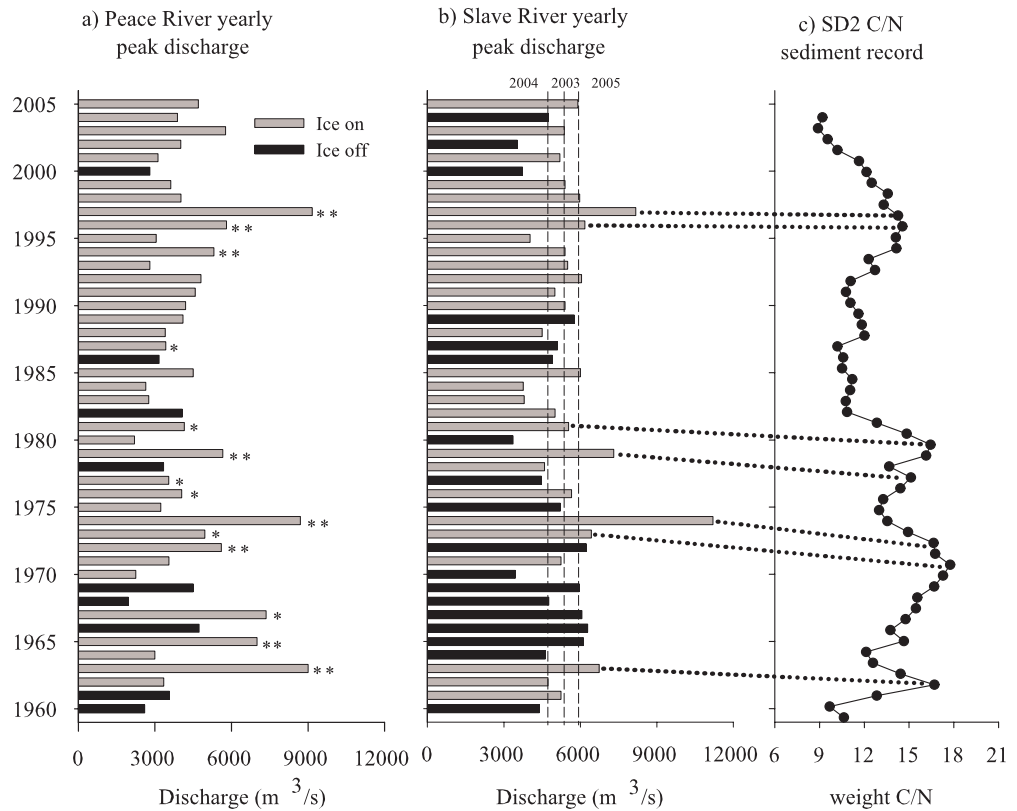


Figure 3.8. Maximum discharge (m^3/s) measured in a) the Peace River at Peace Point, AB and b) the Slave River at Fitzgerald, AB (Water Survey of Canada, 2006) during the period 14 days prior to and three days after the disappearance of solid and floating ice. Grey bands indicate years in which peak discharge occurred while river ice cover was intact, while black bands represent years in which peak discharge occurred following the disappearance of river ice cover. Thus, the likelihood of widespread flooding is greatest during years when high levels of peak discharge occur while river ice cover is still intact (e.g., 2005 for the SRD). Peak discharge conditions measured on the Slave River during 2003-2005 monitoring period are indicated by dashed lines on b). Spring ice-jam floods (**) and lower magnitude flood events (*) observed in the PAD (Peters, 2003; Beltaos et al., 2006a; Wolfe et al., 2006) are indicated on a). Plot c) shows weight C/N ratios measured on sediments collected from a flood-dominated SRD lake dated using ^{137}Cs (Mongeon, 2008; see Figure 3.1 for lake location). Peaks in C/N ratios are believed to closely correspond with peaks in Slave River discharge, as indicated by the dotted lines on b) and c).

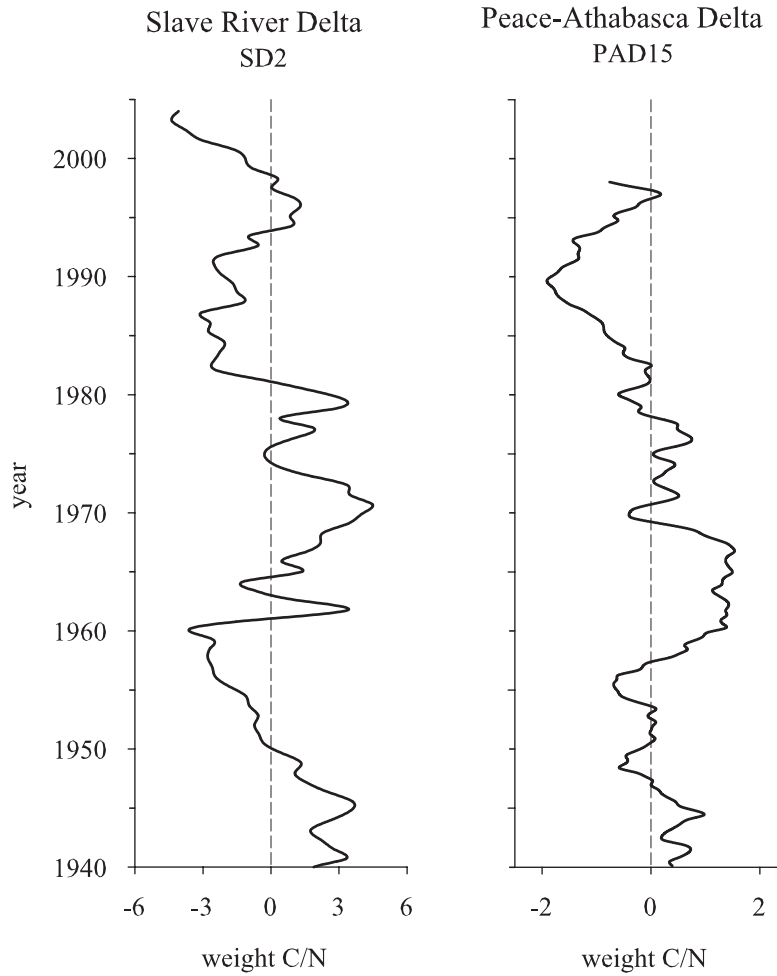


Figure 3.9. Weight C/N ratio sediment records to 1940 from flood-dominated lakes in a) the SRD (Mongeon, 2008; see Figure 3.1 for lake location) and b) the PAD (Wolfe et al., 2006), plotted relative to mean values. Note the PAD15 record has been smoothed by an 11-point running mean to achieve resolution comparable to the SD2 record.

Tables

Table 3.1. Flux-weighted thaw season temperature and relative humidity based on climate normal (1971-2000) conditions (Environment Canada, 2002) and conditions measured in 2003, 2004 and 2005 (Environment Canada, 2005) at Hay River, NWT. Data are flux-weighted based on potential evaporation, using methods described by Malmstrom (1969) and Dingman (1993).

	Temperature (°C)	Relative Humidity (%)
Climate normal	11.4	69.2
2003	13.4	62.8
2004	12.6	63.2
2005	11.9	63.0

Table 3.2. Isotopic framework parameters for 2003-2005.

Parameter	2003	2004	2005
T (K)	286.55	285.78	285.05
h	0.628	0.632	0.630
$\alpha^*_{L-V} (^{18}\text{O}, ^2\text{H})$	1.0104, 1.0925	1.0105, 1.0935	1.0105, 1.0944
$\varepsilon^*_{L-V} (^{18}\text{O}, ^2\text{H})$	10.39, 92.46	10.47, 93.46	10.54, 94.42
$\varepsilon_{K-LV} (^{18}\text{O}, ^2\text{H})$	5.28, 4.65	5.23, 4.60	5.25, 4.63
$\delta_{AS} (^{18}\text{O}, ^2\text{H})$	-27.1‰, -206‰	-27.2‰, -206‰	-27.3‰, -207‰
$\delta^* (^{18}\text{O}, ^2\text{H})$	-2.6‰, -76‰	-2.7‰, -76‰	-2.5‰, -74‰
$\delta_{SSL} (^{18}\text{O}, ^2\text{H})$	-8.8‰, -106‰	-8.9‰, -105‰	-8.7‰, -104‰
LEL equation	$\delta^2\text{H} = 4.13 \delta^{18}\text{O} - 69.74$	$\delta^2\text{H} = 4.19 \delta^{18}\text{O} - 68.71$	$\delta^2\text{H} = 4.33 \delta^{18}\text{O} - 65.94$

Table 3.3. Peak Slave River discharge and last day of observed ice cover for the 2003-2005 spring melt periods (Water Survey of Canada, 2006) and dates of SRD regional water sampling campaigns.

	SR discharge peak (m ³ /s)	Date	Ice breakup	Regional sampling date
2003	5370	May 4	May 11	May 23
2004	4740	May 15	May 15	May 31
2005	5900	May 1	May 1	May 17

Chapter 4: Multi-year landscape-scale assessment of lakewater balances in the Slave River Delta, NWT, using water isotope tracers

Complete citation: Brock BE, Yi Y, Clogg-Wright KP, Edwards TWD, Wolfe BB. 2009. Multi-year landscape-scale assessment of lakewater balances in the Slave River Delta, NWT, using water isotope tracers. *Journal of Hydrology* 379: 81-91.

Introduction

Lakes, wetlands and other riparian freshwater ecosystems are ubiquitous in Canada's north. Freshwaters cover ~350,000 km² in arctic and subarctic North America (Rouse et al., 1997), while wetlands are estimated to cover ~3.5 million km² in the circumpolar Arctic (Huntington and Weller, 2005). These ecosystems provide a rich diversity of habitats, which support biota that have developed a wide range of adaptations for survival in sometimes-severe northern environments (Wrona et al., 2005). Northern freshwater ecosystems provide important permanent and migratory habitats for fish and wildlife populations, notably for migrating waterfowl (Townsend, 1984; Prowse and Conly, 2000; Huntington and Weller, 2005; Wrona et al., 2005). These populations are in turn of vital importance to northern indigenous populations (Rouse et al., 1997; Huntington and Weller, 2005; Wrona et al., 2005), who have been using these resources to support traditional lifestyles for millennia.

Recent studies have highlighted the potential consequences of climate change on lake levels in northern Canadian freshwater ecosystems. Smol and Douglas (2007) documented the disappearance of high Arctic ponds on Ellesmere Island that had existed for thousands of years, as a result of climate change. Emmerton et al. (2007) concluded that water storage in Mackenzie Delta lakes and channels is likely to decline, resulting in lower lake levels, as reductions in spring break-up flood stage and increases in open-water evaporation continue. In the Peace-Athabasca Delta, the combined effects of

declining headwater snowpacks and glacial storage, decreased river discharge and changes in local climate are leading to drying in delta lakes (Wolfe et al., 2008a). These and other studies (e.g., Smith et al., 2005) provide compelling evidence that profound changes are occurring in the hydrology of northern freshwater ecosystems.

The Slave River Delta (SRD) is a key hydrological node at the terminus of the Peace-Athabasca-Slave river corridor, and is subject to multiple stressors, including flow regulation and water extraction, in addition to climate change. Hundreds of shallow lakes in the SRD are part of an important ecosystem that provides significant migratory, breeding and year-round habitats for birds and mammals (Townsend, 1984), upon which the residents of nearby Fort Resolution depend for both recreation and income (Wesche, 2007). Since the mid-1970s, declining snowpacks have been observed in key tributaries of the Peace River (Romolo et al., 2006a), which provides ~66% of annual flow to the Slave River (English et al., 1997). Because melting of the winter snowpack is an important factor influencing spring river discharge, declining snowpacks will alter the hydrograph of both the Peace and Slave rivers during the spring break-up period (Prowse and Conly, 1998; see also Figure 3 in Wolfe et al., 2008a). Flow regulation in the northern headwaters of the Peace River system by the WAC Bennett Dam, established in 1968, may also have affected the geomorphological and botanical evolution of the SRD (English et al., 1997), although paleolimnological studies do not indicate that flood frequency has declined over the past ~40 years (Brock et al., in press; see Chapter 5). Continued water diversion and extraction from the upstream Athabasca River to support the Alberta oil sands industry may threaten the ecological integrity of the SRD, as may potential hydroelectric development along the Slave River near Fort Smith, NWT (Figure 4.1). Incomplete knowledge of the consequences of these stressors on the SRD ecosystem hampers informed water resource management.

In response to this need, research activities in the SRD have been focused on understanding the crucial role of water in the ecosystem (Wolfe et al., 2007a). Stable isotope analysis of water collected in 2003 from a suite of study lakes spanning the active and relict SRD revealed the dominant hydrological factors controlling delta lakewater balances (Brock et al., 2007; see Chapter 2). These include evaporation, river flooding during the spring break-up period, and exchange with the Slave River, via direct channel connections, or with Great Slave Lake via seiche events. These results provided the basis for a lake classification scheme comprising evaporation-, flood- and exchange-dominated lakes (Brock et al., 2007; see Chapter 2). Continued monitoring of delta lakes during the 2003-2005 spring break-up period revealed a positive relationship between Slave River spring discharge and the spatial extent of river flooding in the SRD, and highlighted the importance of upstream runoff generation, relative to several other factors (e.g., local snowmelt runoff, ice thickness, temperature), in producing downstream flood events (Brock et al., 2008; see Chapter 3).

Here, we employ water isotope tracers to quantify the effect of river floodwater and snowmelt input on end-of-thaw-season (fall) SRD lakewater balances and identify areas of the delta susceptible to lake-level drawdown due to expected changes in river discharge and local climate. The isotope mass-balance model uniquely accounts for the varying role of local Great Slave Lake vapour on the individual lakewater balances. These results provide the basis for anticipating future evolution of the delta, and for informed water resource management decisions.

The Slave River Delta and Great Slave Lake

The SRD (61°15'N, 113°30'W) is an actively prograding fluvial delta (Figure 4.1) (Smith, 1991; Vanderburgh and Smith, 1988). The active delta, which occurs downstream of a major bifurcation of the Slave River into secondary distributary channels, currently covers approximately 400 km² (English et al., 1997), while relict alluvial and deltaic sediments extend

approximately 250 km upstream to Fort Smith, NWT (Vanderburgh and Smith, 1988). The SRD is infilling the southern arm of Great Slave Lake, the second largest lake in Canada. Great Slave Lake has a surface area of 28,400 km², a volume of 2088 km³ and a maximum depth of 614 m (CNCID, 1978).

Lakes in the SRD are typically small (<3 km²) and shallow (<4 m deep). Water isotope tracers, total inorganic suspended sediment concentrations and field observations have been used to characterize the dominant hydrological processes affecting lakewater balances and thus classify SRD lakes into three groups: flood-dominated, exchange-dominated and evaporation-dominated (Brock et al., 2007; see Chapter 2). Flood-dominated are lakes situated in the active delta, where levee heights separating the lake from the distributary channel network are typically 0.5–2.5 m above low summer Great Slave Lake water levels (English et al., 1997). These lakes are susceptible to spring flooding, which introduces isotopically-depleted Slave River water and high concentrations of total inorganic suspended sediment to the lake basin. Evaporation-dominated lakes are found in the relict delta, and have higher levee heights than flood-dominated lakes (2.5–3 m above low summer Great Slave Lake water levels (English et al., 1997)). Because of their sill elevations, evaporation-dominated lakes are rarely flooded by the Slave River, and instead receive inputs of catchment-sourced snowmelt in the spring. Water balances in these lakes during the open-water season are dominated by evaporation, leading to increased end-of-season isotopic enrichment in evaporation-dominated lakes when compared with flood-dominated lakes. Exchange-dominated lakes are situated along the Slave River and the delta front. Lakes with direct channel connections to the Slave River receive river water throughout the thaw season (with the strength of the channel connection controlling the amount of river water input to the lake). Exchange-dominated lakes along the outer edges of the delta receive periodic inputs of Great Slave Lake water during seiche events (Gardner et al., 2006). Groundwater exchange is minimal because of the low hydraulic conductivity of the alluvial sediments of the delta, and the occurrence of discontinuous permafrost (Day, 1972).

The SRD experiences cold winters (mean January temperature = -23.1°C) and cool summers (mean July temperature = 15.9°C). Precipitation is evenly divided between rain and snow, with a total of 320 mm falling annually, based on 1971-2000 Canadian Climate Normals for Hay River (Environment Canada, 2002). Similar thaw season conditions prevailed during 2003-2005. While thaw season temperature during the monitoring period was comparable to climate normal conditions, evaporation-flux-weighted relative humidity was several percent lower (Table 4.1). Spring flood conditions were also different in each year of the monitoring period. Aerial distribution maps of the spatial extent of flooding, determined using water isotope tracers, were presented in Brock et al. (2008; see Chapter 3) and show that a moderate spring break-up flood occurred in 2003 and a significant spring ice-jam flood in 2005. No flooding occurred in 2004.

Water sample collection and meteorological data

Lakewater samples were collected for oxygen and hydrogen stable isotope analysis from 40 SRD lakes, which included all three hydrological lake types (flood-dominated lakes = 12; evaporation-dominated lakes = 24; exchange-dominated lakes = 4), as well as Great Slave Lake and the Slave River (Figure 4.1), on multiple occasions during the 2003-2005 ice-free seasons. Results from samples collected near the end of the thaw season, on 15 August 2003, 20 September 2004 and 22 September 2005, are the focus here, and build upon previously published datasets (Brock et al., 2007; 2008; see Chapters 2 and 3). Samples were collected by helicopter from approximately 10 cm below the surface at the centre of each lake, and were sealed in 30 mL high density polyethylene bottles for analysis of $^{18}\text{O}/^{16}\text{O}$ and $^2\text{H}/^1\text{H}$ ratios at the University of Waterloo's Environmental Isotope Laboratory following standard procedures (Drimmie and Heemskerk, 1993; Morrison et al., 2001). Results are reported as δ values, representing deviations in per mil (‰) between the sample and the V-SMOW standard on a scale normalized to Standard Light Antarctic

Precipitation ($\delta^{18}\text{O}$, $\delta^2\text{H} = -55.5\text{‰}$, -428‰) (Coplen, 1996). Analytical uncertainties are $\pm 0.2\text{‰}$ for $\delta^{18}\text{O}$ and $\pm 2\text{‰}$ for $\delta^2\text{H}$.

Thaw season temperature and relative humidity data were collected from Hay River, NWT (Environment Canada, 2002, 2005), where data records are more complete than at Fort Resolution airport. To reflect climate conditions during which open-water evaporation occurs from delta lakes (following recommendations by Gibson (2002)), temperature and relative humidity data were evaporation-flux-weighted prior to their inclusion in isotope mass-balance calculations. Evaporation-flux-weighted values were determined from potential evapotranspiration using methods described by Malmstrom (1969) and Dingman (1993). The isotopic composition of yearly amount-weighted precipitation was estimated from data collected at a Canadian Network for Isotopes in Precipitation (CNIP) station at Fort Smith, NWT (Birks et al., 2004).

Results and discussion

Spring and fall 2003-2005 lakewater isotopic compositions

Results from isotopic analysis of water samples collected from SRD lakes in the spring and fall of 2003-05 capture early and late thaw-season lake water balance conditions (Figure 4.2). The early-season isotopic composition of delta lakes that were flooded by the Slave River in 2003 and 2005 show distinct clusters of lakes that are more isotopically-depleted than non-flooded lakes (Figures 2a, c). In the absence of spring flooding in 2004, lakewater results form a continuous gradient in δ - δ space (Figure 2b).

Fall lakewater isotopic compositions in the SRD have been linked to spring break-up conditions, which influence subsequent evaporative enrichment as the thaw season progresses (Brock et al., 2007; see Chapter 2). In the fall, lakes that were flooded during the spring of 2003 and 2005 continue to be more isotopically-depleted than non-flooded lakes, and are more tightly clustered (Figure 4.2d, f). For all lakes in 2004, and for non-flooded lakes in 2003 and 2005, isotopically-depleted snowmelt from each lake's catchment was the

dominant input during the spring break-up period (Brock et al., 2008; see Chapter 3). By fall, although these lakes have undergone evaporative enrichment, they continue to form a gradient in δ - δ space, in part reflecting the persistent influence of snowmelt from the preceding spring. Lakes with more isotopically-depleted lakewater signatures likely received more spring snowmelt, while more evaporatively enriched lakewater signatures likely reflect lakes that received less spring snowmelt input. Those lakes with the most isotopically-enriched signatures are not exclusively the smallest lakes in the dataset, thus volumetric differences are unlikely to account for patterns in isotopic data. Rather, these patterns reflect a lake's hydrologic setting in the delta landscape, as discussed in more detail below.

In addition to the hydrological influence of spring break-up conditions, direct channel connections between SRD lakes and the distributary channel network (SD10, SD17 and SD28; Figure 4.1) or Great Slave Lake via seiche events (SD39 and SD41; Figure 4.1) also exert strong controls on late-season lakewater isotopic compositions. In 2003, 2004 and 2005, lakewater compositions of some exchange-dominated SRD lakes (SD39 and SD41) are close to the isotopic compositions of the Slave River and Great Slave Lake (Figure 4.2), reflecting the isotopically-depleted dominant input water source to these lakes (i.e., Slave River or Great Slave Lake water). However, in some exchange-dominated SRD lakes, channel connections are long and shallow (SD10, SD17 and SD28) and low late-summer water levels and emergent vegetation growing in the connecting channels impede exchange with the Slave River. This allows for more evaporative enrichment in these lakes than in other lakes where more direct connections to the Slave River are maintained (Brock et al., 2007; see Chapter 2; Figure 4.2).

Quantifying lakewater balances using water isotope tracers

An isotope-mass-balance model was used to quantify lakewater balances during the late-season sampling period. The evaporation-to-inflow (E/I) ratio of

a well-mixed lake at isotopic steady-state is

$$E/I = \left(\frac{\delta_I - \delta_L}{\delta_E - \delta_L} \right) \quad (1)$$

This equation reflects the isotopic compositions of key water budget components, including input water (δ_I), lakewater (δ_L) and the evaporating flux (δ_E). This approach has been applied frequently to assess water balances of lakes (Gonfiantini, 1986; Gibson and Edwards, 2002; Wolfe et al., 2007b; Yi et al., 2008). Mass and isotope conservation dictate that E/I ratios calculated for both $\delta^{18}\text{O}$ - and $\delta^2\text{H}$ -based parameters should be identical, thereby establishing the relationship

$$\frac{\delta^{18}\text{O}_I - \delta^{18}\text{O}_L}{\delta^{18}\text{O}_E - \delta^{18}\text{O}_L} = \frac{\delta^2\text{H}_I - \delta^2\text{H}_L}{\delta^2\text{H}_E - \delta^2\text{H}_L} \quad (2)$$

(Yi et al., 2008).

Solving equations (1) and (2) requires values for δ_L , δ_I and δ_E . The isotopic composition of lakewater can be readily measured. The composition of input water is more difficult to quantify, as it can originate from several different water sources, but can be estimated from the intersection of a regression through a series of lakewater samples and the Local Meteoric Water Line, which approximates the relationship between $\delta^{18}\text{O}$ and $\delta^2\text{H}$ in local precipitation (Gibson et al., 1993). Alternatively, δ_I can be calculated using a variation of the isotope-mass-balance model presented here (Yi et al., 2008). δ_E is commonly estimated from the linear resistance model of Craig and Gordon (1965), using

$$\delta_E = \frac{(\delta_L - \varepsilon^*)/\alpha^* - h\delta_A - \varepsilon_K}{1 - h + \varepsilon_K} \quad (3)$$

(Gonfiantini, 1986). (Equations expressed here are formulated for δ and ε values in decimal notation. δ -values are multiplied by 1000 and expressed in per mil (‰).) α^* , the equilibrium liquid-vapour fractionation, can be calculated using empirical equations given by Horita and Wesolowski (1994). ε^* and ε_K

describe equilibrium and kinetic separation, respectively, between the liquid and vapour phases. The former is related to α^* by $\varepsilon^* = \alpha^* - 1$, while the latter is defined as $\varepsilon_K^{18} = 0.0142 (1 - h)$ and $\varepsilon_K^2 = 0.0125 (1 - h)$ (Gonfiantini, 1986; Araguás-Araguás et al., 2000). (Note that we are referring specifically to liquid-vapour fractionation; i.e., $\alpha^* > 1$.) In cold regions that experience extended periods of ice cover, the isotopic composition of atmospheric vapour (δ_A) is commonly assumed to be in isotopic equilibrium with the isotopic composition of summer precipitation (δ_{PS}), and can therefore be estimated as $\delta_A = (\delta_{PS} - \varepsilon^*)/\alpha^*$ (Gibson, 2002a; Gibson and Edwards, 2002).

This approach to quantifying lakewater balances assumes lakes are well-mixed, and are at isotopic and hydrologic steady-state (Gonfiantini, 1986). By late fall, the water balances of most SRD lakes are more likely to approximate isotopic steady-state, thus justifying the use of this approach to model seasonal water balances as ‘quasi-steady-state’.

Resolving isotope-mass-balance calculations using a vapour mixing model

To quantify the effect of river flooding on late-season SRD lakewater balances and to identify areas of the delta undergoing lake-level drawdown, evaporation-to-inflow (E/I) ratios were calculated for delta lakes using Equation (1) incorporating the measured fall 2003, 2004 and 2005 lakewater isotopic compositions (δ_L). As presented above, this required defining the isotopic compositions of input water (δ_I) and evaporated vapour (δ_E), as well as the isotopic composition of atmospheric vapour (δ_A). Proper characterization of these parameters required careful consideration of the hydrological setting and synoptic climatology of the SRD and surrounding region, as detailed below.

The isotopic composition of input water (δ_I)

For the SRD, the amount-weighted annual precipitation composition (δ_P) measured at the closest CNIP station in Fort Smith, NWT (Figure 4.1) provides one possible value for δ_I ($\delta^{18}\text{O} = -19.0\text{‰}$; $\delta^2\text{H} = -148\text{‰}$; Birks et al., 2004). Based on a regression through all samples collected in fall 2003-2005 from

SRD lakes, this intersection lies at -20.0‰ for $\delta^{18}\text{O}$ ($\delta^2\text{H} = -153\text{‰}$), which is very similar to the CNIP-measured δ_{p} . The slightly more depleted regression-based input estimate probably reflects contributions of early spring snowmelt input to delta lakes, described in the previous section, which can influence lakewater balances into mid-summer (Brock et al., 2007; see Chapter 2). Here we apply the CNIP-measured δ_{p} value to our analysis, because of the close agreement between the CNIP δ_{p} value and the regression-based δ_{i} estimate. This value is also reasonable for flood- and exchange-dominated lakes, although other key input sources have been identified for these lakes (Brock et al., 2007; see Chapter 2). The average spring Slave River isotopic composition, the input source for flood-dominated lakes, is very similar to that of δ_{p} (average Slave River $\delta^{18}\text{O} = -17.4\text{‰}$, $\delta^2\text{H} = -141$), which becomes the input water source for flood-dominated lakes in the absence of flooding and following the spring break-up period. Slave River inputs are also strongest in exchange-dominated lakes in the spring, before vegetative growth in connecting channels later in the thaw season impedes water flow (Brock et al., 2007; see Chapter 2). In these lakes, and in seiche-affected lakes, end-of-thaw-season input waters are a mixture of δ_{p} and Slave River or Great Slave Lake water ($\delta^{18}\text{O}_{\text{GSL}} = -17.5\text{‰}$; $\delta^2\text{H}_{\text{GSL}} = -141\text{‰}$). Because the proportion of both input sources will vary for each exchange-dominated lake, reflecting local catchment characteristics and the spatial distribution of late-season rainfall, it is difficult to estimate the exact input composition to these lakes, although it should be similar to CNIP δ_{p} .

The isotopic composition of atmospheric moisture (δ_{A})

Careful consideration is also required in the quantification of δ_{A} because E/I results are sensitive to this parameter (Gibson et al., 1993). In the SRD, the proximity of the delta to Great Slave Lake suggests that the development of local δ_{A} may be more complex than the simple formation of vapour in equilibrium with local δ_{p} , as Great Slave Lake evaporate contributes isotopically-depleted atmospheric vapour. The contributions of isotopically-depleted local evaporate have also been observed in the Amazon Basin of South

America (Gat and Matsui, 1991), the Great Lakes region of North America (Gat et al., 1994), the Mediterranean (Gat et al., 2003), Madagascar (Vallet-Coulomb et al., 2006; 2008), and California and Nevada (Ingraham and Taylor, 1991). For the present study, this notion is supported by evidence for lake-effect precipitation events, which have been observed in the SRD and Fort Resolution (Brock et al., 2007; see Chapter 2). Additionally, wind-forced seiche events promote water exchange between Great Slave Lake and lakes along the outer fringes of the SRD (e.g., SD39, SD41; Figure 4.1), where levee heights are at or within 0.1 m of Great Slave Lake low summer water levels (English et al., 1997). Wind-forced seiche events are most common in late summer and early autumn, and are typically set up by northwesterly winds (Gardner et al., 2006).

Given that vapour from Great Slave Lake (δ_{E-GSL}) is transported to the delta by prevailing northwest winds, ambient atmospheric vapour (δ_{A-amb}) in the SRD would then comprise contributions from both advected atmospheric vapour (δ_{A-adv}) and δ_{E-GSL} , and thus should fall along a mixing line between the two (Figure 4.3). It is also reasonable to expect local variability in δ_{A-amb} in response to a number of factors, including distance from Great Slave Lake, prevailing wind patterns and synoptic climate conditions. Mixing between these two potential sources of vapour can be described as

$$\delta^{18}O_{A-amb} = f\delta^{18}O_{E-GSL} + (1-f)\delta^{18}O_{A-adv} \quad (4a)$$

$$\delta^2H_{A-amb} = f\delta^2H_{E-GSL} + (1-f)\delta^2H_{A-adv} \quad (4b)$$

where δ_{A-amb} represents ambient atmospheric vapour for each SRD study lake as a function of the fraction of mixing (f) between the two potential vapour sources, δ_{E-GSL} and δ_{A-adv} . A linear system of Equations (2), (4a) and (4b) can be developed, thus producing a unique solution for $d^{18}O_{A-amb}$, d^2H_{A-amb} and f for each SRD study lake. We refer to this approach as the coupled-tracers method, which is a variation of the approach applied by Yi et al. (2008) to the upstream Peace-Athabasca Delta.

In an isotopic survey of lakes in northern Canada, Gibson and Edwards (2002) defined the isotopic composition of δ_{A-adv} as being in equilibrium with thaw season precipitation (δ_{PS} ; Birks et al., 2004), assuming evaporation-flux-weighted temperature, thereby reflecting conditions under which evaporation occurs. This definition of δ_{A-adv} was initially used to calculate the advected vapour composition (Table 4.2). However, when this value is applied using Equations (4a) and (4b) to calculate lake-specific ambient atmospheric vapour conditions for SRD lakes, results span a large isotopic range and are poorly constrained around the LWML (Figure 4.4), and many are not positioned between the two likely sources of vapour (Figure 4.3). These results signify that this definition of δ_{A-adv} , in equilibrium with local δ_{PS} , does not properly characterize atmospheric conditions in the SRD. However, when δ_{A-adv} is defined by equilibrium with amount-weighted (yearly) precipitation (δ_P) (Table 4.2), δ_{A-amb} results cluster around the LMWL (Figure 4.4b) and are much more effectively constrained by the two end-member vapour sources (Figure 4.3). These results indicate that vapour comprising varying mixtures of advected vapour in approximate equilibrium with δ_P and locally derived vapour from Great Slave Lake is a more appropriate characterization of atmospheric conditions in the SRD.

These results also suggest that advected vapour in the SRD develops in an area where δ_{PS} is isotopically similar to the delta's δ_P . Dominant northwesterly winds, especially in the later part of the thaw season (Gardner et al., 2006), likely introduce atmospheric vapour to the SRD that originates in areas having more isotopically-depleted thaw season precipitation. Data interpolated from northern CNIP stations show areas where $\delta_{PS} \sim -19\text{‰}$ for $\delta^{18}\text{O}$ span a swath from south-central Yukon across the Northwest Territories, including Great Bear Lake, and north to the southwest tip of Victoria Island (Figure 4.5; Gibson and Edwards, 2002). When dominant wind directions are considered, it is probable that the majority of advected vapour introduced to the SRD originates in the central Northwest Territories.

Results for lake-specific δ_{A-amb} are very similar in the three monitoring years (Figure 4.4) because thaw season temperature and relative humidity conditions were remarkably similar (Table 4.1). In all three years, advected atmospheric vapour is the dominant source of ambient vapour for SRD lakes, accounting for ~55-100% of δ_{A-amb} , while evaporate from Great Slave Lake contributes ~0-45%. These results are similar to other aforementioned studies examining recycling of evaporated vapour from large water bodies (Table 4.3). While δ_{A-amb} likely represents the greatest uncertainty in our isotope mass-balance calculations, results described below effectively capture hydrological differences across this complex landscape.

Quantification of E/I ratios for SRD lakes, 2003-2005

E/I ratios calculated for SRD lakes using lake-specific δ_{A-amb} reveal systematic patterns in late-season lakewater balances associated with the different hydrological categories (Figure 4.6). All exchange-dominated lakes, where connectivity is facilitated via direct channel connections to the Slave River, or by seiche events on Great Slave Lake, have *E/I* ratios less than 1 for all three monitoring years (Figure 4.6). However, results are typically lower in lakes where seiche events are the primary mechanism controlling water exchange. The consistency of low *E/I* ratios in seiche-affected lakes during the fall monitoring period (*E/I* range = 0.06 – 0.18) is likely related to the increased frequency of seiche events in the SRD during this part of the ice-free season (Gardner et al., 2006). In river-connected lakes, the strength of the channel connection likely controls the degree of variability in *E/I* ratios at each lake over the monitoring period. Dense stands of emergent aquatic vegetation grow in the channel connections of SD17 and SD28, and are likely also present in the channel connecting SD10 and the Slave River, which impedes Slave River inputs to each lake. However, exchange continues to be the dominant hydrological process controlling these lakes, which is reflected by their low *E/I* ratios (*E/I* range = 0.17 – 0.53).

E/I ratios for flood-dominated lakes are also consistently below 1, reflecting the dominance of flood inputs to lakewater balances (with the exception of SD38 in 2004 ($E/I = 0.98$); Figure 4.6), even though not all lakes in this category were known to have flooded during the spring break-up period in each of the monitoring years (see Figure 4.2). The average difference between the minimum and maximum *E/I* ratios for each lake in this category over the monitoring period is low (~ 0.30), also with the exception of SD38 (~ 0.69), in comparison to the evaporation-dominated lakes (~ 0.90). As expected, *E/I* ratios are highest in most flood-dominated lakes in 2004, a year in which there was no known spring flooding in the delta. In contrast, ratios are lowest in 2005, following a significant spring flood that replenished these lakes with Slave River water (Brock et al., 2008; see Chapter 3). A moderate spring flood in 2003 led to *E/I* ratios in these lakes that are more similar to results for 2005 than for 2004. Notably, these results confirm that even in late summer and fall, spring flood status affects the seasonal water balances of flood-dominated delta lakes (Brock et al., 2007; see Chapter 2).

There is considerably more variability in the *E/I* ratios of evaporation-dominated lakes compared to lakes in other hydrological categories (Figure 4.6), but no consistent yearly trends are evident. For example, lakes in this category that were flooded in 2005 (SD8, SD18, SD29 and SD32) do not show consistently low *E/I* ratios relative to their 2003 and 2004 ratios. However, there do appear to be two classes of lakes in this category. One group of lakes (lakes SD16 - SD25 on Figure 4.6) has generally lower *E/I* ratios with less variability (0.42 – 1.59) over the monitoring period than lakes in the second group (lakes SD14-SD35 on Figure 4.6), where the range in *E/I* ratios is much greater (0.47 – 6.08). The first group of lakes, where water balances for most lakes tend to cluster around $E/I = 1$, are mainly located adjacent to the Jean River, a distributary of the Slave River (Figure 4.1). The consistency of *E/I* ratios in lakes in this area indicates that these lakes may be influenced by greater amounts of snowmelt, which offsets the effects of evaporation. Many of the lakes in this area of the delta are surrounded by mature spruce forest, which

accumulates deeper winter snowpacks than other areas of the delta and likely results in more snowmelt input to local lakes in the spring. Snowmelt inputs are probably lower for the second group of lakes, which are generally located along the upstream Slave River, where forest vegetation is more sparse. Evaporative enrichment in these lakes is a more significant process controlling lakewater balances than snowmelt input.

Spatial patterns in spring flooding and fall E/I ratios across the delta over the three-year monitoring period can be used to examine how the degree of spring flooding influences late-season water balances in delta lakes (Figure 4.7). During the monitoring period, fall E/I ratios in the active delta are <1 , consistent with the hydrological classification of these lakes as flood-dominated. However, there are year-to-year differences in water balance status in lakes in this area of the delta. Spring flooding in 2005 was more spatially extensive than in 2003 (Figure 4.7a, c), which is reflected in lower fall E/I ratios in 2005 in several lakes adjacent to the Slave River upstream of the active delta. In the absence of spring flooding in 2004 (Figure 4.7b), flood-dominated lakes in the active delta attained slightly higher fall E/I ratios, although they are lower than those for evaporation-dominated lakes in the relict delta. This suggests the hydrological effects of flooding on lakewater balances in the active delta may persist in years following a flood event.

Under these circumstances, annual flooding may not be necessary to maintain the low, input-dominated water balances of flood-dominated lakes. However, because the monitoring period only included one flood-free year, it is unclear how long flood-dominated lakes would be capable of maintaining positive water balance conditions, particularly over several subsequent seasons with no spring break-up flooding. In the Mackenzie Delta, modeling studies have suggested that high-closure lakes could disappear within 10 years in the absence of flooding (Marsh and Lesack, 1996), depending on precipitation and catchment contributions. Elsewhere, in the Athabasca Delta, areas that have become less susceptible to river flooding in recent decades have undergone

drying (Wolfe et al., 2008b), whereas other lakes have persisted for hundreds of years (Wolfe et al., 2008a).

In contrast to the active delta, E/I ratios consistently exceed 1 along upstream reaches of the Slave River, and in some areas along the Jean River (northeast area of maps in Figure 4.7), reflecting the dominance of evaporation on lakewater balances in these regions of the delta (Figure 4.7d-f). The number of evaporation-dominated lakes with E/I ratios >1 increased from 2003 ($n = 10$) to 2005 ($n = 14$). These results, showing persistent non-steady-state evaporation along the Jean and upstream Slave rivers during the monitoring period, reveal that these areas may be most susceptible to drying, especially if snowmelt or thaw season precipitation inputs to these lakes decline over the course of several consecutive seasons, or if evaporation increases.

Conclusions and management recommendations

Quantifying fall lakewater balances provides important insight about landscape-scale hydrological processes that control SRD lakes and reveals that broad patterns are related to spring break-up flooding and hydrological setting. Low E/I ratios in exchange-dominated lakes in the active delta throughout the 2003-2005 monitoring period reflect both the strength of the lake-river channel connection and the increasing frequency of seiche events on Great Slave Lake in late summer and fall (Gardner et al., 2006). Although isotopic results from lakewater samples examined here were collected at the end of the thaw season, flood-dominated lakes in the active delta have persistently low E/I ratios. This reflects the role of spring flooding in re-setting the starting point for hydrological evolution of flood-dominated lakes throughout the thaw season. In 2004, in the absence of a spring break-up flood, lakewater balances in flood-dominated lakes continue to be positive. These results suggest that the hydrological influence of the previous year's flood persists in lakes in the absence of spring flooding, although several consecutive years with no flooding would likely lead to increased cumulative evaporation.

In contrast to flood-dominated lakes in the active delta, fall lakewater balances in evaporation-dominated lakes in the relict delta are highly variable and do not show consistent inter-annual trends. Rather, two classes of lakes appear to comprise this category of lakes. In lakes in the northeast sector of the delta, where lake catchments are largely composed of mature forest and entrainment of winter snowpacks is likely high, generally low variability is evident in lakewater balances at the end of the thaw season and over successive years. Snowmelt input may be lower for lakes along the upstream reaches of the Slave River, where mature forest is less prevalent, resulting in a greater range in E/I ratios in these lakes. Declining snowmelt inputs and increased evaporation in both classes of evaporation-dominated lakes have the potential to increase lake-level drawdown, and may promote drying of the relict delta. As we have demonstrated here and elsewhere (Brock et al., 2007; 2008; see Chapters 2 and 3), multi-seasonal and multi-annual surveys of lakewater isotope compositions have been extremely effective in deciphering the relative roles of hydrological processes on lakewater balances in this large, remote, northern freshwater landscape.

Results from these studies provide important context for policy regarding water resource management in the delta and along the upstream Slave River and its tributaries. For example, hydroelectric development on the Slave River and continued or increased water extraction and diversion associated with the Alberta oil sands production have the potential to alter the amount and timing of Slave River discharge. Because river discharge is positively correlated to spring flooding in the active delta (Brock et al., 2008; see Chapter 3), a decline in river discharge, particularly during the spring break-up period, will result in less frequent and less widespread flooding in the active delta. A decline in flood frequency and magnitude will cause the water balances of flood-dominated lakes in the active delta to, eventually, become increasingly influenced by evaporation, resulting in drier conditions in the active SRD. Increases in northern air temperatures, extending the ice-free season (ACIA, 2004), could exacerbate such conditions. Careful management of water

resources in the Peace-Athabasca-Slave river corridor requires recognition of such stressors and their potential impacts.

Figures

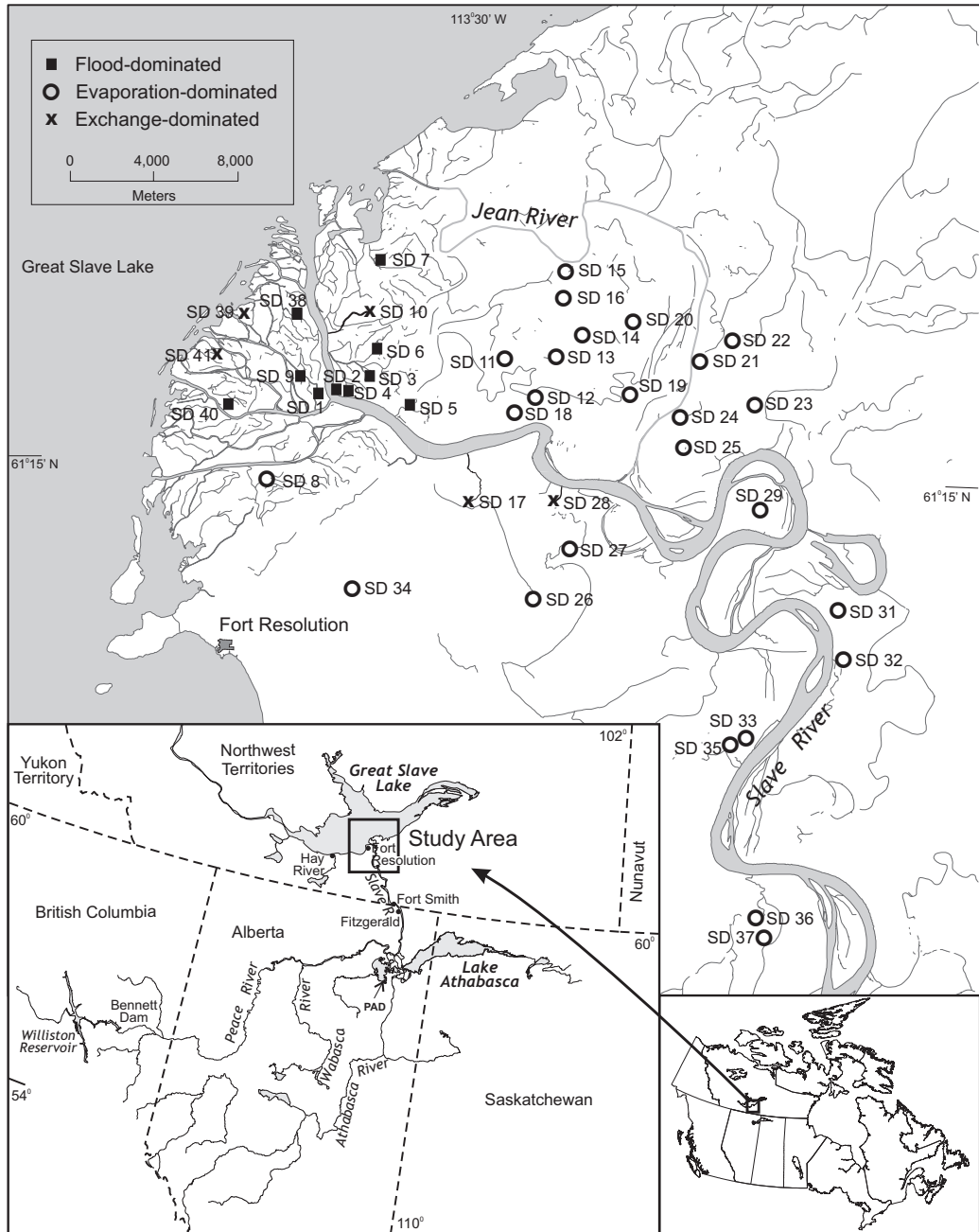


Figure 4.1. Location of the Slave River Delta, NWT, including lake and river sampling sites.

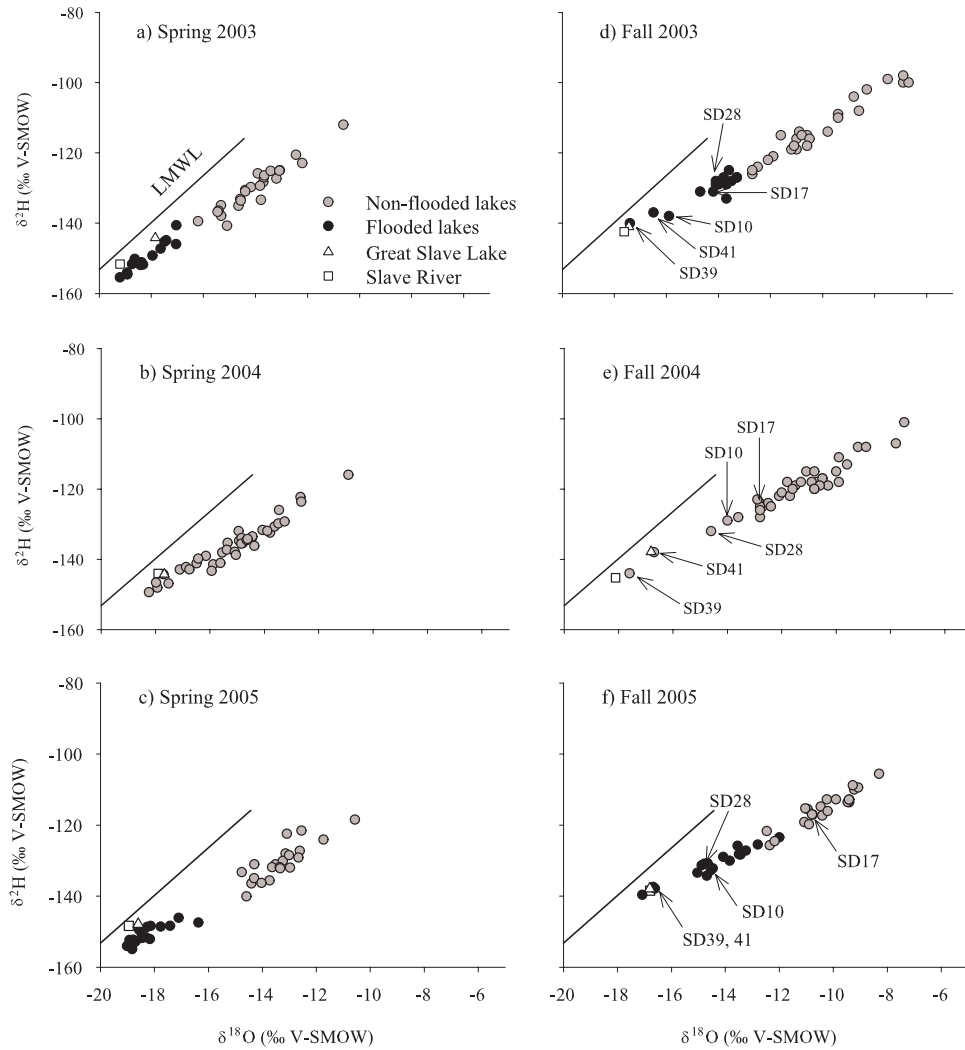


Figure 4.2. Water isotope results from SRD lakes in the spring of a) 2003, b) 2004 and c) 2005 (Brock et al., 2008; see Chapter 3), and the fall of the same years (d-f). Lakes that were flooded by the Slave River in the spring of each monitoring year are shown in black circles, while lakes that did not flood are shown in grey circles. No flooding occurred in 2004. Isotope results are shown relative to the Local Meteoric Water Line (LMWL: $\delta^2\text{H} = 6.7 \delta^{18}\text{O} - 19.2$; Birks et al., 2004), which approximates the relationship between $\delta^{18}\text{O}$ and $\delta^2\text{H}$ in local precipitation. Great Slave Lake and Slave River values are shown as open triangles and squares, respectively. Lakes identified in the text are labeled.

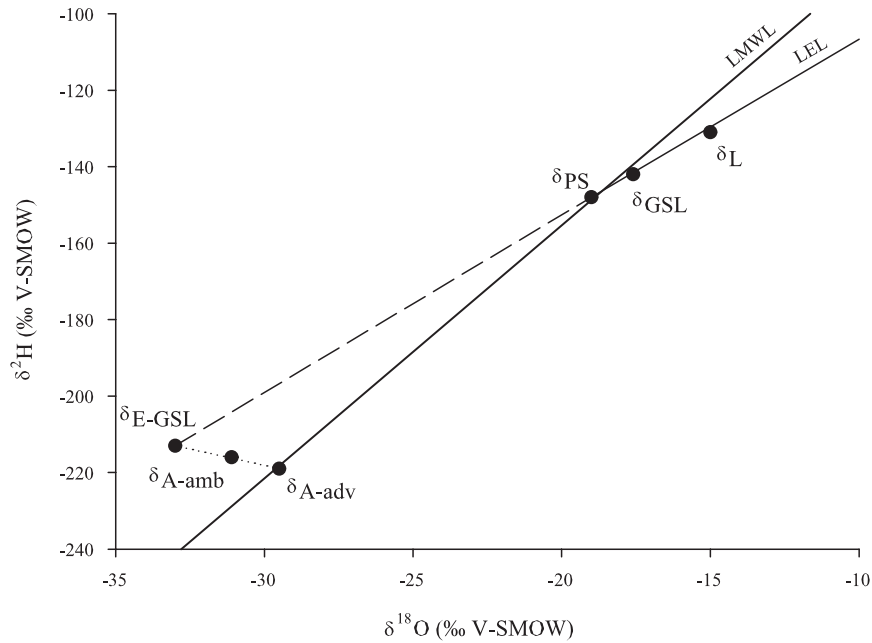


Figure 4.3. Conceptual diagram showing lake-specific ambient vapour ($\delta_{\text{A-amb}}$) for lake δ_{L} as a function of mixing between evaporate from Great Slave Lake ($\delta_{\text{E-GSL}}$) and advected vapour ($\delta_{\text{A-adv}}$). $\delta_{\text{E-GSL}}$ is calculated using Equation (3), incorporating $\delta_{\text{A-adv}}$. The local meteoric water line (LMWL) approximates the relationship between $\delta^{18}\text{O}$ and $\delta^2\text{H}$ in local precipitation, while a lake (δ_{L}) with input δ_{p} undergoing evaporation plots along the local evaporation line (LEL). This conceptual diagram incorporates climate normal (1971-2000) conditions measured at Hay River, NWT (Environment Canada, 2002), and vapour compositions are in equilibrium with amount-weighted (yearly) precipitation (δ_{p} ; Birks et al., 2004).

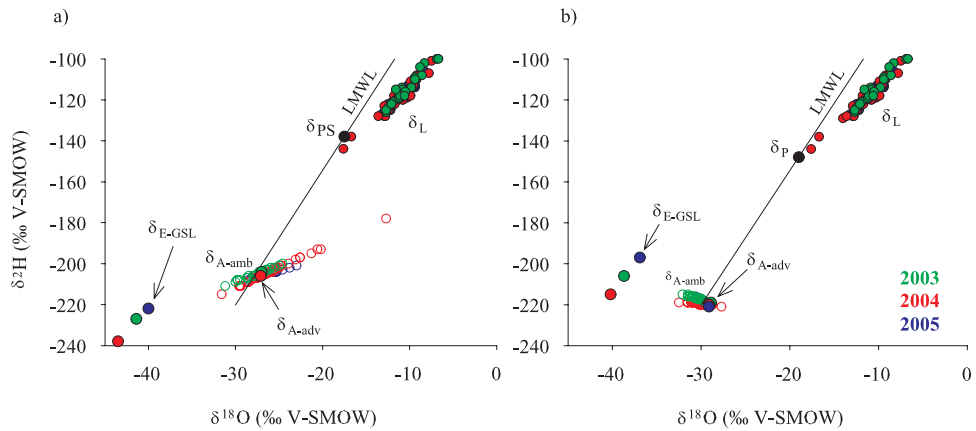


Figure 4.4. Ambient vapour mixing results (δ_{A-amb}) for fall 2003-2005 calculated using advected vapour (δ_{A-adv}) in equilibrium with a) evaporation-flux-weighted (thaw season) precipitation (δ_{PS} , Gibson and Edwards, 2002) and b) amount-weighted (yearly) precipitation (δ_P , Birks et al., 2004). Also shown are the isotopic compositions of SRD study lakes (δ_L), Great Slave Lake (δ_{GSL}) and Great Slave Lake vapour (δ_{E-GSL}). In a), the definition of δ_{A-adv} in equilibrium with δ_{PS} does not properly characterize atmospheric conditions in the SRD, and δ_{A-amb} results are poorly constrained between δ_{A-adv} and δ_{E-GSL} . Improved characterization of atmospheric conditions is achieved in b), when δ_{A-adv} is defined as being in equilibrium with δ_P .

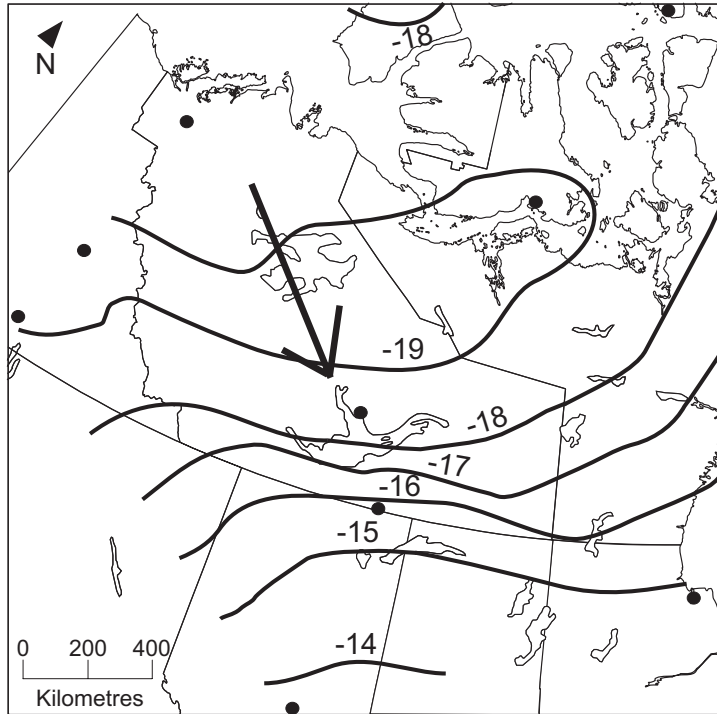


Figure 4.5. $\delta^{18}\text{O}$ composition of precipitation for northern Canada, reproduced from Gibson and Edwards (2002). Isolines are interpolated from Canadian Network for Isotopes in Precipitation stations, shown as black dots. Similar trends are noted for $\delta^2\text{H}$. The black arrow represents the direction of dominant winds affecting the SRD in the fall.

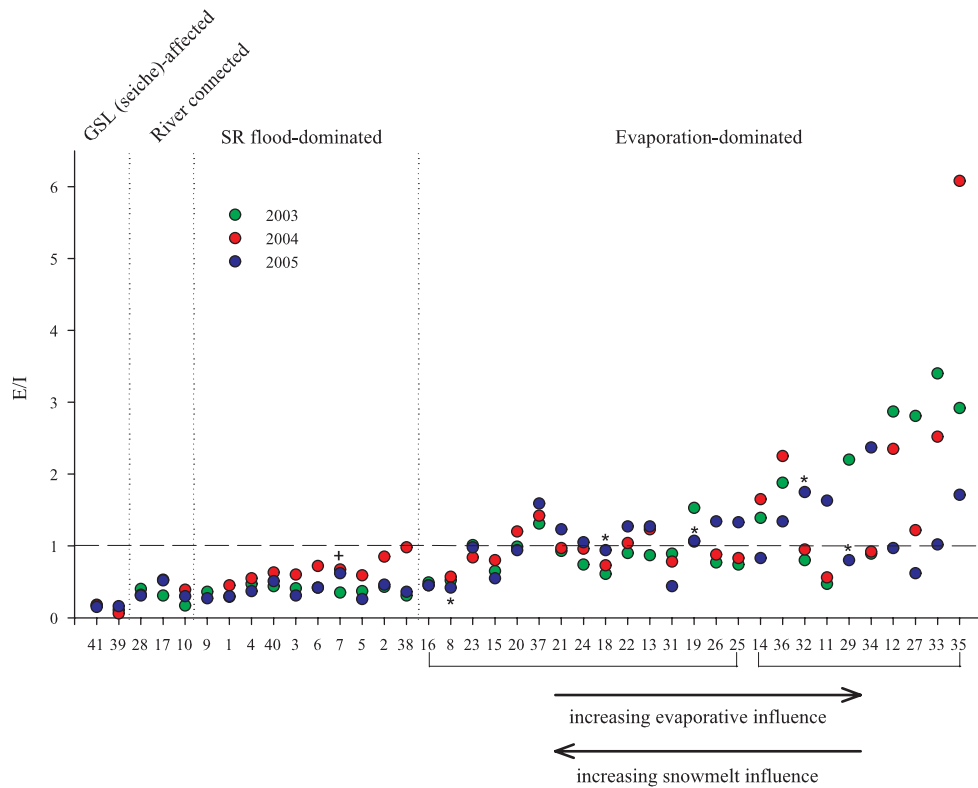


Figure 4.6. E/I results for SRD lakes in fall 2003-2005. Lakes are grouped according to dominant hydrological processes affecting their water balances (Brock et al., 2007; see Chapter 2) and are sorted in ascending order based on the difference between the minimum and maximum E/I ratio at each lake over the 2003-2005 monitoring period. One lake (SD7) in the flood-dominated category that did not flood in 2005 is indicated by a + sign. Lakes in the evaporation-dominated category that flooded in 2005 (SD8, 18, 19, 29, 32) are indicated by a * sign. Brackets on the x-axis identify lakes more strongly affected by snowmelt versus evaporation. An E/I ratio of 1 represents steady-state hydrological conditions for a terminal basin. Results are modeled based on the assumption that lakes are at “quasi-steady-state” (see the section titled “Quantifying lakewater balances using water isotope tracers”), thus E/I ratios >1 are not physically meaningful, but have comparative value.

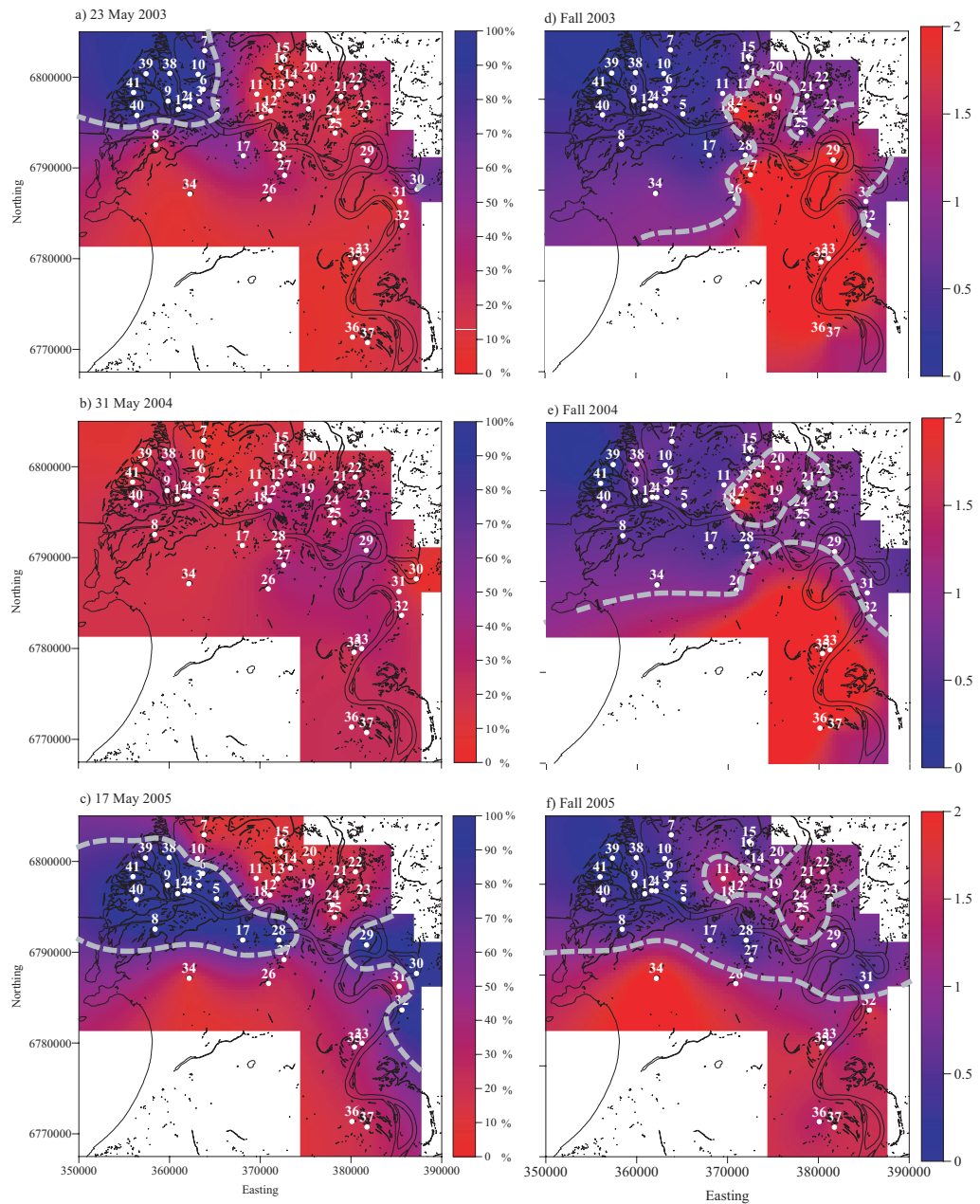


Figure 4.7. Percent dilution in SRD lakes by Slave River water or snowmelt in spring of a) 2003, b) 2004 and c) 2005. Percent dilution for each lake was calculated by dividing the difference between a lake's isotopic composition in the spring and the preceding fall by the difference between the isotopic composition of the diluting sourcewater (Slave River water or snowmelt) and

the preceding fall's lakewater composition (see Brock et al., 2008; see Chapter 3). The observed spatial extent of flooding in 2003 and 2005 corresponds with the 70% dilution isoline, shown as a grey contour in a) and c). Fall E/I ratios for d) 2003, e) 2004 and f) 2005 show lakes with positive water balances ($E/I < 1$) as blue areas and lakes with negative water balances ($E/I > 1$) as red areas. The grey contour on d) – f) represents an E/I ratio of 1.

Tables

Table 4.1. Evaporation-flux-weighted thaw season temperature and relative humidity for the SRD in 2003, 2004 and 2005, and 1971-2000 Canadian Climate Normals for Hay River (Environment Canada, 2002; 2005).

	Temperature (°C)	Relative humidity (%)
2003	13.4	62.8
2004	12.6	63.2
2005	11.9	63.0
Climate normal	13.4	69.2

Table 4.2. Isotopic composition of advected atmospheric vapour (δ_{AS-adv} and δ_{A-adv}) in equilibrium with evaporation-flux-weighted (thaw season) precipitation ($\delta^{18}O_{PS}$, $\delta^2H_{PS} = -17.0\text{‰}$; -132‰ ; Gibson and Edwards, 2002) and amount-weighted (yearly) precipitation ($\delta^{18}O_P$, $\delta^2H_P = -19.0\text{‰}$; -148‰ ; measured at the Fort Smith, NWT, CNIP station (Birks et al., 2004)), respectively.

	δ_{AS-adv}		δ_{A-adv}	
	$\delta^{18}O$ (‰)	δ^2H (‰)	$\delta^{18}O$ (‰)	δ^2H (‰)
2003	-27.0	-204	-28.9	-219
2004	-27.1	-205	-29.1	-220
2005	-27.1	-206	-29.1	-221

Table 4.3. The percent contribution of recycled or re-evaporated vapour to atmospheric vapour pools in isotope-based studies of atmospheric vapour compositions.

Recycled vapour contribution (%)	Location	Source
20-40	Amazon Basin	Gat and Matsui, 1991
~20	Northern and central California	Ingraham and Taylor, 1991
5-16	North American Great Lakes	Gat et al., 1994
≥16 - 50	Lake Ihorty, Madagascar	Vallet-Coulomb et al., 2008
0-45	Slave River Delta, NWT	This study

Chapter 5: Flood frequency variability during the past 80 years in the Slave River Delta, NWT, as determined from multi-proxy paleolimnological analysis

Complete citation: Brock BE, Martin ME, Mongeon CL, Sokal MA, Wesche SD, Armitage D, Wolfe BB, Hall RI, Edwards TWD. In press. Flood frequency variability in the Slave River Delta, NWT, over the past 80 years from multi-proxy paleolimnological analysis. *Canadian Water Resources Journal*.

Introduction

The flow regime of northern rivers is among the most important factors controlling the structure and function of their floodplains and deltas (Milburn et al., 1999, Beltaos and Prowse, 2009). The spring break-up is an influential period in the seasonal flow regime (Beltaos and Prowse, 2001; Romolo et al., 2006a) and it is often accompanied by flooding. Pulses of water associated with spring break-up flooding replenish water levels in lakes elevated above the main-stem and distributary channels (Prowse and Lalonde, 1996; Rouse et al., 1997; Beltaos et al., 2006b; Peters et al., 2006a,b) and introduce sediment to lake beds (Milburn et al., 1999). Spring flooding is especially important in northern delta ecosystems such as the Peace-Athabasca (Prowse and Conly, 1998; Beltaos et al., 2006a; Peters et al., 2006a,b; Wolfe et al., 2006, 2008a), Slave (Brock et al., 2007; 2008; Sokal et al., 2008, 2010) and Mackenzie (Marsh and Hey, 1989; Marsh and Lesack, 1996; Woo and Thorne, 2003; Emmerton et al., 2007) river deltas in the Mackenzie River Basin. These ecosystems provide important aquatic and terrestrial habitat for a wide assortment of communities of vegetation, birds, mammals and aquatic life (Milburn et al., 1999). The habitat and wildlife resources associated with northern deltas are also important to the cultural integrity and livelihood of First Nations land users.

Regulation of the Peace River since 1968 by the WAC Bennett hydroelectric dam has led to concerns regarding declining downstream flood

frequency. In the Peace-Athabasca Delta (PAD; Figure 5.1), land users report less frequent and extensive spring flooding, declining lake levels and loss of habitat for waterfowl and muskrat. However, investigation of these concerns is hindered by northern Canada's spatially-limited network of river gauge stations and short duration of hydrometric records (Shiklomanov et al., 2002; Kane, 2005; Rood et al., 2005; Schindler and Donahue, 2006; Prowse, 2009). Longer hydrological records beyond those available from hydrometric stations in this region are needed to evaluate natural variability in river discharge - knowledge that is essential for informed management of water resources (Sear and Arnell, 2006). To supplement discharge data from the sparse river gauge network, multi-proxy paleolimnological studies of lake sediment records have been conducted in the PAD to investigate long-term variability in flood frequency. These studies aimed to tease apart the effects of multiple stressors on the hydrological regime of northern rivers, and to provide context within which to evaluate causes of contemporary hydrological change (Wolfe et al., 2005, 2006, 2008a,b). Results have revealed that lakes perched above the river system may persist for decades in the absence of spring flooding (Wolfe et al., 2005), while others may dry up within a decade following a flood event (Peters et al., 2006a; Jaques, 1989). Additionally, there have been oscillating multi-decadal periods of both high and low flood frequency over the last several hundred years, suggesting marked natural variability in flood recurrence intervals (Wolfe et al., 2006, 2008a). Importantly, the current period of low flood frequency in the PAD began several decades before regulation of the Peace River by the WAC Bennett Dam. Changes in headwater climate (Wolfe et al., 2008a) and local changes in Athabasca River tributary flow (Wolfe et al., 2008b) appear to be the main drivers influencing the frequency and magnitude of river flooding in the PAD.

Similar concerns about declining flood frequency have developed in the Slave River Delta (SRD; Figure 5.1) downstream of the PAD. For example, SRD land users suspect that the WAC Bennett Dam has reduced discharge on the Slave River (of which the Peace River is a major tributary) and thus the

frequency of spring floods (Wesche, 2007). Previous studies using aerial photographs of the active delta from the 1970s and 1990s document drying that has been attributed to changes in river discharge subsequent to regulation of the Peace River (English et al., 1997). While river regulation has been identified as a driver of hydrological change, a host of other factors may contribute to reduced flood frequency in the SRD. These include natural changes in distributary flow in the active delta and multiple potential consequences of climatic changes on Slave River discharge and the SRD (Prowse et al., 2006). Distinguishing the relative roles of these hydrological drivers, however, is hampered by insufficient knowledge of the variability in flood frequency in the delta.

Here we provide an extended record of flood frequency in the SRD that spans the past ~80-years using information contained in lake sediments from SD2, a shallow lake in the active delta where recent spring break-up flood waters have entered the basin. This continuous record provides a unique opportunity to assess the relative roles of multiple stressors on Slave River discharge and flood frequency. Consumptive water use from the upstream Athabasca River for oil sands development and recent interest in hydropower generation at the Slave River rapids heightens the need for improved understanding of long-term patterns in flood frequency in the SRD to enable appropriate allocation of water resources.

The Slave River and its delta

Deltaic and alluvial sediments delivered by the Slave River began infilling the southern arm of Great Slave Lake after the retreat of the Keewatin Ice Sheet (Vanderburgh and Smith, 1988). The modern delta (~400 km²) fans into Great Slave Lake (Figure 5.1; English et al., 1997). The delta is a large wetland complex consisting of numerous river channels, marshes, fens, bogs, swamps and forests. Scattered throughout this landscape are hundreds of small, shallow (<4 m deep) lakes spanning a wide hydrological gradient, consisting of lakes with thaw season (May-October) water balances dominated by spring break-up

flooding, open-water evaporation or exchange with the Slave River or Great Slave Lake (Brock et al., 2007; see Chapter 2). Lakes in the SRD are macrophyte-rich, with productive shoreline communities that provide diverse habitats for a variety of plant and animal communities (English et al., 1997; Sokal et al., 2008).

The Slave River begins at the confluence of the Peace River and Rivière des Rochers in northern Alberta, and flows north 420 km into Great Slave Lake. The Peace River contributes $\sim 2/3$ of the overall discharge of the Slave River (English et al., 1996), but the river also receives water from other north-flowing channels in the PAD that carry Athabasca River flow and outflow from Lake Athabasca. The hydrograph of the Slave River is characteristic of a subarctic nival flow regime, in which snowmelt generates high spring flows (Figure 5.2a; Woo and Thorne, 2003). Discharge along the Slave River is low through the winter, but increases rapidly after the onset of the spring melt in response to upstream snowmelt runoff. Subsequently, discharge declines over the course of the thaw season, until the development of winter ice cover.

The Smoky River catchment, an important upstream tributary for the Peace River, is the source of spring snowmelt inducing augmented spring flows on the Slave River (Figure 5.1 and Figure 5.2). Thick snowpacks and early and rapid melting in the Smoky River catchment are conducive to high flow events and spring ice jams on the Peace River (Prowse and Conly, 1998; Romolo et al., 2006a), and hence also contribute to high flow events on the Slave River and flooding in the SRD (Brock et al., 2008; see Chapter 3). Higher-than-average spring discharge on the Slave River in 2005 (Figure 5.2a), associated with high discharge on the Smoky River (Figure 5.2b), produced widespread spring break-up flooding in the SRD. Similarly, a moderate spring break-up flood was observed in the SRD in 2003, while an absence of flooding in 2004 can be associated with low spring discharge on the Slave, Peace and Smoky rivers (Brock et al., 2008; see Chapter 3), evidently due to a loss of snowpack in the late winter and a more protracted melt that caused peak discharge on the Smoky River to occur later in the season (Figure 5.2b).

Spring break-up flooding is the key water input to lakes with flood-dominated hydrological regimes in the active delta (Brock et al., 2007; see Chapter 2) and promotes positive lakewater balances with low inter-annual variability, even in the absence of flooding (Brock et al., 2009; see Chapter 4). In frequently-flooded lakes in the SRD, spring flooding temporarily introduces planktonic, centric diatoms to the water column and results in decreased concentrations of dissolved nutrients and ions, lakewater with stable physical and chemical conditions year-to-year, reduced water transparency, and reduced macrophyte biomass. However, nutrient concentrations and macrophyte growth in intermittently-flooded SRD lakes increase over the course of the thaw season (Sokal et al., 2008, 2010).

Study Site – SD2

SD2 is a small (~1.2 km²), shallow (maximum depth ~1.5 m), flood-dominated lake in the active SRD (Figure 5.1) where levee heights are 0.5-2.5 m above low summer water levels in Great Slave Lake (English et al., 1997). Adjacent to SD2, the Slave River divides into multiple distributary channels that fan across the active delta. SD2 is at the junction of the Slave River and Resdelta Channel, which carries ~90% of Slave River flow through the active delta and into Great Slave Lake (English et al., 1997). The 90° angle formed by the Slave River and Resdelta Channel is a prime location for the development of ice jams during the spring break-up period, making SD2 particularly sensitive to Slave River flooding early in the thaw season, and likely to preserve a record of flood frequency in its sediments. Flooding was observed at SD2 during the spring break-up in 2003 and 2005, when discharge was high (Figure 5.2; Brock et al., 2008; see Chapter 3).

The morphology of the SRD's distributary channel network at SD2 has changed over the last ~50 years (Figure 5.3; Hill, 1996; Prowse et al., 2006). Prior to 1954, most of the water flowing through the active delta exited to Great Slave Lake via Mid Channel West. By 1966, a cleavage bar had developed at the junction of the Slave River and Mid Channel West. Continued

sedimentation restricted the entrance to Mid Channel West, routing the majority of Slave River distributary flow through Resdelta Channel by 1973 (English et al., 1997). This flow configuration has persisted to the present day.

Field observations show vegetation at SD2 consists of an open water area dominated by submerged macrophytes (*Myriophyllum exalbescens*, *Potamogeton pusillus*, *P. freseii*, *P. richardsoni* and *P. zosteriformis*, with isolated patches of *Ceratophyllum demersum* and the macroalgae *Chara* sp.), emergent vegetation, grasses and herbs along the lake margin (*Equisetum fluviale*, *Typha latifolia*, *Carex* spp. and *Calamagrostis canadensis*), and low shrubs (*Salix* spp.) that transition to mature trees (*Betula* spp., *Populus tremuloides* and *Picea glauca*) in the surrounding catchment.

Field and laboratory methods

Core collection and extrusion

A fully-recovered 49.5 cm-long sediment core was collected from SD2 in July 2004 using a Glew (1989) gravity corer. The chosen coring site is distal to the known point of entry of floodwaters, maximizing the length of time captured by the gravity core. The core was sectioned vertically into 0.5-cm intervals at the field station. Core sections were stored at 4°C until analysis.

Slave River sediment collection

A sample of river-lain sediment was collected from the flood path between the Slave River and SD2 following the spring flood of 2005. Elemental and stable carbon and nitrogen isotope compositions were measured on this sample, as described below. This information is used here as a benchmark for the geochemical composition of Slave River sediment to infer periods of fluvial sediment influx to SD2.

Sediment core chronology

A sediment core chronology was developed for SD2 by counting gamma emissions from radioactive isotopes ^{210}Pb and ^{137}Cs using an Ortec GWL Series HPGe coaxial-well gamma spectroscopy system. Gamma emissions from 2-

cm³ aliquots of freeze-dried sediment were sealed with epoxy and counted following a minimum 14-day equilibration period (Appleby, 2001).

Physical and geochemical proxies

Water content of the sediment core was determined for every 0.5-cm-thick sediment sample by weight loss after drying subsamples of ~0.5 g at 90°C for 24 hours.

Elemental and stable carbon and nitrogen isotope compositions were measured for each 0.5-cm sediment interval. Prior to analysis, carbonates were dissolved with 10% (by volume) hydrochloric acid and samples were then rinsed to neutral with deionized water. Acid-washed samples were freeze-dried and sieved through a 500- μ m screen to remove coarse-grained material. Subsamples from the fine fraction were analyzed by the University of Waterloo Environmental Isotope Laboratory using an elemental analyzer interfaced with a continuous-flow isotope-ratio mass spectrometer. Percent dry weight organic carbon and nitrogen contents were used to calculate carbon-to-nitrogen ratios. Carbon and nitrogen stable isotope results are reported in δ -notation, representing deviations in per mil (‰) from the Vienna-Peedee Belemnite (VPDB) and atmospheric nitrogen (AIR) standards, respectively. Analytical uncertainties for elemental carbon and nitrogen are $\pm 0.1\%$ and $\pm 0.01\%$, respectively, while uncertainties for both $\delta^{13}\text{C}$ and $\delta^{15}\text{N}$ are $\pm 0.1\text{‰}$.

Biological proxies

Microscope slides for diatom analysis were prepared from wet sediment samples by acid digestion following standard methods (Hall and Smol, 1996). Generally, alternate 0.5-cm samples were analyzed to determine taxon percent abundance of the total sum of diatom valves. For each sample, at least 400 diatom valves were identified and enumerated along transects using a Zeiss Axioskop II_{Plus} compound microscope with differential interference contrast optics (1000X magnification, numerical aperture = 1.30). Diatom taxonomy followed Krammer and Lange-Bertalot (1986-1991).

To quantify periods of high river influence from the diatom record, a diatom-based flood index was developed. Z-scores were calculated for each sediment interval, based on the sum of diatoms previously identified as indicators of high river influence in SRD lakes (Sokal et al., 2008).

Macrofossil samples were prepared following standard techniques outlined by Birks and Birks (1980). Briefly, 10 cm³ of wet sediment from every 0.5-cm sediment interval were washed through a 125- μ m screen with tap water. Materials retained on the sieve were sorted in water using a binocular dissecting microscope at 8-40X magnification and all identifiable macrofossils were enumerated. Identifications were made to the highest taxonomic resolution possible, with the aid of modern reference samples and relevant reference keys (Jessen, 1955; Martin and Barkley, 1961; Wood, 1967; Berggren, 1969, 1981; Delorme, 1970a-c, 1971; Montgomery, 1977; Lévesque et al., 1988; Schoch et al., 1988; Artjushenko, 1990). Data were recorded as concentrations of macrofossils per volume of sediment.

Results and interpretation

Sediment core chronology

²¹⁰Pb activities at SD2 do not decline exponentially with sediment depth (Figure 5.4a), as is often otherwise the case (Appleby, 2001). Instead, values range between 0.017 and 0.070 Bq/g in the upper 10 cm, and are constrained to a narrow range spanning 0.028-0.049 Bq/g below this depth. These values are similar to those measured from sediment cores from two oxbow lakes in the PAD, where ²¹⁰Pb concentrations fell within a similar narrow range, and average values for both lakes were ~0.033 Bq/g (Wolfe et al., 2006). As was concluded for these two PAD lakes, frequent flooding introduces pulses of old, re-worked sediment to the lake bed that dilutes ²¹⁰Pb activity, which accounts for the generally constant measured ²¹⁰Pb. Thus, we were unable to use ²¹⁰Pb to develop a sediment chronology for this core.

Fortunately, the ¹³⁷Cs activity profile provides the basis for estimating a sediment core chronology. Results show a clear ¹³⁷Cs peak (0.021 Bq/g)

measured at 25.0-25.5 cm in the core (Figure 5.4b). Average ^{137}Cs values measured above and below the peak are much lower (0-0.005 Bq/g). A ^{137}Cs peak occurs at approximately the same depth (26.5-27.0 cm) in another core from SD2, collected in August 2003 (Jermyn, 2004), and the peak ^{137}Cs activity is of similar magnitude (~ 0.017 Bq/g) to that measured in the sediments of the PAD lakes mentioned above (Wolfe et al., 2006). We use the measured ^{137}Cs peak at SD2 to represent the 1963 stratigraphic horizon, representing maximum ^{137}Cs fallout as a result of above-ground nuclear weapons testing (Appleby, 2001). A chronology was developed for SD2 by calculating the average sedimentation rate (0.62 cm/yr) from the top of the core to the 1963 ^{137}Cs horizon at 25.0-25.5 cm and was extrapolated down-core, giving a basal date of ~ 1925 for the 49.5 cm core (Figure 5.4c).

Physical and geochemical proxies

Moisture and organic contents, bulk organic carbon (C_{org}) and nitrogen (N), carbon ($\delta^{13}\text{C}_{\text{org}}$) and nitrogen ($\delta^{15}\text{N}$) isotopic signatures and carbon-to-nitrogen (C/N) ratios at SD2 are variable over the last ~ 80 years (Figure 5.5). Water content spans 23.0-78.0% of wet sediment mass. The uppermost sediments have the highest water content; below 3 cm, water content does not exceed $\sim 50\%$. $\delta^{13}\text{C}_{\text{org}}$ values range between -26.0‰ and -24.5‰ , while $\delta^{15}\text{N}$ values range between -0.9‰ and 2.2‰ . Percent dry weight organic nitrogen and carbon values are both low, ranging between 0.9% and 5.7%, and 0.07% and 0.61%, respectively. C/N ratios vary between 8.9 and 17.8. The contents of water, organic carbon and nitrogen are positively correlated with each other, and are negatively correlated with $\delta^{15}\text{N}$ and C/N ratios. Variations in $\delta^{13}\text{C}_{\text{org}}$ do not appear to correlate with any other proxy.

The sample of Slave River sediment collected in 2005 from the flood-path to SD2 is predominantly inorganic, with low C_{org} (1.0%) and N (0.06%) contents. $\delta^{13}\text{C}_{\text{org}}$ is -24.6‰ , $\delta^{15}\text{N}$ is 1.7‰ , and the C/N ratio is 15.9. Comparison of fluctuations in the SD2 sediment sequence to the geochemical profile of Slave River sediment (shown as dashed lines on Figure 5.5b – f) can

be used to identify periods of high and low flood frequency at SD2. Six periods of Slave River sediment input are identified in the SD2 sediment sequence, by distinguishing intervals when measured proxy values at SD2 are similar to those measured for the Slave River flood sediment deposit. Periods of increased flood frequency (~1930-1932, ~1937-1947, ~1961-1962, ~1968-1974, ~1976-1981 and ~1992-1998, shown as grey bars on Figure 5.5) generally have low water, organic carbon and nitrogen contents, while $\delta^{15}\text{N}$ and C/N values are high.

Associated with river floodwaters are high C/N ratios, which may reflect organic matter derived from terrestrial sources (Meyers and Teranes, 2001). However, high C/N ratios may also be due to the influx of C-rich, N-poor hydrocarbons (i.e., bitumen) derived from upstream oil sand deposits, as has been suggested for similar geochemical signatures in the stratigraphic records of oxbow lakes in the PAD (Wolfe et al., 2006; Jarvis, 2008). During non-flood intervals, increases in autochthonous production generate sediment that is more organic-rich with higher water content, and possess lower $\delta^{15}\text{N}$ values and C/N ratios, the latter typical of aquatic organic matter (Meyers and Teranes, 2001). The lack of clear oscillations in $\delta^{13}\text{C}_{\text{org}}$ values that can be correlated to the other physical and geochemical proxies suggests this parameter is less sensitive to fluctuating hydrological conditions at SD2.

Biological proxies

Composition of diatom assemblages varies markedly in the sediment record from SD2 (Figure 5.6). Twelve diatom taxa with abundances $\geq 5\%$ were identified. Taxa include diatoms indicative of both high (*Navicula libonensis*, *Rhopalodia gibba*) and low (*Achnanthes lanceolata* var. *frequentissima*, *Achnanthes minutissima*, *Navicula pupula*, *Nitzschia amphibia*) river influence (Sokal, 2007). In addition, several common epiphytic taxa were identified (*Cocconeis placentula* var. *placentula*, *Epithemia adanta*, *Fragilaria capucina* var. *mesolepta*). Several taxa occur at relatively low abundance ($\leq 10\%$; *Fragilaria capucina* var. *mesolepta*, *Navicula radiosa*, *Navicula cryptocephala*,

Rhopalodia gibba). The most abundant taxa include *Navicula libonensis*, *A. minutissima* and *C. placentula* var. *placentula*, with maximum abundances of ~25-30% each.

The diatom-based flood index identifies three periods of elevated flood frequency (Figure 5.6). These periods span ~1935-1953, ~1966-1979, and ~1989-2003. The first two periods of strong flood influence are mainly captured by increased percent abundance of *N. libonensis*. Compared to these first two periods, increases in *N. libonensis* abundance and diatom-based flood index values are more subdued during the most recent period of elevated flood frequency.

Remains of several macrofossil taxa were identified in the sediments of SD2, including both vegetative and reproductive parts of submerged and emergent aquatic macrophytes (*Potamogeton*, *Myriophyllum*, *Equisetum*, *Carex* spp., *Sagittaria cuneata*), aquatic moss leaves (*Drepanocladus*) and invertebrate fauna (Figure 5.7). The most striking feature of the SD2 macrofossil stratigraphy is the abundance of *S. cuneata* seeds between ~1948 and ~1958. During this period, the concentration of *S. cuneata* remains increases rapidly from 0 to 16 specimens/cm³.

Modern vegetation assessments at SD2 indicate that *S. cuneata* is concentrated on the edge of the sedge marsh fringing the lake, where the water level is ~5-15 cm deep. Where *S. cuneata* has been observed growing in deeper water (~0.5-1 m) at SD2 it did not flower, despite the presence of extensive stands of flowering plants growing in the sedge marsh periphery. No *S. cuneata* seeds were found in the surface sediments of the SD2 core, despite the presence of flowering plants along the margins of SD2 at the time of coring, making the possibility of flood-induced seed transport to the centre of the lake unlikely. Therefore, the presence of *S. cuneata* seeds in the sediments of SD2 between ~1948 and ~1958 suggests that water levels at the coring site were substantially lower than present (~5-15 cm), probably due to an extended period with no Slave River spring break-up flooding.

Discussion

Multi-proxy records of flood frequency in the Slave River Delta

Although each proxy responds with different sensitivity to different environmental factors, broadly concurrent periods of increased flood frequency can be identified in the SD2 sediment sequence (Figure 5.8). While flooding may not have occurred in each of the years contained within the shaded grey bars on Figure 5.8a and b, the frequency of floods was generally higher than during the intervening periods. Three major periods of relatively high flood frequency occurred at SD2, spanning 1) the late 1930s to late 1940s, 2) the early 1960s to early 1980s, and 3) the early 1990s to ~2000. Additionally, the peak abundance of *S. cuneata* seeds between ~1948-1958 identifies the period of lowest water levels (~5-15 cm) at SD2 over the last ~80 years. Based on these results, SD2 has been subject to a variable flooding regime over the period of record, with shifts between high and low flood frequency occurring on an approximately decadal to multi-decadal scale.

Measured Slave River discharge and oral history records of flooding

We compared our multi-proxy paleolimnological flood record to two independent sources of hydrological information: hydrometric data and oral history. Slave River discharge has been measured at Fitzgerald, AB, upstream of the SRD, since 1960 (Water Survey of Canada, 2006; Figure 5.8d). This discharge record has been used to identify past flood events in the SRD, because spring floods occur in years when discharge on the Slave River is high (Brock et al., 2008; see Chapter 3). In 2003, elevated spring discharge (5370 m³/s) flooded much of the active SRD, including SD2 (Figure 5.2; Brock et al., 2007; see Chapter 2). By identifying spring discharge peaks that met or exceeded that of 2003, years when the Slave River was capable of flooding SD2 can be identified. Over the past 45 years, peak discharge exceeded 5370 m³/s on 24 occasions. Maximum discharge was measured in 1974, at 11200 m³/s. Peak discharge exceeded 5370 m³/s for several consecutive multi-year intervals,

including 1965-1967, 1972-1974, 1992-1994, and 1996-1999 (Water Survey of Canada, 2006).

The oral history record of flood events was assembled through interviews with SRD land users (Wesche, 2009; Figure 5.8d). While there is potential for slight inaccuracies due to the difficulty of recalling specific floods, the validity of knowledgeable land user observations of this type is well documented in analyses of environmental change (Huntington et al., 2004). Land users describe flooding by the Slave River and its tributaries in the early and mid-1960s, as well as in the early and mid-1970s, corresponding with high (>5370 m³/s) discharge on the Slave River. Two flood events in the late 1970s were also reported, corresponding to high Slave River discharge, while no floods were reported during the 1980s. Land users recalled consecutive years of flooding in the late 1990s, but no floods in the early 2000s.

Periods of high Slave River discharge and the oral flood history correspond to periods of high flood frequency inferred from multiple proxies in the SD2 sediment core (Figure 5.8). As described, the sedimentary record exhibits a period of high flood frequency beginning in the early 1960s and lasting through the early 1980s. During this period, there were 11 discharge events on the Slave River capable of flooding SD2, including two periods with multiple consecutive years of high spring peak discharge, and several corresponding flood events documented in the oral flood history. The most recent period of high flood frequency inferred from the sediment sequence, beginning in the early 1990s and ending ~2000, has eight measured discharge events capable of flooding SD2, and includes consecutive years of flooding reported by land users. In the intervening period, during the mid-1980s and early 1990s, there were only three discharge events capable of flooding SD2, no recollections of floods by SRD land users, and non-flood conditions exhibited in the sedimentary record. The marked co-variance between measured Slave River discharge, the oral flood history, and geochemical and biological proxies preserved in the sediments of SD2 demonstrates that flood frequency at SD2

can be reconstructed using lake sediments beyond the duration of the Slave River hydrometric record.

Assessing the effects of river regulation and change in distributary flow on flood frequency at SD2

Since the construction of the WAC Bennett Dam on the Peace River in 1968, several studies have attempted to assess the impacts of river regulation on downstream flow using measured river discharge records (English et al., 1997, Prowse and Conly, 1998; Prowse et al., 2002a, Beltaos et al., 2006a). However, the Slave River gauging station at Fitzgerald, AB and Peace River gauging station at Peace Point, AB, have discharge records with only eight and nine years of pre-impoundment data, respectively. Notably, this includes the high flood frequency interval of the 1960s, but immediately post-dates the driest 10-year interval at SD2. The ~80-year record of flood frequency at SD2 presented here doubles the length of available flood records and substantially extends our understanding of Slave River hydrology prior to upstream river regulation. Importantly, this provides improved temporal context required to ascertain the effects of river regulation on discharge and flooding in the active SRD.

Multi-proxy paleolimnological evidence presented here identifies periods of both high and low flood frequency prior to impoundment (Figure 5.8). Flood frequency was low until the late 1930s but increased over the subsequent ~10 years. The period of lowest water levels (~1948-1958) pre-dates river regulation and reflects an extended period without Slave River flooding. Flooding increased again at SD2 in the early 1960s. Regular flooding continued following the regulation of the Peace River and lasted until the early 1980s. Flooding was largely absent in the active delta during the 1980s, although the lack of *S. cuneata* seeds during this interval suggests that water levels at SD2 were not as low as those during the late 1940s and 1950s. Because the decline in flood frequency in the 1980s occurred ~10 years post-regulation and is not unprecedented in the pre-dam era, we suggest it is more likely related to climate-driven variability in discharge at the headwaters of the Slave River

rather than to river regulation. Our results at SD2 indicate that previously identified shifts to drier conditions in the SRD following regulation, which were attributed to the effects of river regulation (English et al., 1997), may instead mainly reflect the 1980s decline in river discharge driven by lower headwater snowpack accumulation (Romolo et al., 2006a).

Changes in distributary channel configuration can also affect flood frequency of delta lakes. For example, in the southern Athabasca sector of the PAD, an engineered meander cutoff and the natural bifurcation of a distributary channel have recently changed the frequency of flooding in nearby lakes, leading to notable directional changes in hydroecological conditions (Wolfe et al., 2008b). In the SRD, however, changes in distributary channel configuration do not appear to have had a significant effect on flood frequency at SD2. An increase in flood frequency beginning in the early 1960s (Figure 5.8) predates the shift in distributary flow from Mid Channel West to Resdelta Channel, at the point where development of a cleavage bar restricted channel access (Figure 5.3). It also predates the beginning of the impoundment period, further supporting the notion that river regulation did not trigger the channel switch (Prowse et al., 2006). Additionally, had the channel switch promoted higher flood frequency at SD2, the subsequent period of low flood frequency during the 1980s evident in the sediment record (Figure 5.8) may not have been as pronounced. Based on this evidence, it is likely that the effects of upstream flow generation (discussed below) play a much stronger role in determining flood frequency at SD2 than local changes in distributary flow.

Past flood frequency in the upper Mackenzie Drainage Basin

While many factors contribute to the occurrence of riverine spring break-up flooding (Beltaos et al., 2006a,b), Slave River discharge is likely the most important in the SRD (Brock et al., 2008; see Chapter 3). The magnitude of Slave River discharge is in turn driven by discharge on the Peace River, the main tributary to the Slave River, and to snowmelt and discharge in key tributaries like the Smoky River (Prowse and Conly, 1998; Romolo et al.,

2006a), upstream of the Peace River (Figure 5.2). Low snow accumulation and a protracted spring melt in the catchment of the Smoky River result in low flow on both the Peace and Slave rivers, and an absence of flooding in the rivers' deltas. Conversely, major flooding results from high snow accumulation and a rapid spring melt in the Smoky River basin. A major ice-jam flood occurred in the PAD in 1974 (Peters et al., 2006b), which likely extended downstream to the SRD (Figure 5.8), was generated by extremely high discharge on the Peace River (8700 m³/s, Water Survey of Canada, 2006) as a result of historical maximum peak snow accumulation in the Smoky River catchment (Romolo et al., 2006a). The strong correlation between Peace and Slave river discharge (Brock et al., 2008; see Chapter 3) is also evident in the sediment records of flood-dominated lakes in both deltas. The flood history record from SD2 is similar to a flood-frequency record from PAD15 (Figure 5.9), an oxbow lake in the northern Peace sector of the PAD. The SD2 and PAD15 sediment records show broadly parallel decadal-scale oscillations in C/N ratios, with high values reflecting inputs of riverine sediment during floods. The consistency of the two records from lakes several hundred kilometres apart confirms that upstream drivers of discharge are the main factors determining whether spring flooding occurs in the SRD and the northern Peace sector of the PAD.

Concluding comments

Multi-proxy paleolimnological evidence from a shallow flood-prone lake in the SRD has provided a detailed flood history for the Slave River for the past ~80 years. Biological and geochemical proxies reveal three periods of high flood frequency spanning the late 1930s to late 1940s, early 1960s to early 1980s, and early 1990s to ~2000. The intervening periods are characterized by low flood frequency. Water levels at SD2 were very low (~5-15 cm) between ~1948 and ~1958, based on the abundance of *S. cuneata* seeds. Slave River discharge and oral history records of flood events in the SRD since the 1960s are also consistent with this flood reconstruction, verifying the sediment core

chronology and the appropriateness of our multi-proxy paleolimnological approach for extending the record of flood frequency.

The SD2 sediment record reveals oscillating decadal-scale intervals of both high and low flood frequency, but provides no evidence of a shift to lower flood frequency attributable to the effects of river regulation. While the last period of high flood frequency ended ~2000, low flow conditions during the subsequent ~4 years are well within the range of natural variability over the last century. In fact, the absence of *S. cuneata* seeds in the most recent sediments of the core, combined with field observations at SD2, suggest water levels were lower during the 1950s than they are at present. Importantly, the driest period recorded by lake sediments at SD2 ended ~5 years before upstream river regulation, and was followed by an increase in Slave River flood frequency initiated in the early 1960s. Hence, regulation of the Peace River began during a period of relatively high Slave River flood frequency.

Correspondence between proxy flood records for the SRD and the PAD reveal that upstream drivers of discharge strongly influence the flood regime of the upper Mackenzie River Basin. Discharge in key tributaries such as the Smoky River is likely a major cause of parallel variations in flood frequency in both deltas (Brock et al., 2008; see Chapter 3). A shift to lower snowpacks in the Smoky River basin since the 1970s (Prowse and Conly, 1998; Romolo et al., 2006a) may signify the beginning of a trend towards lower headwater discharge during the spring melt. Other evidence suggests that this trend towards lower snowpacks will continue (Lapp et al., 2005; Rood et al., 2005), and thus we anticipate a reduction in flood frequency in the SRD in the coming decades, as has also been suggested for the PAD (Wolfe et al., 2008a).

Our findings highlight the critical role of headwater flow generation in determining the frequency of downstream flooding in the upper Mackenzie River Basin, a watershed spanning the three jurisdictions of British Columbia, Alberta and the Northwest Territories. Thus, water management strategies must acknowledge the transboundary nature of river discharge in this region, and its

importance for promoting water replenishment of downstream ecosystems like the PAD and SRD. Prudent decision-making is required, particularly with respect to allocating upstream consumptive water use, as declines in water availability will affect the ecological integrity of the PAD and SRD and increase the vulnerability of First Nations communities that remain closely connected to these delta ecosystems.

Figures

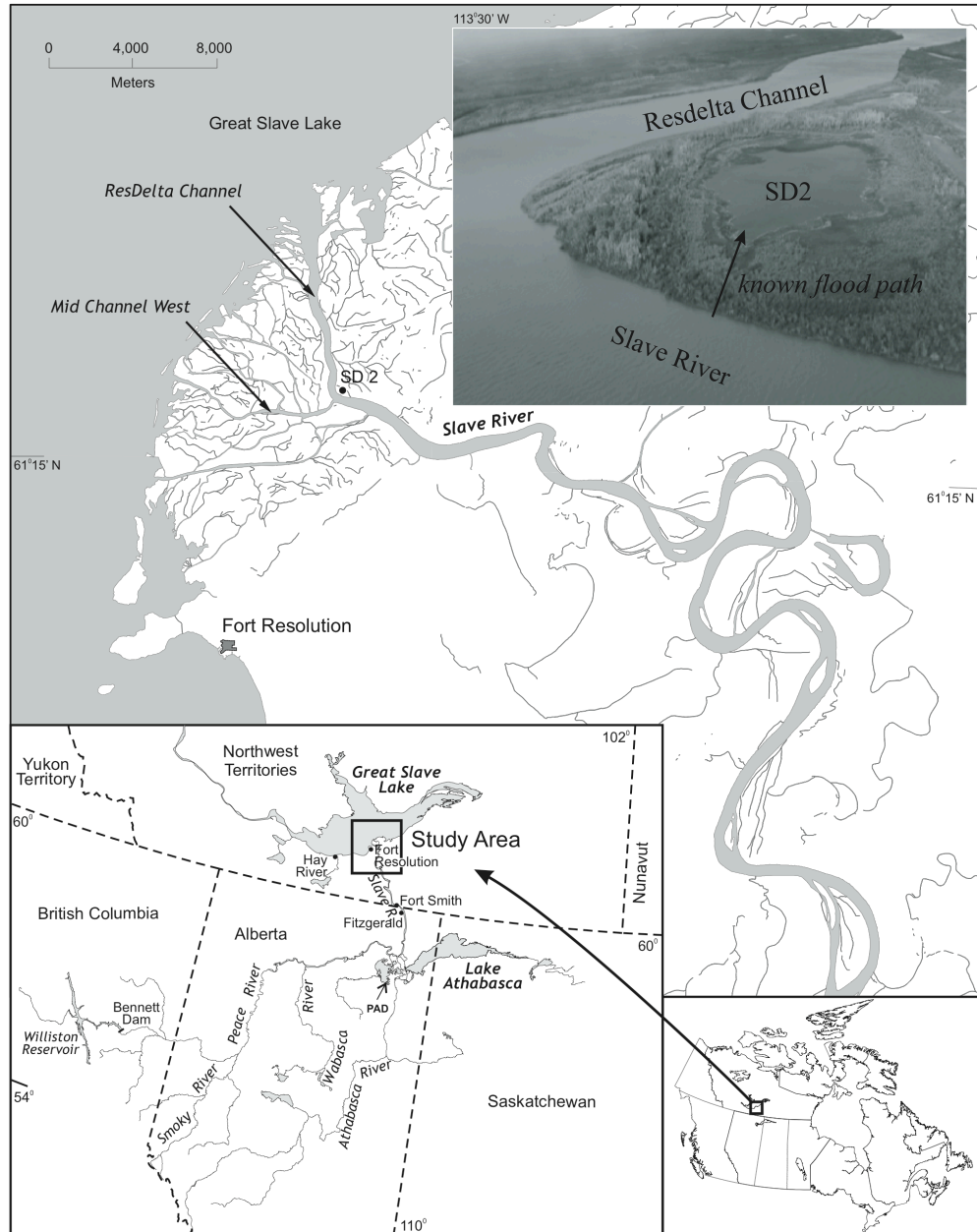


Figure 5.1. Location of the Peace-Athabasca (PAD) and Slave River (SRD) deltas and lake SD2. Inset image shows SD2 and depicts the observed path of floodwater entry in 2003 and 2005.

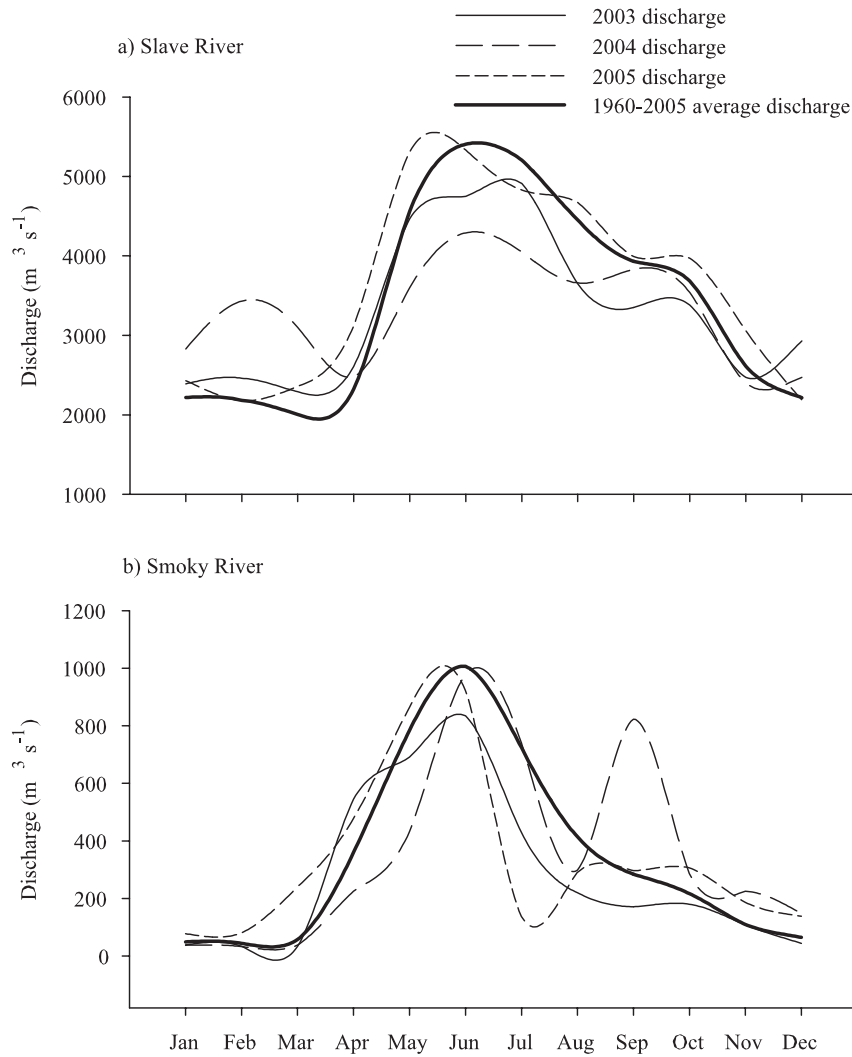


Figure 5.2. Hydrographs showing average monthly discharge over the period 1960-2005, and for the years 2003-2005, for a) the Slave River, measured at Fitzgerald, AB, and b) the Smoky River, measured at Watino, AB (Water Survey of Canada, 2006).

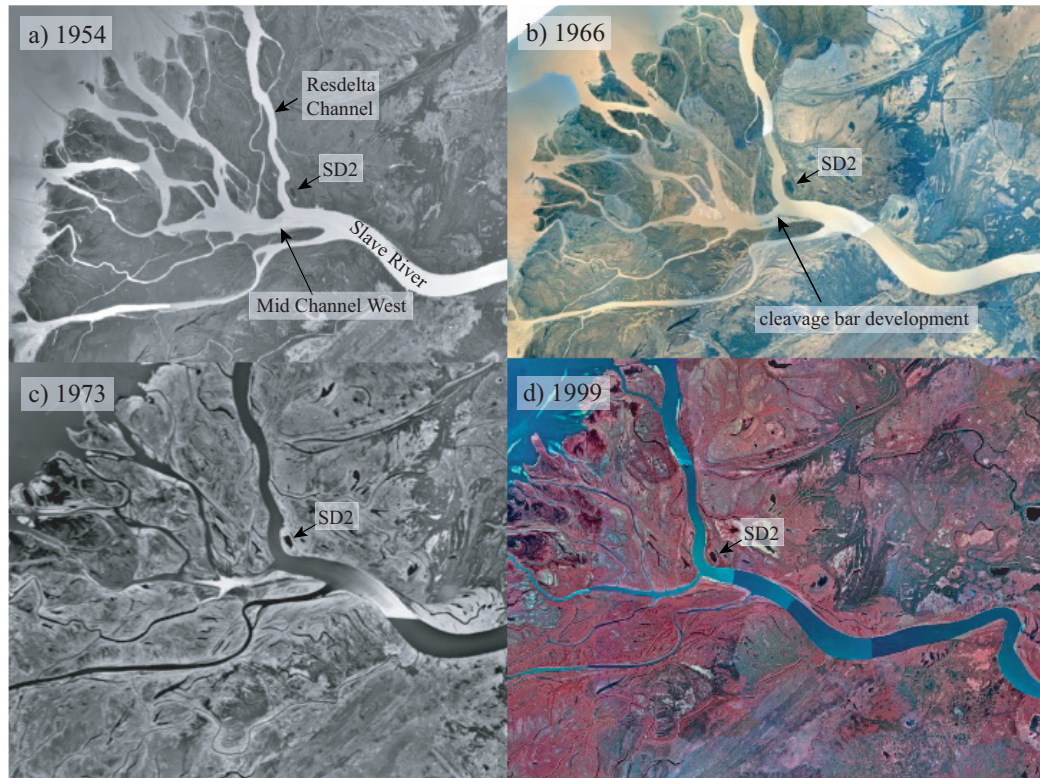


Figure 5.3. Aerial photographs showing shifts in distributary channel routing in the active Slave River Delta: a) in 1954, the majority of flow passed through Mid Channel West; b) by 1966, a cleavage bar had developed at the entrance of Mid Channel West; c) by 1973, most distributary flow was diverted via Resdelta Channel; and d) in 1999, the majority Slave River distributary flow continued to pass through Resdelta Channel (see also Hill, 1996; Prowse et al., 2006). Study site SD2 is also shown. Scales are not identical in each photograph.

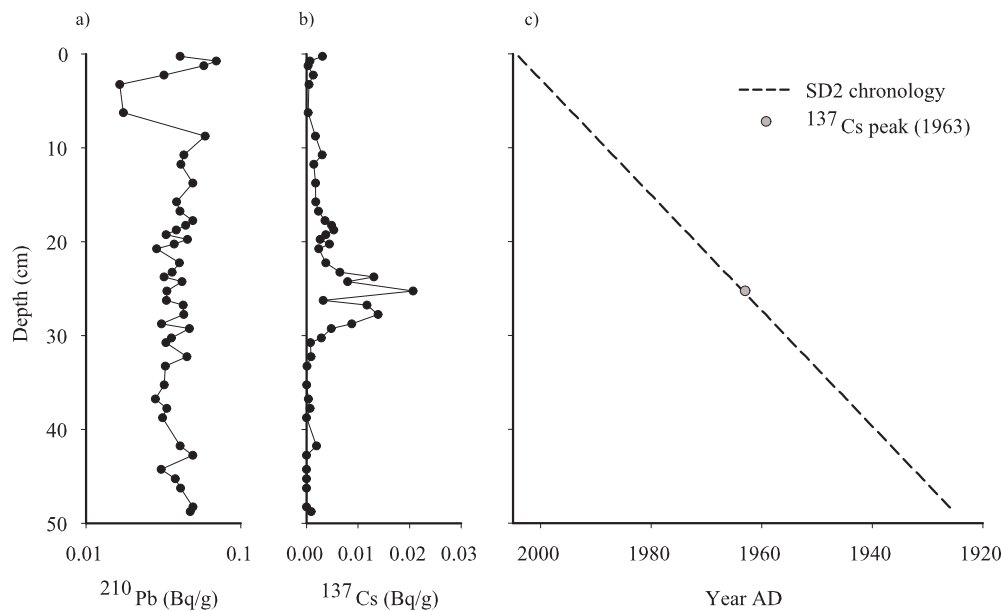


Figure 5.4. a) ^{210}Pb activity versus depth, b) ^{137}Cs activity versus depth and c) the sediment core chronology for SD2. The ^{137}Cs activity peak at 25.0-25.5 cm depth corresponds to the 1963 above-ground nuclear weapons testing fallout peak (Appleby, 2001), and constrains the sediment core chronology.

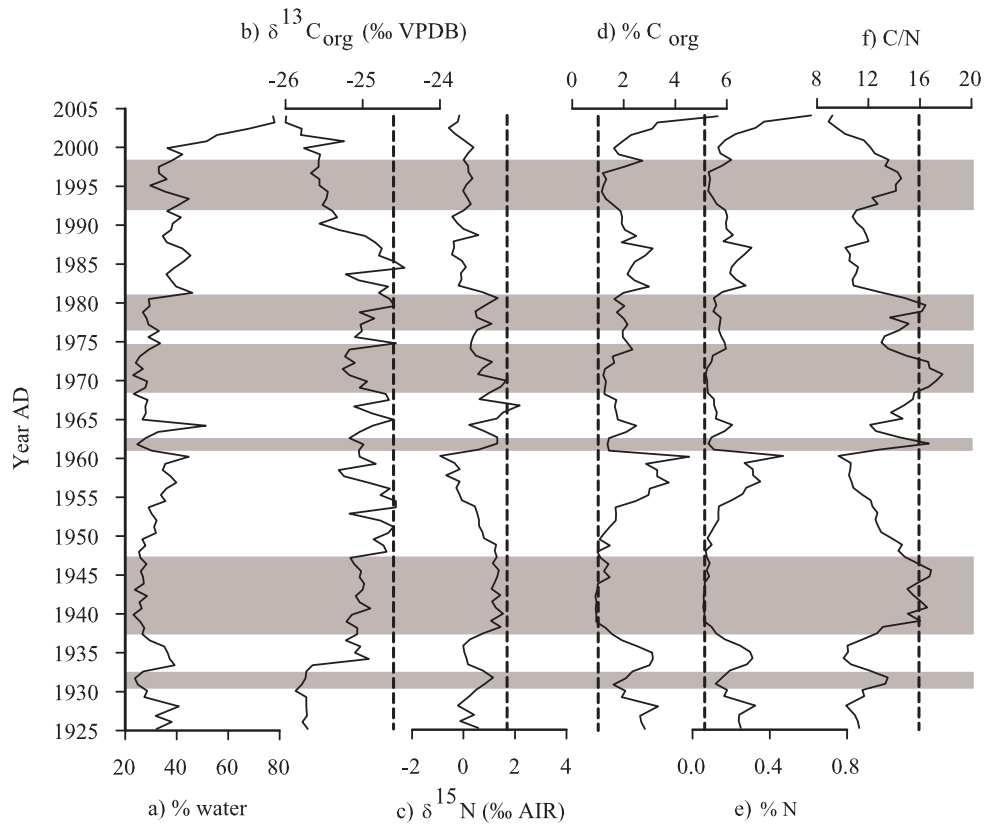


Figure 5.5. Physical and geochemical proxies for the SD2 sediment sequence, showing a) water content as percent of wet weight, b) $\delta^{13}\text{C}_{\text{org}}$, c) $\delta^{15}\text{N}$, d) organic carbon content as percent of dry mass, e) nitrogen content as percent of dry mass and f) carbon-to-nitrogen ratios. The vertical dashed line on b) – f) represents the composition of Slave River sediment, collected in the catchment of SD2 during the spring flood of 2005. Horizontal grey bars represent inferred periods of high flood frequency.

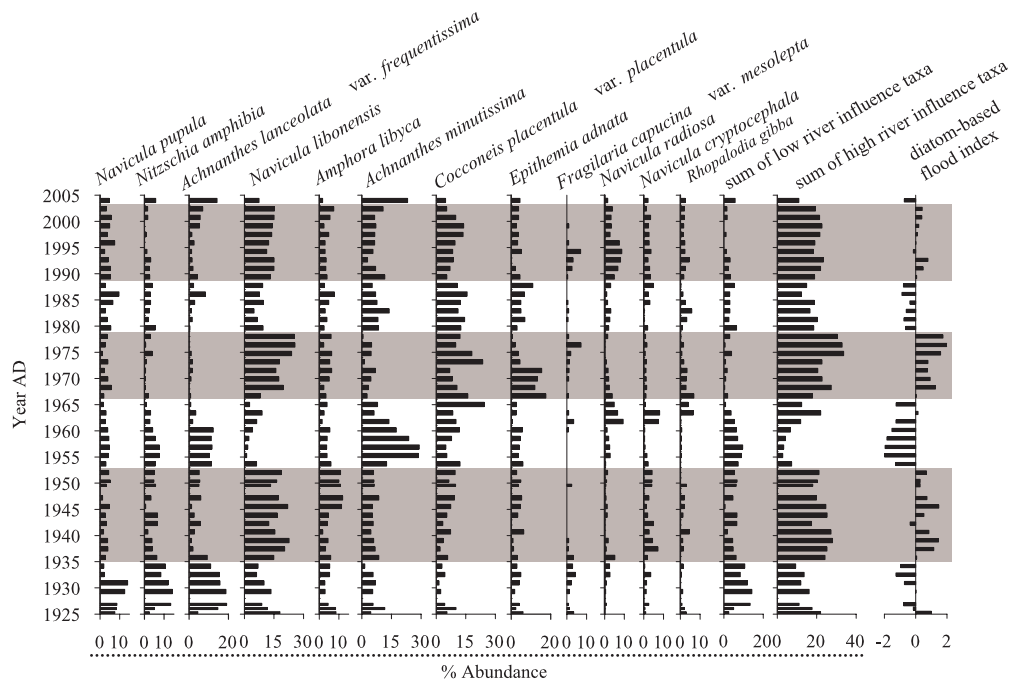


Figure 5.6. Relative abundance profiles of the dominant diatom taxa (i.e., those with relative abundances of $\geq 5\%$ in at least one sediment interval) from the SD2 sediment sequence. The flood index (right hand panel) is developed from z-scores based on the abundances of taxa indicating high river influence.

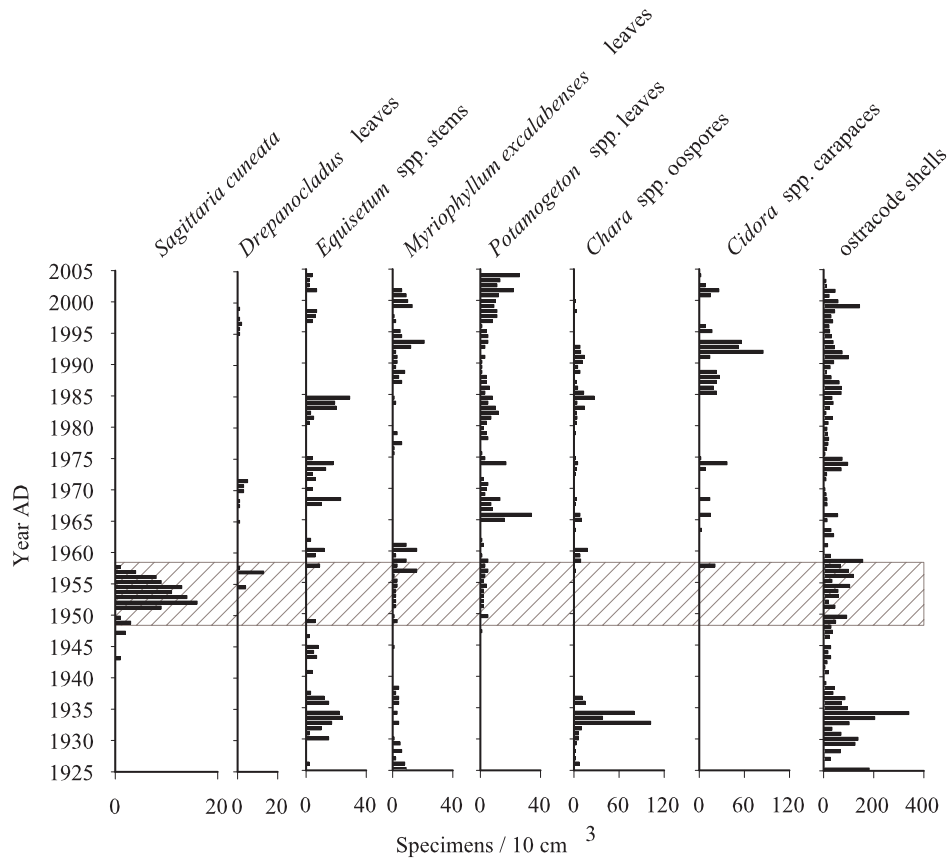


Figure 5.7. A stratigraphic plot of the abundance of the eight most abundant macrofossil taxa in the sediment core from SD2. The peak in *S. cuneata* seeds is highlighted with a hatched box, and identifies the period of lowest water level at SD2, as described in the text.

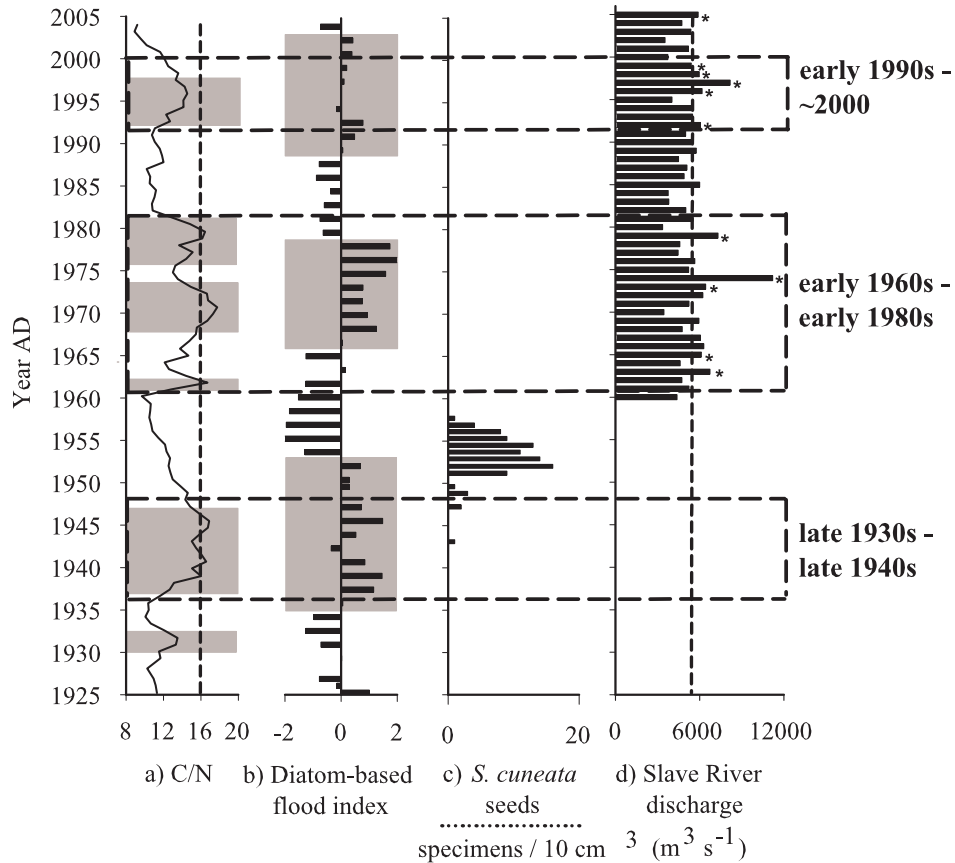


Figure 5.8. Key geochemical and biological geochemical proxies for the SD2 sediment sequence, and measured Slave River discharge (Water Survey of Canada, 2006). The horizontal shaded grey boxes on the proxy records represent periods of high flood frequency, inferred from each proxy. The vertical short-dashed line on a) indicates the C/N value of modern Slave River sediment. The vertical short-dashed line on d) indicates peak spring discharge attained during the 2003 spring break-up flood. Asterisks on d) represent flood events reported in the oral flood history (Wesche, 2009). Horizontal long-dashed boxes outline the main periods of high flood frequency at SD2, inferred from the proxy records.

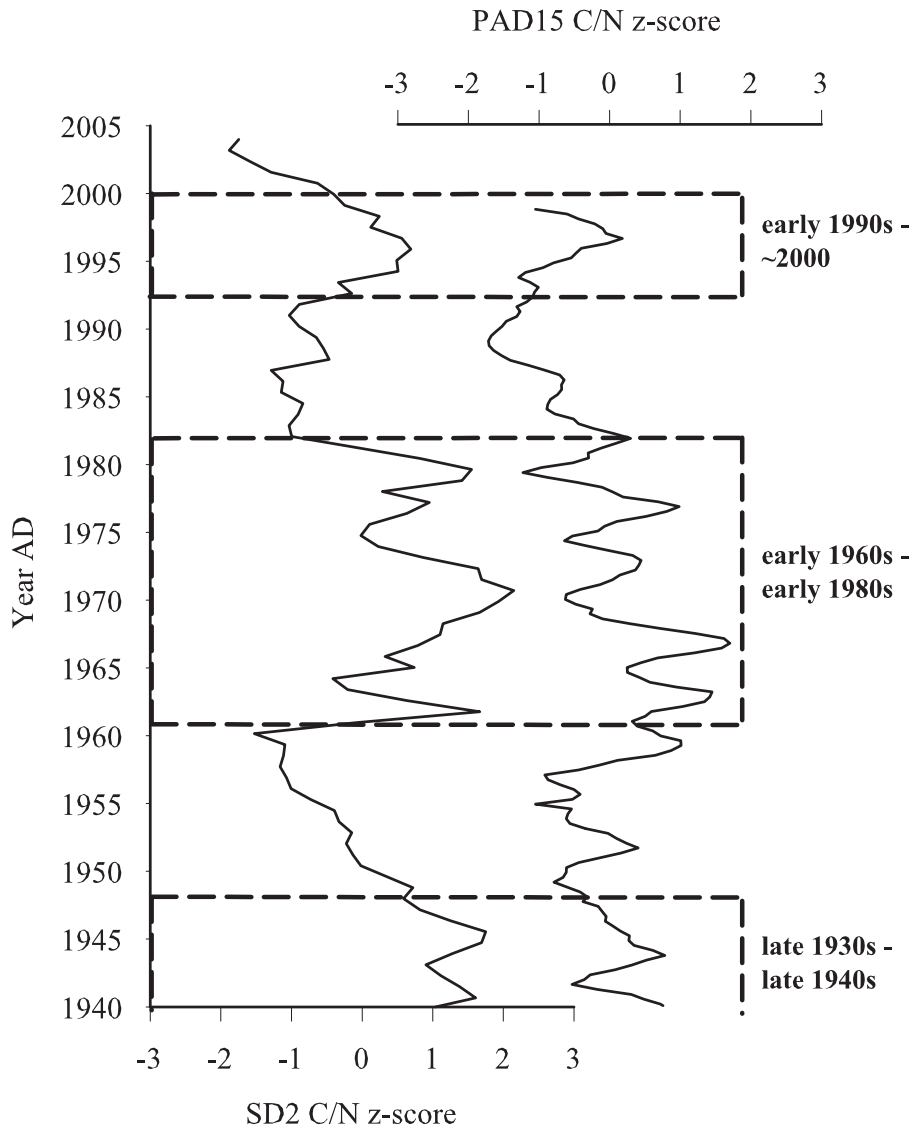


Figure 5.9. Carbon-to-nitrogen ratios (normalized as z-scores) for SD2 and PAD15, a flood-dominated lake in the upstream Peace-Athabasca Delta (Wolfe et al., 2006). The PAD15 record has been smoothed by an 11-point running mean to achieve comparable resolution to the SD2 sequence. Periods of high flood frequency inferred from the SD2 sediment record (Figure 8) are outlined with dashed boxes.

Chapter 6: Thesis summary and applications

Thesis summary

The Slave River Delta is an active, heterogeneous landscape made up of lakes that exhibit strong spatial and temporal hydrological responses to river and climate dynamics. This thesis has provided important insight into the relative roles of spring break-up flooding, snowmelt and open-water evaporation on contemporary lakewater balances in the delta at the landscape scale. In turn, this knowledge has been used to develop a record of Slave River flood frequency that extends beyond available instrumental data and provides important context within which to evaluate past hydroecological changes in the delta. Cumulatively, results provide the basis for anticipating future evolution of the SRD in response to multiple natural and anthropogenic stressors, and address key concerns expressed by local land users about present and past environmental change in the delta.

Contemporary hydrological studies in the SRD used water isotope tracers and total suspended sediment concentrations to characterize the hydrology of 41 lakes spanning previously identified hydrological and ecological gradients in the delta (Brock et al., 2007; see Chapter 2). Study lakes were sorted into three categories, based on the dominant hydrological process affecting each lake's hydrology. Flood-dominated lakes had water balances primarily influenced by contributions of turbid Slave River floodwater during the spring break-up, exhibited by relatively isotopically-depleted lakewater compositions and high suspended sediment concentrations. Immediately following the spring melt period, evaporation-dominated lakes generally had more enriched isotopic compositions and lower suspended sediment concentrations than flood-dominated lakes. Snowmelt influence was variable among evaporation-dominated lakes, with the greatest response to snowmelt input exhibited by lakes in areas of the delta with mature spruce forest (for example, along the Jean River), where deeper winter snowpacks may accumulate. Evaporative enrichment was evident in both flood- and

evaporation-dominated lakes as the thaw season progressed, although the two groups remained isotopically-distinct throughout the season. In contrast, the isotopic compositions of exchange-dominated lakes, capable of exchanging water with the Slave River via direct channel connections or with Great Slave Lake via seiche events, varied over the course of the thaw season in response to the strength of the channel connection and the occurrence of seiche events on Great Slave Lake. Importantly, this component of research identified that the course of hydrological evolution of a lake during the thaw season is set during the highly influential spring melt period. Subsequent research benefits from the classification of delta lakes, as it provides a baseline for teasing apart the relative influences of local climate and Slave River hydrology and for identifying target coring sites for paleohydrological reconstructions.

Because the spring melt period is so influential in setting the course of seasonal hydrological evolution in SRD lakes, subsequent research focused on examining this period in more detail (Brock et al., 2008; see Chapter 3). Spring lakewater samples collected for isotopic analysis from all study lakes during 2003-2005 allowed for a comparison of the effects of moderate (2003), absent (2004) and significant (2005) flooding by the Slave River. Lakes flooded by the Slave River were identified by relatively depleted isotopic signatures and high suspended sediment concentrations, while the opposite was evident in non-flooded lakes. Results were used to quantify the amount of dilution by Slave River floodwater (70-100%) or snowmelt (0-56%) in delta lakes during the spring melt period, and spatial analysis of the results revealed a positive relationship between the spatial extent of spring flooding and discharge on the Slave River. Examination of spring river discharge in upstream tributaries (specifically the Peace and Smoky rivers) showed that upstream flow generation plays a key role in determining the magnitude of downstream flooding. High discharge in these tributaries causes high discharge on the Slave River, resulting in spring flooding in the SRD. Parallel variations in a 46-year instrumental record of Slave River discharge and a Slave River flood history developed from a lake sediment sequence confirmed the potential for developing an extended

flood record from lake sediments of flood-dominated lakes in subsequent phases of research.

The final phase of contemporary hydrological studies conducted as part of this thesis quantified fall lakewater balances for SRD study lakes during 2003-2005 (Brock et al., 2009; see Chapter 4). The influence of evaporated vapour from Great Slave Lake on evaporation from delta lakes was quantified and integrated in this phase of research. Evaporated vapour from Great Slave Lake contributed 0-45% to the ambient atmospheric vapour pool, and this contribution was incorporated into the quantification of lakewater balances (E/I ratios) for each SRD study lake. E/I ratios for delta lakes continued to reflect the hydrological classification scheme developed in Chapter 2, with consistently low E/I ratios (<0.5) in exchange-dominated lakes during the study period. E/I ratios in flood-dominated lakes were positive and relatively consistent in each lake over the study period (0.26-0.98), despite the absence of spring flooding in 2004. This indicates that annual spring flooding is not necessary to maintain positive water balances in flood-dominated lakes in the delta. In evaporation-dominated lakes, E/I ratios were higher and more variable (0.42 - >1), although lakes in sectors of the delta supporting mature spruce forest had lower and more consistent water balances, likely because higher spring snowmelt runoff offset evaporative losses. These results confirm that spring inputs to delta lakes are crucial for their subsequent hydrological evolution during the ensuing thaw season. Importantly, this chapter distinguished areas of the delta most susceptible to changes in Slave River discharge, particularly in multiple consecutive years with no spring flooding, as well as those most susceptible to changes in climate that may reduce snowmelt inputs and increase evaporative losses.

Finally, based on the understanding of contemporary SRD hydrology developed in this thesis, an ~80-year flood history record from a flood-dominated lake in the active SRD was developed (Brock et al., in press; see Chapter 5). A multi-proxy paleolimnological approach was taken, incorporating

biological and geochemical analyses. Results revealed oscillating decadal-scale intervals of high and low flood frequency over the course of the record. Three periods of high flood frequency were identified, spanning the late 1930s and 1940s, the early 1960s and 1970s, and the early 1990s to ~2000. While land users have expressed concerns about declining flood frequency in the delta since regulation of the upstream Peace River in 1968, sedimentary records revealed that the lowest water levels at the study site over the past ~80 years occurred between ~1948 and 1958, prior to regulation and independent of known geomorphological changes to Slave River distributary flow. Additionally, the flood record developed here parallels a flood history developed from lake sediments in the upstream Peace-Athabasca Delta (PAD), suggesting that flood frequency in both deltas is driven by forcings upstream of both deltas. It is likely that spring snowmelt runoff generating elevated tributary flow in the headwaters of the Mackenzie River Basin (MRB) is a major contributor to the occurrence of downstream flooding in the PAD and SRD.

Cumulatively, research findings from this thesis reveal that the SRD is a dynamic landscape, with lakes in different regions of the delta responding differently to variations in river discharge and changes in local and upstream climate. This landscape-scale, multi-year assessment of contemporary SRD hydrology provides important insight into the influence of the spring melt period on delta lakes, as well as the influence of Great Slave Lake evaporate on thaw season evaporation in the delta, and how both contribute to end-of-thaw-season lakewater balances. Further, it highlights the crucial role played by flow generation in the headwaters of the MRB on the occurrence of downstream spring flooding in the PAD and SRD. Paleolimnological reconstructions of Slave River flood frequency, developed based on our understanding of contemporary SRD flood dynamics, generated previously unavailable records of past flood frequency in the active delta. This reconstructed flood history encompasses the period of upstream river regulation, thus providing important context within which to evaluate concerns about declining flood frequency in the SRD. Cumulatively, these research findings can contribute to the

development of water resource management strategies for the upper MRB. This research has also raised new research questions regarding past SRD hydrology, and has highlighted the need for further research into aspects of upstream climate and river dynamics and their effects on downstream ecosystems, as described below.

Water resource management in the upper Mackenzie River Basin

Results from this thesis clearly demonstrate that the hydrology of the SRD is intimately linked to climate and river dynamics in the upper MRB. Should any water management plans be developed for the delta, they must not simply concentrate on local water resources. Rather, water resource management for the SRD should be considered in the context of a broader MRB water management strategy. Ideally, a water management strategy for the basin should reflect the importance of upstream hydrology on downstream ecosystems, and hence should include a distinct component focused on water management in the southwestern half of the basin. It is in this regard that research results from the SRD would be the most relevant and useful.

It is important to note, however, that potential water management strategies for the upper MRB would likely be primarily focused on factors affecting river discharge (e.g., river regulation and water extraction). Subsequent potential management outcomes would then most likely affect flood- and exchange-dominated lakes in the active SRD, rather than evaporation-dominated lakes in more relict portions of the delta. Further, while climate variability has a strong impact on river discharge, as has been discussed in this thesis, good and effective management strategies should not focus on preventing projected climate variability but rather on mitigation and adaptation strategies responding to future predictions of change (e.g., Wesche, 2009). This will be discussed in more detail below.

Importantly, this thesis has demonstrated that the occurrence and magnitude of downstream flooding is directly related to upstream contributions

to discharge. Because of this, careful upstream water use and water extraction policies should be a primary focus of water resource management in the upper MRB. This relates to water extraction from the Athabasca River for oil sands development and potential hydroelectric production at the Slave River rapids, as well as other future water use operations in the upper MRB. Both water extraction and river regulation have the potential to disrupt natural patterns of river discharge and hence the occurrence and magnitude of downstream flooding. In the case of water extraction, a successful management strategy may include flexibility in water resource allocations, reflecting variable river discharge patterns. For example, water extraction could be limited should several consecutive years with no downstream flooding. Careful consideration of seasonal and multi-year river discharge data would be necessary to assist with identifying periods during which water extraction should be limited. One approach may be to use the 2005 Slave River spring discharge peak as a benchmark when examining consecutive years of river discharge data. For example, if there are multiple (>2, for example) years with spring peak discharge <2005 amounts, it may be prudent to limit water extraction, especially during the critical spring melt period. Considering winter river discharge amounts may also be useful. For example, low spring discharge in 2004 followed an increase in Slave River discharge between January and March, suggesting a mid-winter loss of snowpack and reduced potential for downstream flooding. Strategies such as these may prevent upstream water withdrawals from reducing the potential for downstream spring flooding. Where hydroelectric production is concerned, a run-of-the-river operation may have a much less significant impact on river discharge and the riverine hydrograph than a dam and impoundment structure, hence limiting the effects of such a project on downstream flooding. As with water extraction, careful and on-going examinations of multi-year discharge data would minimize the impacts of hydroelectric generation on downstream ecosystems. In both cases, it is important to recognize that economic pressures (e.g., demands for oil and hydroelectric power) are unlikely to decline in the near future, and that

management strategies should likely focus on minimizing their impacts, rather than preventing them.

Other research findings presented in this thesis highlight important additional factors that should be reflected in decisions regarding water resource management. For example, yearly flooding is not necessary to maintain positive water balances ($E/I < 1$) of flood-dominated SRD lakes, and thus promoting yearly flooding is not an appropriate management goal. Engineering solutions for promoting flooding in the PAD (e.g., Prowse et al., 2002b) were only moderately successful, and should not be applied in the SRD. Secondly, management decisions should reflect the fact that the delta is a constantly-shifting system. For example, changes in distributary flow occur naturally (e.g., the switch in distributary channel flow from Mid Channel West to Resdelta Channel in the active delta between ~1950 and 1990). The delta is a naturally heterogeneous landscape, and should not be expected to exist indefinitely in its current geomorphological or hydrological state. It is also important for water resource managers to clearly understand that flooding is not the only mechanism responsible for maintaining water balances of SRD lakes. Direct snowmelt inputs and thaw season precipitation are also important contributors to maintaining lake levels. In the case of evaporation-dominated lakes, these are the primary mechanisms of water delivery. Hence, frequent flooding causing high water levels in flood-dominated lakes in the active delta may occur simultaneously with low water levels in evaporation-dominated lakes if direct snowmelt or precipitation inputs are also low.

While potential water resource management strategies for the upper MRB would likely focus on anthropogenic effects on river discharge, the research presented here suggests that climate variability is likely the dominant factor affecting the hydrology of all SRD lakes. Climate conditions affect flood- and exchange-dominated lakes because the depth of the headwater winter snowpack and the timing of melt in upstream tributaries directly affects downstream discharge and the potential for spring flooding. Climate conditions

also control the potential for mid-winter melts, as well as the timing of freeze-up and break-up, which both contribute to the incidence of spring flooding. In evaporation-dominated lakes, water inputs and losses are a direct product of the local climate. Spring snowmelt in a lake's catchment, as well as thaw-season precipitation, are the primary hydrological inputs to these lakes, while evaporative losses draw down water levels during the ice-free period. Climate variability has a strong influence on delta lake hydrology, and it is important that this be reflected in resource management plans for the entire upper MRB. It is in this regard that paleohydrological reconstructions of a lake's responses to climate variability can be especially useful for water resource managers, when used in conjunction with predictions of future climate variability such as those provided by the IPCC. For example, warm temperatures during the Medieval Warm Period may be similar to temperature increases predicted for northern Canada, but the spring melt of deep alpine snowpacks during the Medieval Warm Period was an important contributor to frequent spring flooding in the downstream PAD and SRD (Wolfe et al., 2008a). Predicted warmer winter temperatures (IPCC, 2007) may result in lower winter snowpack accumulations, while receding headwater glaciers will also lessen contributions to downstream flow, hence reducing the potential for downstream flooding. Predicting future climate variability and subsequent ecosystem responses is difficult, but this must be incorporated into water management plans for the upper MRB, as the effects of a changing climate will have a strong influence on hydroecological evolution in the basin. Successful stewardship of water resources in the upper MRB and the SRD should focus on preparing for and adapting to environmental change, rather than on preventing it. It is perhaps in this way that the residents of Fort Resolution and SRD land users may make their most valuable contributions to water management decisions.

Future research directions and applications

The research approach taken in this thesis, integrating both contemporary and paleolimnological techniques, has been highly successful in

the SRD, as well as in the PAD. Contemporary hydrological studies using water isotope tracers have many advantages over conventional hydrological monitoring, and are especially suited to remote northern environments. For example, water samples were collected from all 41 study lakes in the SRD over the course of a single day. Early-, mid- and late-season lakewater sampling, as well as sampling over consecutive years, provides a suite of data from which much information about the seasonal and multi-year evolution of lake hydrology can be extracted. In addition to characterizing contemporary hydrology, these data can then be used to select coring sites for paleolimnological analysis, as has been done here. The selection of SD2 as an archive of Slave River flood frequency was based on field observations and contemporary lakewater samples showing the lake's susceptibility to spring flooding during both moderate and significant flood events. Application of this approach is highly warranted in other complex freshwater ecosystems where a more comprehensive understanding of present and past hydrology would be advantageous (for example, in the Saskatchewan River Delta, a designated Important Bird Area affected by the Grand Rapids hydroelectric project).

In addition to initiating research programs in other delta or wetland environments, there are several possible extensions to this research. These include:

- 1. Continued research in the SRD*

Continued collection of contemporary SRD lakewater samples for isotopic analysis would increase the quantity of contemporary data available for analysis, and may provide new insight into SRD hydrology. More importantly, however, continued monitoring of SRD lakes would allow for on-going assessment of the hydroecological vitality of the SRD, and for the identification of major hydrological changes. Further, if an SRD or MRB water resource management plan were developed, on-going isotopic monitoring of SRD lakes would allow for the evaluation of the effectiveness of such a plan and provide the basis for revision, should results demonstrate this is necessary. Based on the

research findings presented here, water samples collected from a subset of SRD study lakes, rather than the entire suite of study lakes, could provide an adequate basis for monitoring. Lakes from each hydrological category should be selected, and selected lakes should span the active and relict SRD. The following lists 15 sampling lakes that could be monitored on an on-going basis, in spring and fall, to provide an overall evaluation of hydrological trends in delta lakes:

Exchange-dominated lakes

SD39: Samples could be used to monitor the frequency Great Slave Lake seiche events and the susceptibility of outer delta lakes to changes in these water inputs. For example, a decline in mid-season isotopic depletion could indicate a decline in the occurrence of seiche events, or the development of outer delta landforms (e.g., cleavage bars) or successional communities capable of preventing seiche inputs. Field observations and meteorological data could be used to further investigate such a scenario.

SD28: Samples would provide information about the influence of Slave River flow on lakes with channel connections to the river. For example, mid-season isotopic depletion in SD28 may indicate increased mid-summer flows on the Slave River.

Flood-dominated lakes

SD2: This lake has been demonstrated to be susceptible to both major and moderate Slave River flood events because of its location in the active delta, and lakewater samples can therefore be used to identify the occurrence of both. This lake is accessible by boat, and sampling this lake should be of high priority.

SD5: This lake is distanced from the Slave River but floodwaters generated during a major flood are capable of entering the lake through a

channel connection and small buffering wetland and pond. Water samples from this lake could be used to distinguish major and moderate flood events. This lake is accessible by boat, and sampling this lake should be of high priority.

SD7: This lake is on the eastern margins of the flood-dominated lakes sampled over the course of the 2002-2005 SRD monitoring program and can provide information about the spatial extent of flooding.

SD40: This lake is on the southwest margin of the flood-dominated lakes sampled over the course of the 2002-2005 SRD monitoring program and can provide information about the spatial extent of flooding.

SD1 or SD9: These lakes are in the centre of the active delta and, like SD2, can provide information about the occurrence of moderate or major flood events.

Evaporation-dominated lakes

SD8, SD29 and SD32: Although these lakes are classified as evaporation-dominated, they were all flooded during the major flood of 2005 and can therefore be used to identify the spatial limits of major flood events.

SD12 or SD18: These lakes were just beyond the margins of the major 2005 flood but could be flooded should an even larger flood event occur and thus could be used to identify such an event.

SD33 or SD35 and SD36 or 37: These lakes are along the upstream reaches of the Slave River and had *E/I* ratios generally >1 during the study period. Lakewater samples from these lakes could be used to monitor the potential for desiccation in the upper relict delta. Collecting water samples from one of these lakes should be of high priority, because they are highly sensitive to water level drawdown. SD33 is accessible by boat and a short hike.

SD20: This lake is located along the Jean River, and has provided a ~215 year sediment record showing marked hydrological responses to climate variability (see Mongeon, 2008). It had fall *E/I* ratios ~1 during the 2003-2005 study period, and could provide information about lake responses to climate variability.

SD21 or 22: These lakes are in the relict delta, removed from the Jean River. One of these lakes could be included in an on-going monitoring program to provide good spatial coverage of the relict delta.

In addition, on-going research in the SRD continues to focus on paleohydrological reconstructions from cores taken from other delta lakes during the March 2007 vibracoring campaign (Ennis, MSc in progress). Reconstructing paleohydrological conditions from cores collected from other flood-dominated lakes in the delta, as well as those from evaporation-dominated lakes, will contribute to the development of a more comprehensive picture of river discharge and climate variability in the SRD over the past several centuries. Vibracores were also extracted from lakes in areas of the delta that may have been affected by geomorphic changes, such as shifting patterns of distributary flow in the active delta, as well as fluctuating Great Slave Lake water levels, which may be similar to those identified in Lake Athabasca (Johnston et al., 2010). Interpretations of the sedimentary records from these lakes may provide more insight into Great Slave Lake dynamics during periods of major climate variability, such as the Little Ice Age and the Medieval Warm Period. Additionally, x-ray analysis was conducted on all SRD vibracores, and creative use and interpretation of these x-ray images (for example, see Lofi and Weber, 2001) may yield more detailed information about sedimentary characteristics and past hydrological conditions at the coring sites than has been obtained thus far.

2. *Initiation of a similar research program in the Mackenzie Delta*

A logical step ahead for this research approach is to apply it to the lakes of the Mackenzie Delta (MD). The success of the PAD and SRD research programs could be replicated in the MD, where there is a similarly complex system of lakes and river channels. Concern about changing flood frequency and climate variability is also a reality in the MD, while additional potential stressors to the delta include thawing permafrost and the possible development of the Mackenzie Valley pipeline. Characterizing the hydrology of the 13 000 km² delta would be exceptionally difficult using traditional hydrological monitoring, but would be greatly facilitated using water isotope tracers in early-, mid- and late-season sampling campaigns over consecutive thaw seasons. However, if applied in the MD, the sampling method presented in this thesis should be modified to accommodate the area of the delta. For example, sampling lakes along carefully chosen transects, identified based on previously published investigations of MD hydrology (e.g., Marsh and Hey, 1989; Marsh and Lesack, 1996; Emmerton et al., 2007) and intersecting different regions of the delta may be more appropriate and logistically feasible than sampling lakes spread across the entire region.

Recent reconstructions of patterns in break-up and ice-jam flooding in the delta, completed using data from local hydrometric stations, extend back to 1974 (e.g., Goulding et al., 2009). As with the hydrometric records for the rivers of the upper MRB, a much longer record is required before assessing long-term changes in flood frequency and lake hydrology. Hence, research in the MD would be significantly advanced if long-term paleohydrological reconstructions of delta lake responses to past changes in flood frequency or climate variability were developed. This could be achieved using methods followed in this thesis. As in the SRD, contemporary isotopic characterization of lakes would assist in identifying target coring sites, and a combination of gravity, Russian and vibracores could produce extended records of past lake dynamics and responses to multiple forcings. Ideally, these records would be developed for different regions of the delta, to provide a landscape-scale view of past hydrological change. They may also be useful in identifying future

scenarios of change in response to continued exploration and development of oil and gas resources in the area of the MD.

3. *Lake sediment coring in upper Mackenzie River Basin lakes*

The research presented in this thesis has demonstrated that headwater contributions to river discharge are a key component of the contemporary downstream hydrograph. Collecting sediment cores from oxbow lakes along MRB headwater tributaries such as the Smoky River may provide a record of past river dynamics in the upper reaches of the basin. When compared with downstream flood frequency records from the PAD and the SRD, headwater discharge records will strengthen our understanding of the drivers of changing downstream flood frequency patterns and trends in headwater climate conditions, and may be useful in predicting future responses of the upper MRB to changes in climate and river discharge.

4. *Synthesis of upper MRB, PAD, SRD and MD results*

Contemporary and past hydrological data from the headwaters and deltas of the MRB, including multi-century records of flood frequency and landscape-scale responses to climate change, would provide an unprecedented suite of records across a vast area of western and northern Canada. Such a compilation would be an essential component of responsible water management in the MRB, and would be invaluable in predicting and developing adaptations to future climate variability in both southern and northern areas of the watershed.

Figures

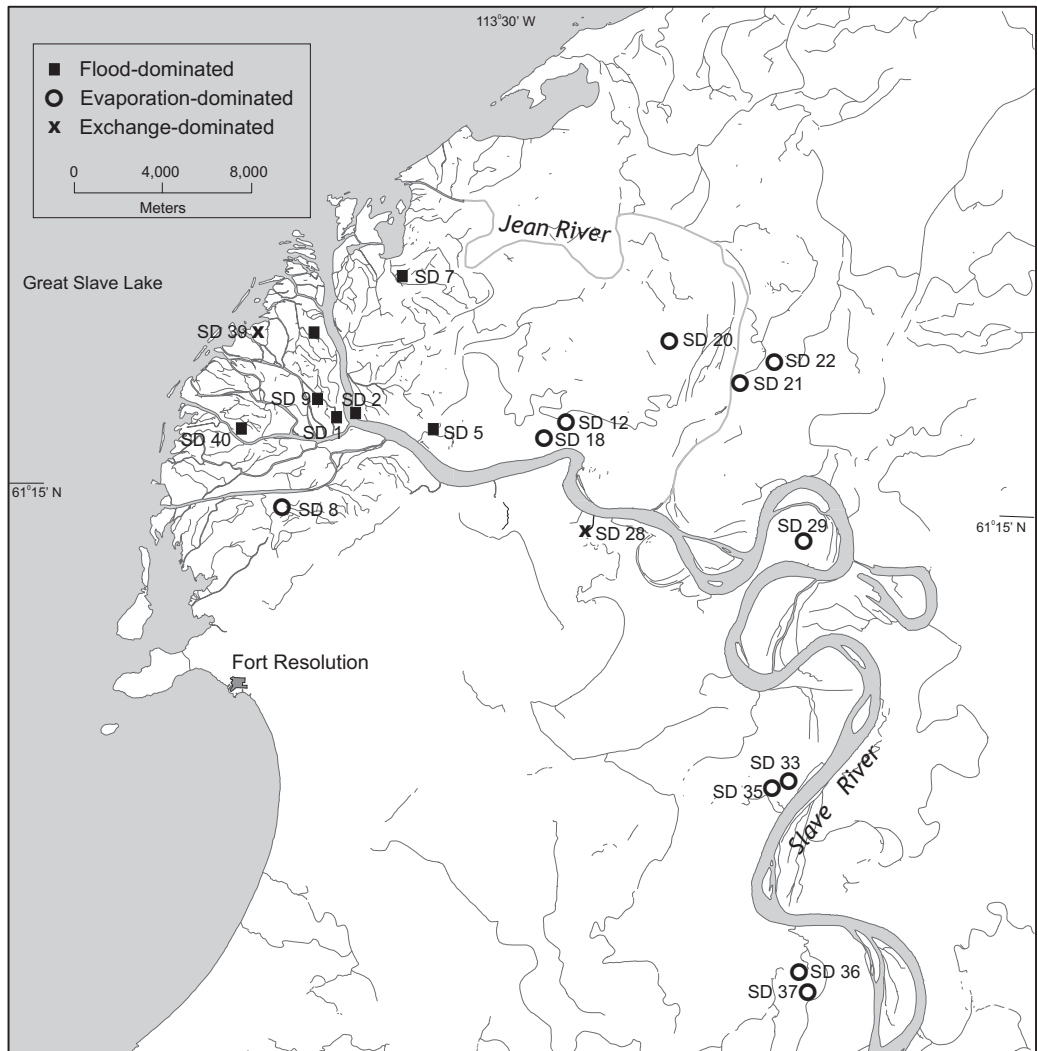


Figure 6.1. Map of potential SRD monitoring lakes.

Permissions

The chapters of this thesis have been previously published as manuscripts in the journals Arctic, Antarctic and Alpine Research, Hydrological Processes, Journal of Hydrology and Canadian Water Resources Journal. Written permission was required by Arctic, Antarctic and Alpine Research before reproducing the manuscript in this thesis, while the other three journals allow reproduction of these manuscripts here without written permission. Written permission was obtained from Arctic, Antarctic and Alpine Research via email, and the text of that email conversation is included below.

March 23, 2010

Hi Dr. Bowlds,

I published an article in AAAR in 2007 (39: 388-401). Now I'd like to include that article as part of my PhD thesis. Do I need to obtain permission from AAAR before I do so? How should I go about obtaining that permission?

Thanks a lot for your help!

Bronwyn (Brock) Benkert.

March 23, 2010

Hi Bronwyn,

Yes, you do need to obtain permission, but we are happy to grant it. Congratulations on finishing your PhD.

Larry

March 23, 2010

That's great, thanks Larry! Do I need to do anything else more formal, or is this enough to secure the permission?

And thanks for the congratulations!

Bronwyn.

March 24, 2010

Hi Bronwyn,

We don't require anything more formal. Good luck.

References

- ACIA. 2004. *Impacts of a Warming Arctic: Arctic Climate Impact Assessment*. Cambridge University Press.
- Adam ME. 2007. *Development and application of plant macrofossils for paleolimnological reconstructions in the Slave River Delta, NWT*. Unpublished MSc thesis, University of Waterloo. 170 p.
- Appleby PG. 2001. Chronostratigraphic techniques in recent sediments. In *Tracking Environmental Change Using Lake Sediments: Basin Analysis, Coring, and Chronological Techniques, Developments in Paleoenvironmental Research, Volume 1*. Last WM, Smol JP (eds). Kluwer Academic Publishers, Dordrecht. pp 171-203.
- Araguás-Araguás L, Froehlich K, Rozanski K. 2000. Deuterium and oxygen-18 isotope composition of precipitation and atmospheric moisture. *Hydrological Processes* 14: 1341-1355.
- Artjuschenko Z. 1990. *Organographia Illustrata Plantarum Vascularium*. Institutum Botanicum Nomina V. Kamrovii (in Russian and Latin). 204 p.
- Barnes CJ, Allison GB. 1983. The distribution of deuterium and ^{18}O in dry soils, 1. Theory. *Journal of Hydrology* 60: 141-156.
- Bell S. 2009. *ATCO's vision for the NWT*. Published online in *Slave River Journal*, 10 February 2009. [<http://srj.ca>]
- Beltaos S. 1995. Ice jam processes. In *River Ice Jams*. Beltaos S (ed). Water Resources Publications: Highlands Ranch, CO. pp 71-104.
- Beltaos S. 1997. Onset of river ice breakup. *Cold Regions Science and Technology* 25: 183-196.
- Beltaos S. 1998. Scale effects on river ice fracture and breakup. In *Ice in Surface Waters*. Shen HT (ed). Balkema, The Netherlands. pp 631-636.

- Beltaos S, Prowse TD. 2001. Climate impacts on extreme ice-jam events in Canadian rivers. *Hydrological Sciences Journal* 46: 157-181.
- Beltaos, S, Prowse, TD, Bonsal BR, MacKay R, Romolo LA, Pietroniro A, Toth B. 2006a. Climatic effects on ice-jam flooding of the Peace-Athabasca Delta. *Hydrological Processes* 20: 4031-4050.
- Beltaos S, Prowse TD, Carter T. 2006b. Ice regime of the lower Peace River and ice-jam flooding of the Peace-Athabasca Delta. *Hydrological Processes* 20: 4009-4029.
- Beltaos S, Prowse TD. 2009. River-ice hydrology in a shrinking cryosphere. *Hydrological Processes* 23: 122-144.
- Berggren G. 1969. *Atlas of Seeds and Small Fruits of Northwest European Plant Species: Part 2. Cyperaceae*. Swedish Natural Science Research Council, Stockholm. 68 p.
- Bill L, Crozier J, Surrendi D. 1996. A report of wisdom synthesized from the Traditional Knowledge component studies. *Northern River Basins Study Synthesis Report No. 12*. Northern River Basins Study, Edmonton.
- Birks HJB, Birks HH. 1980. *Quaternary Palaeoecology*. Blackburn Press, Caldwell New Jersey. 289 p.
- Birks SJ, Edwards TWD, Gibson JJ, Drimmie RJ, Michel FA. 2004. *Canadian Network for Isotopes in Precipitation*. Accessed 6 January 2006. [<http://www.science.uwaterloo.ca/~twdedwar/cnip/cniphome.html>]
- Burn D. 2008. Climatic influences on streamflow timing in the headwaters of the Mackenzie River Basin. *Journal of Hydrology* 352: 225-238.
- Brock BE, Wolfe BB, Edwards TWD. 2007. Characterizing the hydrology of shallow floodplain lakes in the Slave River Delta, NWT, using water isotope tracers. *Arctic, Antarctic and Alpine Research* 39: 388-401.

- Brock BE, Wolfe BB, Edwards TWD. 2008. Spatial and temporal perspectives on spring break-up flooding in the Slave River Delta, NWT. *Hydrological Processes* 22: 4058-4072.
- Brock BB, Yi Y, Clogg-Wright KP, Edwards TWD, Wolfe BB. 2009. Multi-year landscape-scale assessment of lakewater balances in the Slave River Delta, NWT, using water isotope tracers. *Journal of Hydrology* 379: 81-91.
- Brock BE, Martin ME, Mongeon CL, Sokal MA, Wesche SD, Armitage D, Wolfe BB, Hall RI, Edwards TWD. In press. Flood frequency variability in the Slave River Delta, NWT, over the past 80 years from multi-proxy paleolimnological analysis. *Canadian Water Resources Journal*.
- Canadian National Committee for the International Decade (CNCIHD). 1978. *Hydrological Atlas of Canada*. Fisheries and Environment Canada, Ottawa. 6 p + 68 leaves.
- Clogg-Wright KP. 2007. *Isotope-inferred water balances of Slave River Delta lakes, NWT, Canada*. Unpublished MSc thesis, University of Waterloo. 80 p.
- Coleman ML, Shepherd TJ, Durham JJ, Rouse JE, Moore GR. 1982. Reduction of water with zinc for hydrogen isotope analysis. *Analytical Chemistry* 54: 993-995.
- Coplen TB. 1996. New guidelines for reporting stable hydrogen, carbon, and oxygen isotope-ratio data. *Geochimica et Cosmochimica Acta* 60: 3359-3360.
- Craig H. 1961. Isotopic variations in meteoric waters. *Science* 133: 1702-1703.
- Craig H, Gordon LI. 1965. Deuterium and oxygen 18 variations in the ocean and marine atmosphere. In *Stable Isotopes in Oceanographic Studies and*

- Paleotemperatures*. Tongiorgi E. (ed.). Laboratorio di Geologia Nucleare, Pisa, Italy. pp 9-130.
- Day JH. 1972. *Soils of the Slave River Lowland in the Northwest Territories*. Research Branch, Canada Department of Agriculture, Ottawa, 60 p + map.
- Dean WE. 1974. Determination of carbonate and organic matter in calcareous sediments and sedimentary rocks by loss on ignition: comparison with other methods. *Journal of Sedimentary Petrology* 44: 242-248.
- Delorme LD. 1970a. Freshwater ostracodes of Canada. Part I. Subfamily Cypridinae. *Canadian Journal of Zoology* 48: 153-168.
- Delorme LD. 1970b. Freshwater ostracodes of Canada. Part II. Subfamilies Cypridopsinae and Herpetocypridinae and family Cyclocyprididae. *Canadian Journal of Zoology* 48: 253-266.
- Delorme LD. 1970c. Freshwater ostracodes of Canada. Part III. Family Candonidae. *Canadian Journal of Zoology* 48: 1099-1127.
- Delorme LD. 1971. Freshwater ostracodes of Canada. Part V. Families Ilyocyprididae, Notodromadidae, Darwinulidae, Cytherideidae and Entocytheridae. *Canadian Journal of Zoology* 49: 43-64.
- Déry SJ, Wood EF. 2005. Decreasing river discharge in northern Canada. *Geophysical Research Letters* 32: doi:10.1029/2005GL022845.
- Dingman LS. 1993. *Physical Hydrology*. Prentice-Hall, Englewood Cliffs, New Jersey. 575 p.
- Drimmie RJ, Heemskerk RA. 1993. *Water ¹⁸O by CO₂ Equilibration. Technical Procedure 13.0, Rev. 02*. Environmental Isotope Laboratory, Department of Earth Sciences, University of Waterloo.

- Edwards TWD, Wolfe BB, Gibson JJ, Hammarlund D. 2004. Use of water isotope tracers in high latitude hydrology and paleohydrology. In *Long-Term Environmental change in Arctic and Antarctic Lakes*. Pienitz R, Douglas MSV, Smol JP. (eds.). Springer, Dordrecht, The Netherlands. pp 187-207.
- Emmerton CA, Lesack LFW, Marsh P. 2007. Lake abundance, potential water storage, and habitat distribution in the Mackenzie River Delta, western Canadian Arctic. *Water Resources Research* 43, W05419.
- English MC, Stone MA, Hill RB, Wolfe PM, Ormson R. 1996. *Assessment of impacts on the Slave River Delta of Peace River Impoundment at Hudson Hope, British Columbia*. Northern River Basins Study Project Report No. 74. Edmonton, Alberta. 91 p.
- English M, Hill R, Stone M, Ormson R. 1997. Geomorphological and botanical change on the outer Slave River Delta, NWT, before and after impoundment of the Peace River. *Hydrological Processes* 11: 1707-1724.
- Environment Canada. 2002. *Canadian Climate Normals 1971-2000*. Environment Canada.
- Environment Canada. 2004. *Climate Data Online*. Accessed 4 March 2005. [http://www.climate.weatheroffice.ec.gc.ca/climateData/hourlydata_e.html]
- Environment Canada. 2005. *Climate Data Online*. Environment Canada.
- Epstein S, Mayeda TK. 1953. Variations in the $^{18}\text{O}/^{16}\text{O}$ ratio in natural waters. *Geochimica et Cosmochimica Acta* 4: 213.
- Evans MS. 2000. The large lake ecosystems of northern Canada. *Aquatic Ecosystem Health and Management* 3: 65-79.

- Gardner JT, English MC, Prowse TD. 2006. Wind-forced seiche events on Great Slave Lake: Hydrologic implications for the Slave River Delta, NWT, Canada. *Hydrological Processes* 20: 4051-4072.
- Gat JR, Bowser CJ, Kendall C. 1994. The contribution of evaporation from the Great Lakes to the continental atmosphere: estimate based on stable isotope data. *Geophysical Research Letters* 21: 557-560.
- Gat JR, Klein B, Kushnir Y, Roether W, Wernli H, Yam R, Shemesh A. 2003. Isotope composition of air moisture over the Mediterranean Sea: an index of the air-sea interaction pattern. *Tellus* 55B: 953-965.
- Gat JR, Matsui E. 1991. Atmospheric water balance in the Amazon Basin: An isotopic transpiration model. *Journal of Geophysical Research* 96: 13179-13188.
- Gibson J. 2001. Forest-tundra water balance signals traced by isotopic enrichment in lakes. *Journal of Hydrology* 251: 1-13.
- Gibson JJ. 2002a. A new conceptual model for predicting isotopic enrichment in lakes in seasonal climates. *PAGES News* 10: 10-11.
- Gibson J. 2002b. Short-term evaporation and water budget comparisons in shallow Arctic lakes using non-steady isotope mass balance. *Journal of Hydrology* 264: 242-261.
- Gibson JJ, Edwards TWD. 2002. Regional water balance trends and evaporation-transpiration partitioning from a stable isotope survey of lakes in Northern Canada. *Global Biogeochemical Cycles* 16: 1026 doi:10.1029/2001GB001839.
- Gibson JJ, Edwards TWD, Bursley GG, Prowse TD. 1993. Estimating evaporation using stable isotopes: quantitative results and sensitivity analysis for two catchments in northern Canada. *Nordic Hydrology* 24: 79-94.

- Gibson JJ, Prowse TD, Peters DL. 2006a. Partitioning impacts of climate and regulation on water level variability in Great Slave Lake. *Journal of Hydrology* 329: 196-206.
- Gibson JJ, Prowse TD, Peters DL. 2006b. Hydroclimatic controls on water balance and water level variability in Great Slave Lake. *Hydrological Processes* 20: 4155-4172.
- Glew J. 1989. A new trigger mechanism for sediment samplers. *Journal of Paleolimnology* 5: 241-244.
- Gonfiantini R. 1986. Environmental isotopes in lake studies. In *Handbook of Environmental Isotope Geochemistry, Volume 2*. Fritz P, Fontes JC (eds). Elsevier, New York. pp 113-168.
- Goulding HL, Prowse TD, Beltaos S. 2009. Spatial and temporal patterns of break-up and ice-jam flooding in the Mackenzie Delta, NWT. *Hydrological Processes* 23: 2654-2670.
- Gray DM, Prowse TD. 1993. Snow and floating ice. In *Handbook of Hydrology*, Maidment D. (ed.). McGraw-Hill, New York. pp 7.1-7.58.
- Hannah DM, Sadler JP, Wood PJ. 2007. Hydroecology and ecohydrology: a potential route forward? *Hydrological Processes* 21: 3385-3390.
- Hall RI, Smol JP. 1996. Paleolimnological assessment of long-term water-quality changes in south-central Ontario lakes affected by cottage development and acidification. *Canadian Journal of Fisheries and Aquatic Sciences* 53: 1-17
- Hall RI, Wolfe BB, Edwards TWD, Karst-Riddoch TL, Vardy S, McGowan S, Sjunneskog C, Paterson A, Last W, English MC, Sylvestre F, Leavitt PR, Warner BG, Boots B, Palmini R, Clogg-Wright K, Sokal M, Falcone M, van Driel P, Asada T. 2004. *A Multi-Century Flood, Climatic, and Ecological History of the Peace-Athabasca Delta, Northern Alberta*,

- Canada*. Final Report to B.C. Hydro. 163 p + appendices.
- Hayashi M, Quinton WM, Pietroniro A, Gibson JJ. 2004. Hydrologic functions of wetlands in a discontinuous permafrost basin indicated by isotopic and chemical signatures. *Journal of Hydrology* 296: 81-97.
- Hill RB. 1996. *An assessment of hydrological process and landform change: Slave River Delta, NWT*. Unpublished MES thesis, Wilfrid Laurier University. 185 pp.
- Horita J, Wesolowski D. 1994. Liquid-vapour fractionation of oxygen and hydrogen isotopes of water from the freezing to the critical temperature. *Geochimica et Cosmochimica Acta* 58: 3425-3497.
- Huntington HP, Callaghan T, Fox SL, Krupnik I. 2004. Matching traditional and scientific observations to detect environmental change: A discussion on Arctic terrestrial ecosystems. *Ambio* Special Report 13: 18-23.
- Huntington H, Weller G. 2005. Chapter 1: An Introduction to the Arctic Climate Impact Assessment. In *Arctic Climate Impact Assessment Scientific Report*. Symon C, Arris L, Heal B. (eds.). Cambridge University Press. pp 1-20.
- Ingraham NL, Taylor BE. 1991. Light stable isotope systematics of large-scale hydrologic regimes in California and Nevada. *Water Resources Research* 27: 77-90.
- IPCC. 2007a. Climate Change 2007: Synthesis Report. Contribution of Working Groups I, II and III to the Fourth Assessment Report of the Intergovernmental Panel on Climate Change. Pachauri RK, Reisinger A. (eds.). IPCC, Geneva, Switzerland. 104 p.
- IPCC. 2007b. Working Group II Contribution to the Intergovernmental Panel on Climate Change. Climate Change 2007: Climate Impacts, Adaptations and Vulnerability. Summary for Policymakers. IPCC, Geneva,

- Switzerland. 23 p.
- Jarvis SR. 2008. *Reconstruction of Peace River flood frequency and magnitude for the past ~600 years from oxbow lake sediments, Peace–Athabasca Delta, Canada*. Unpublished MSc thesis, Wilfrid Laurier University. 228 p.
- Jaques DR. 1989. *Topographic mapping and drying trends in the Peace–Athabasca Delta, Alberta using LANDSAT MSS imagery*. Report prepared by Ecostat Geobotanical Surveys Inc. for Wood Buffalo National Park, Fort Smith, Northwest Territories, Canada, 36 p + appendix.
- Jermyn CE. 2004. *Paleohydrological reconstruction of a closed-basin lake in the Slave Delta, using stable isotope methods*. Unpublished BSc Thesis, University of Waterloo. 49 p.
- Jessen K. 1955. Key to subfossil Potamogeton. *Botanisk Tidsskrift* 52: 1-7
- Johnston JW, Köster D, Wolfe BB, Hall RI, Edwards TWD, Enders A, Martin ME, Wiklund JA, Light C. 2010. Reconstruction of Lake Athabasca (Canada) water level during the Little Ice Age from paleolimnological and geophysical analyses of a transgressive barrier-beach complex. *The Holocene* doi:10.1177/0959683610362816.
- Kane DL. 2005. High-latitude hydrology, what do we know? *Hydrological Processes* 19: 2453-2454.
- Krammer K, Lange-Beralot H. 1986-1991. *Bacillariophyceae*. In *Süßwasserflora von Mitteleuropa Band 2/1-4*. Ettl H, Gerloff J, Heynig H, Mollenhauer D (eds). Gustav Fischer Verlag, Stuttgart.
- Lammers RB, Shiklomanov AI, Vorosmarty CJ, Fekete BM, Peterson BJ. 2001. Assessment of contemporary Arctic river runoff based on observational discharge records. *Journal of Geophysical Research* 106: 3321-3334.

- Lapp S, Byrne J, Townshend I, Kienzle S. 2005. Climate warming impacts on snowpack accumulation in an alpine watershed. *International Journal of Climatology* 25: 521-536.
- Lévesque PEM, Dinel H, Larouche A. 1988. *Guide to the identification of plant macrofossils in Canadian peatlands*. Research Branch, Agriculture Canada Publication No. 1817. Land Resource Centre, Ottawa. 65 p.
- Lofi J, Weber O. 2001. SCOPIX – digital processing of X-ray images for the enhancement of sedimentary structures in undisturbed core slabs. *Geo-Marine Letters* 20: 182-186.
- Magnuson JJ, Robertson DM, Benson BJ, Wynne RH, Livingstone DM, Arai T, Assel RA, Barry RG, Card V, Kuusisto E, Granin NG, Prowse TD, Stewart KM, Vuglinski VS. 2000. Historical trends in lake and river ice cover in the northern hemisphere. *Science* 289: 1743-1746.
- Malmstrom VH. 1969. A new approach to the classification of climate. *Journal of Geography* 68: 351-357.
- Marsh P, Hey M. 1989. The flooding hydrology of Mackenzie Delta lakes near Inuvik, N.W.T., Canada. *Arctic* 42: 41-49.
- Marsh P, Lesack LFW. 1996. The hydrologic regime of perched lakes in the Mackenzie Delta: Potential responses to climate change. *Limnology and Oceanography* 41: 849-856.
- Martin AC, Barkley WD. 1961. *Seed Identification Manual*. University of California Press, Berkeley. 221 p.
- Meyers PA, Teranes JL. 2001. Sediment Organic Matter. In *Tracking Environmental Change Using Lake Sediments: Physical and Geochemical Methods, vol. 2*. Last WM, Smol JP (eds). Kluwer Academic Publishers, Dordrecht, The Netherlands. pp 239-269.

- Milburn D, MacDonald DD, Prowse TD, Culp JM. 1999. Ecosystem maintenance indicators for the Slave River Delta, N. W. T., Canada. In *Environmental Indices Systems Analysis Approach*. Pykh YA, Hyatt DE, Lenz RMJ (eds). EOLSS Publishers Co LTD, Oxford, UK. pp 329-348.
- Mongeon CL. 2008. *Paleolimnological reconstructions of three shallow basins, Slave River Delta, NWT, using stable isotope tracers*. Unpublished MES Thesis, Wilfrid Laurier University. 141 p.
- Montgomery F. 1977. *Seeds and Fruits of Plants of Eastern Canada and Northeastern United States*. University of Toronto Press, Toronto, Canada. 232 p.
- Morrison J, Brockwell T, Merren T, Fourel F, Phillips AM. 2001. A new on-line method for high precision stable-hydrogen isotopic analyses on nanolitre water samples. *Analytical Chemistry* 73: 3570-3575.
- Muzik I. 1985. Recent hydrological changes of the Peace-Athabasca Delta. In *Climate and Paleoclimate of Lake, Rivers and Glaciers*. Muzik I, Kuhn M (eds). Universitätsverlag Wagner, Innsbruck. pp. 175-182.
- Overland JE, Wang M, Bond NA. 2002. Recent temperature changes in the western Arctic during spring. *Journal of Climate* 15: 1702-1716.
- PADPG (Peace-Athabasca Delta Project Group). 1973. *Peace-Athabasca Delta Project, Technical Report and Appendices. Volume 1: Hydrological Investigations, Volume 2: Ecological Investigations*. Governments of Canada, Alberta and Saskatchewan.
- PADTS. 1996. *Peace-Athabasca Delta Technical Studies Final Report*. Fort Chipewyan, Canada. 88 p.
- Peters DL. 2003. *Controls on the persistence of water in perched basins of a northern delta*. Unpublished PhD thesis, Trent University, Peterborough, Canada. 194 p.

- Peters DL, Prowse TD, Marsh P, Lafleur PM, Buttle JM. 2006a. Persistence of water within perched basins of the Peace-Athabasca Delta, Northern Canada. *Wetlands Ecology and Management* 14: 221-243.
- Peters DL, Prowse TD, Pietroniro A, Leconte R. 2006b. Flood hydrology of the Peace-Athabasca Delta, northern Canada. *Hydrological Processes* 20: 4073-4096.
- Prowse TD. 2009. Introduction: hydrological effects of a shrinking cryosphere. *Hydrological Processes* 23: 1-6.
- Prowse TD, Beltaos S, Gardner JT, Gibson JJ, Granger RJ, Leconte R, Peters DL, Pietroniro A, Romolo LA, Toth B. 2006. Climate change, flow regulation and land-use effects on the hydrology of the Peace-Athabasca-Slave system; Findings from the Northern Rivers Ecosystem Initiative. *Environmental Monitoring and Assessment* 113: 167-197.
- Prowse TD, Conly FM. 1998. Effects of climatic variability and flow regulation on ice-jam flooding of a northern delta. *Hydrological Processes* 12: 1589-1610.
- Prowse TD, Conly FM. 2000. Multiple-hydrologic stressors of a northern delta ecosystem. *Journal of Aquatic Ecosystem Stress and Recovery* 8: 17-26.
- Prowse TD, Conly FM. 2002. A review of hydro-ecological studies of the Northern River Basins Study, Canada: Part 2, Peace-Athabasca Delta. *River Research and Applications* 18: 447-460.
- Prowse TD, Conly FM, Church M, and English MC. 2002a. A review of hydroecological results of the Northern River Basis Study, Canada. Part 1. Peace and Slave River. *River Research and Applications* 18: 429-446.
- Prowse TD, Lalonde V. 1996. Open-water and ice-jam flooding of a northern delta. *Nordic Hydrology* 27: 85-100.

- Prowse TD, Peters DL, Beltaos S, Pietroniro A, Romolo LA, Toyra J, Leconte R. 2002b. Restoring ice-jam floodwater to a drying delta ecosystem. *International Water Resources Association* 27: 58-69.
- Romolo LA, Prowse TD, Blair D, Bonsal BR, Martz WL. 2006a. The synoptic climate controls on hydrology in the upper reaches of the Peace River Basin. Part I: snow accumulation. *Hydrological Processes* 20: 4097-4111.
- Romolo LA, Prowse TD, Blair D, Bonsal BR, Marsh P, Martz WL. 2006b. The synoptic climate controls on hydrology in the upper reaches of the Peace River Basin. Part II: Snow ablation. *Hydrological Processes* 20: 4113-4129.
- Rood SB, Samuelson GM, Weber JK, Wywrot KA. 2005. Twentieth-century decline in streamflow from the hydrographic apex of North America. *Journal of Hydrology* 306: 215-233.
- Rouse WR, Douglas MSV, Hecky RE, Hershey AE, Kling GW, Lesack L, Marsh P, McDonald M, Nicholson BJ, Roulet NT, Smol JP. 1997. Effects of climate change on the freshwaters of Arctic and subarctic North America. *Hydrological Processes* 11: 873-902.
- Schindler DW, Donahue WF. 2006. An impending water crisis in Canada's western prairie provinces. *Proceedings of the National Academy of Sciences* 103: 7210-7216.
- Schindler DW, Smol JP. 2006. Cumulative effects of climate warming and other human activities on freshwaters of Arctic and Subarctic North America. *Ambio* 35: 160-168.
- Schoch W, Pawlik B, Schweingruber F. 1988. *Botanical Macro-Remains*. Paul Haupt, Berne and Stuttgart. 227 p.
- Sear DA, Arnell NW. 2006. The application of palaeohydrology in river management. *Catena* 66: 169-183.

- Shiklomanov AI, Lammers RB, Vörösmarty CJ. 2002. Widespread decline in hydrological monitoring threatens pan-Arctic research. *EOS* 83: 13-17.
- Sinnatamby RN, Yi Y, Sokal MA, Clogg-Wright KP, Asada T, Vardy SR, Karst-Riddoch TL, Last WM, Johnston JW, Hall RI, Wolfe BB, Edwards TWD. 2010. Historical and paleolimnological evidence for expansion of Lake Athabasca (Canada) during the Little Ice Age. *Journal of Paleolimnology* 43: 705-717.
- Smith DM. 1982. *Moose-Deer Island House People: A history of the native people of Fort Resolution* (Vol. 81). Ottawa: National Museum of Man, National Museums of Canada.
- Smith D. 1991. Lacustrine Deltas. *The Canadian Geographer* 35: 311-316.
- Smith LC, Sheng Y, MacDonald GM, Hinzman LD. 2005. Disappearing Arctic lakes. *Science* 308: 1429.
- Smol JP, Douglas MSV. 2007. Crossing the final ecological threshold in high Arctic Ponds. *Proceedings of the National Academy of Sciences* 104: 12395-12397.
- Sokal MA. 2007. *Assessment of hydroecological changes at the Slave River Delta, NWT, using diatoms in seasonal, interannual and paleolimnological experiments*. Unpublished PhD thesis, University of Waterloo. 287 p.
- Sokal MA, Hall RI, Wolfe BB. 2008. Relationships between hydrological and limnological conditions in lakes of the Slave River Delta (NWT, Canada) and quantification of their roles on sedimentary diatom assemblages. *Journal of Paleolimnology* 39: 533-550.
- Sokal MA, Hall RI, Wolfe BB. 2010. The role of flooding on inter-annual and seasonal variability of lake water chemistry, phytoplankton diatom communities and macrophyte biomass in the Slave River Delta

- (Northwest Territories, Canada). *Ecohydrology* 3: 41-54.
- Squires MM, Lesack LFW. 2002. Water transparency and nutrients as controls on phytoplankton along a flood-frequency gradient among lakes of the Mackenzie Delta, western Canadian Arctic. *Canadian Journal of Fisheries and Aquatic Sciences* 59: 1339-1349
- Townsend GH. 1984. Wildlife resources of the Slave River and Peace-Athabasca Delta. *Journal of the National and Provincial Parks Association of Canada* 20: 5-7.
- Vallet-Coulomb C, Gasse F, Robinson L, Ferry L. 2006. Simulation of the water and isotopic balance of a closed tropical lake at a daily time step (Lake Ihotry, South-West of Madagascar). *Journal of Geochemical Exploration* 88: 153-156.
- Vallet-Coulomb C, Gasse F, Sonzogni C. 2008. Seasonal evolution of the isotopic composition of atmospheric water vapour above a tropical lake: Deuterium excess and implication for water recycling. *Geochimica et Cosmochimica Acta* 72: 4661-4674.
- Vanderburgh S, Smith D. 1988. Slave River Delta: geomorphology, sedimentology, and Holocene reconstruction. *Canadian Journal of Earth Sciences* 25: 1990-2004.
- Water Survey of Canada. 2006. *National Water Quantity Survey Program*. Environment Canada.
- Wesche S. 2007. Adapting to change in Canada's north: Voices from Fort Resolution, NWT. *Meridian* Spring/Summer 2007: 19-25.
- Wesche S. 2009. Responding to change in a northern aboriginal community: linking social and ecological perspectives. Unpublished PhD thesis. Wilfrid Laurier University. 501 p.

- Wolfe BB, Armitage D, Wesche S, Brock BE, Sokal MA, Clogg-Wright KP, Mongeon CL, Adam ME, Hall RI, Edwards TWD. 2007a. From isotopes to TK interviews: Towards interdisciplinary research in Fort Resolution and the Slave River Delta, NWT. *Arctic* 60: 75-87.
- Wolfe BB, Hall RI, Edwards TWD, Jarvis SR, Sinnatamby RN, Yi Y, Johnston JW. 2008a. Climate-driven shifts in quantity and seasonality of river discharge over the past 1000 years from the hydrographic apex of North America. *Geophysical Research Letters* 35: doi:10.1029/2008GL036125.
- Wolfe BB, Hall RI, Edwards TWD, Vardy SR, Falcone MD, Sjunneskog C, Sylvestre F, McGowan S, Leavitt PR, van Driel P. 2008b. Hydroecological responses of the Athabasca Delta, Canada, to changes in river flow and climate during the 20th century. *Ecohydrology* 1: 131-148.
- Wolfe BB, Hall RI, Last WM, Edwards TWD, English MC, Karst-Riddoch TL, Paterson A, Palmi R. 2006. Reconstruction of multi-century flood histories from oxbow lake sediments, Peace-Athabasca Delta, Canada. *Hydrological Processes* 20: 4131-4153.
- Wolfe BB, Karst-Riddoch TL, Hall RI, Edwards TWD, English MC, Palmi R, McGowan S, Leavitt PR, Vardy SR. 2007b. Classification of hydrologic regimes of northern floodplain basins (Peace-Athabasca Delta, Canada) from analysis of stable isotopes ($\delta^{18}\text{O}$, $\delta^2\text{H}$) and water chemistry. *Hydrological Processes* 21: 151-168.
- Wolfe BB, Karst-Riddoch TL, Vardy SR, Falcone MD, Hall RI, Edwards TWD. 2005. Impacts of climate and river flooding on the hydro-ecology of a floodplain basin, Peace-Athabasca Delta, Canada, since A.D. 1700. *Quaternary Research* 64: 147-162.
- Woo M-K, Thorne R. 2003. Streamflow in the Mackenzie Basin, Canada. *Arctic* 56: 328-340.

- Wood RD. 1967. *Charophytes of North America. A Guide to the Species of Charophyta of North America, Central America and the West Indies*. Stella's Printing, West Kingston, Rhode Island. 72 p.
- Wrona F, Prowse TD, Reist JD. 2005. Chapter 8: Freshwater Ecosystems and Fisheries. In *Arctic Climate Impact Assessment Scientific Report*. Symon C, Arris L, Heal B (eds.). Cambridge University Press. 139 p.
- Yi Y, Brock BE, Falcone MD, Wolfe BB, Edwards TWD. 2008. A coupled isotope tracer method to characterize input water to lakes. *Journal of Hydrology* 350: 1-13.

Appendix A: Slave River Delta study lakes

Table A 1. Name, hydrological classification (see Brock et al., 2007; see Chapter 2) and UTM coordinates for all 41 SRD study lakes.

	Category	UTM Co-ordinates	
		Latitude	Longitude
SD1	Flood-dominated	6796450	360900
SD2	Flood-dominated	6796800	361650
SD3	Flood-dominated	6797350	363250
SD4	Flood-dominated	6796760	362150
SD5	Flood-dominated	6795888	365177
SD6	Flood-dominated	6798670	363650
SD7	Flood-dominated	6802929	363807
SD8	Evaporation-dominated	6792549	358400
SD9	Flood-dominated	6797369	359764
SD10	Exchange-dominated	6800325	363078
SD11	Evaporation-dominated	6798140	369545
SD12	Evaporation-dominated	6796301	371053
SD13	Evaporation-dominated	6798099	371918
SD14	Evaporation-dominated	6799258	373304
SD15	Evaporation-dominated	6802209	372375
SD16	Evaporation-dominated	6801021	372195
SD17	Exchange-dominated	6791348	368063
SD18	Evaporation-dominated	6795593	370045
SD19	Evaporation-dominated	6796500	375250
SD20	Evaporation-dominated	6800033	375441
SD21	Evaporation-dominated	6797868	378831
SD22	Evaporation-dominated	6798855	380493
SD23	Evaporation-dominated	6795825	381409
SD24	Evaporation-dominated	6795230	377971
SD25	Evaporation-dominated	6793846	378186
SD26	Evaporation-dominated	6786563	370914
SD27	Evaporation-dominated	6789184	372615
SD28	Exchange-dominated	6791339	372046
SD29	Evaporation-dominated	6790800	381718
SD30	Exchange-dominated	6787657	387222
SD31	Evaporation-dominated	6786252	385316
SD32	Evaporation-dominated	6783643	385619
SD33	Evaporation-dominated	6779992	381208
SD34	Evaporation-dominated	6787134	362162
SD35	Evaporation-dominated	6779578	380385
SD36	Evaporation-dominated	6771359	380103
SD37	Evaporation-dominated	6770753	381762
SD38	Flood-dominated	6800416	359957
SD39	Exchange-dominated	6800378	357341
SD40	Flood-dominated	6795784	356331
SD41	Exchange-dominated	6798317	355966

Appendix B: Lakewater isotope and total suspended sediment results

Table B 1. Lakewater isotope results for SRD study lakes, the Slave River and Great Slave Lake, collected between September 2002 and September 2005.

Lake name	Sep-02		23-May-03		23-Jun-03		25-Jul-03	
	$\delta^{18}\text{O}$	$\delta^2\text{H}$	$\delta^{18}\text{O}$	$\delta^2\text{H}$	$\delta^{18}\text{O}$	$\delta^2\text{H}$	$\delta^{18}\text{O}$	$\delta^2\text{H}$
SD1	-15.0	-131	-18.6	-150	-16.6	-145	-15.0	-136
SD2	-14.3	-127	-19.2	-155	-16.9	-144	-14.8	-134
SD3	-14.2	-128	-17.6	-147	-15.8	-138	-14.4	-132
SD4	-14.1	-127	-18.4	-152	-15.3	-140	-14.2	-129
SD5	-13.4	-124	-17.1	-146	-15.9	-140	-14.8	-132
SD6	-14.4	-129	-18.0	-149	-15.9	-141	-14.5	-132
SD7	-12.9	-120	-17.5	-145	-16.0	-141	-15.0	-134
SD8	-13.8	-126	-15.3	-138	-14.1	-132	-13.1	-128
SD9	-15.0	-131	-18.4	-152	-16.0	-146	-14.5	-134
SD10	-15.7	-133	-18.9	-154	-17.4	-148	-16.6	-142
SD11	-13.6	-128	-14.6	-135	-14.1	-132	-13.2	-129
SD12	-9.9	-108	-12.2	-123	-10.0	-114	-7.9	-104
SD13	-12.4	-118	-13.7	-128	-12.7	-125	-11.7	-119
SD14	-10.9	-113	-13.1	-125	-11.6	-121	-10.4	-114
SD15	-12.6	-122	-14.4	-131	-13.5	-127	-12.5	-123
SD16	-13.4	-125	-14.2	-130	-13.7	-132	-13.3	-128
SD17	-16.1	-134	-17.4	-145	-16.1	-141	-15.1	-136
SD18	-13.6	-126	-15.3	-135	-14.0	-132	-12.8	-126
SD19	-11.1	-114	-14.6	-133	-14.1	-125	-10.0	-114
SD20	-11.5	-115	-13.7	-127	-12.8	-122	-11.7	-118
SD21	-11.6	-118	-13.8	-133	-13.0	-128	-11.5	-120
SD22	-11.5	-117	-14.6	-134	-13.1	-126	-11.4	-120
SD23	-11.7	-119	-13.9	-126	-12.8	-127	-11.1	-116
SD24	-12.6	-122	-13.8	-129	-13.7	-128	-11.9	-119
SD25	-13.3	-125	-15.4	-136	-12.8	-125	-12.2	-121
SD26	-13.5	-126	-16.2	-139	-14.4	-134	-12.3	-123
SD27	-10.1	-111	-15.1	-141	-9.5	-110	-6.3	-96
SD28	-16.6	-136	-17.0	-141	-15.4	-134	-14.6	-130
SD29	-10.5	-112	-14.4	-131	-12.0	-122	-9.4	-110
SD30	-17.7	-142	-18.4	-151	-17.9	-147	-17.7	-144
SD31	-12.4	-121	-13.2	-127	-12.3	-123	-11.1	-117
SD32	-12.7	-123	-15.5	-137	-13.5	-129	-11.8	-120
SD33	-10.2	-108	-12.4	-121	-10.1	-112	-8.1	-102
SD34	-12.6	-118	-13.7	-126	-12.9	-123	-12.3	-119
SD35	-9.4	-106	-10.6	-112	-9.5	-109	-8.5	-103
SD36	-12.5	-119	-13.4	-125	-12.1	-120	-9.7	-108
SD37	-11.6	-116	-13.1	-125	-11.9	-123	-10.5	-115
SD38	-15.4	-132	-18.9	-155	-16.7	-144	-15.4	-135
SD39	-17.0	-138	-18.7	-152	-17.0	-142	-16.4	-138
SD40	-14.2	-129	-18.3	-152	-16.2	-142	-14.7	-132
SD41	-17.2	-139	-17.9	-144	-16.9	-143	-16.6	-139
Great Slave Lake	-17.6	-142	-17.5	-144	-18.1	-145	-17.9	-142
Slave River			-19.2	-152	-18.5	-146	-18.1	-145

Lake name	05-Aug-03		31-May-04		20-Jul-04		20-Sep-04	
	$\delta^{18}\text{O}$	$\delta^2\text{H}$	$\delta^{18}\text{O}$	$\delta^2\text{H}$	$\delta^{18}\text{O}$	$\delta^2\text{H}$	$\delta^{18}\text{O}$	$\delta^2\text{H}$
SD1	-13.7	-133	-16.5	-141	-14.0	-134	-12.8	-128
SD2	-14.3	-129	-16.2	-139	-12.8	-126	-11.5	-119
SD3	-13.5	-128	-17.1	-143	-13.6	-128	-12.8	-124
SD4	-13.6	-125	-17.9	-148	-13.8	-132	-12.7	-125
SD5	-14.0	-129	-15.6	-138	-13.3	-130	12.5	-124
SD6	-13.3	-127	-15.4	-135	-13.0	-127	-11.7	-122
SD7	-14.1	-129	-15.0	-132	-13.7	-128	-12.9	-123
SD8	-12.5	-124	-14.9	-135	-13.1	-127	-12.1	-122
SD9	-13.7	-129	-17.5	-147	-14.2	-133	-12.8	-125
SD10	-15.9	-138	-16.9	-142	-15.8	-137		
SD11	-12.7	-126	-14.5	-134	-13.0	-129	-12.4	-125
SD12	-6.9	-100	-13.8	-132	-7.6	-106	-9.2	-108
SD13	-11.0	-116	-14.4	-133	-11.4	-118	-11.1	-115
SD14	-9.4	-109	-13.6	-131	-10.4	-115	-9.9	-111
SD15	-12.4	-122	-14.8	-135	-12.1	-126	-11.6	-120
SD16	-12.7	-125	-14.8	-134	-13.2	-129	-13.6	-128
SD17	-14.2	-131	-16.4	-140	-14.6	-133	-12.8	-126
SD18	-12.1	-122	-15.9	-141	-12.8	-127	-12.0	-121
SD19	-8.6	-108	-15.4	-137	-12.6	-120	-10.5	-117
SD20	-10.9	-114	-12.7	-122	-11.2	-118	-10.8	-115
SD21	-10.6	-115	-14.9	-136	-11.2	-121	-10.7	-118
SD22	-10.8	-115	-14.1	-132	-11.2	-120	-10.5	-117
SD23	-9.8	-114	-15.6	-141	-10.6	-123	-10.3	-119
SD24	-11.0	-119	-15.1	-138	-11.9	-126	-10.9	-118
SD25	-11.2	-119	-14.7	-135	-11.9	-125	-10.8	-120
SD26	-11.1	-118	-15.1	-139	-11.4	-124	-10.6	-119
SD27	-6.7	-100	-14.4	-136	-5.2	-100	-10.0	-115
SD28	-14.6	-128	-16.5	-142	-14.7	-134	-14.6	-132
SD29	-8.4	-104	-15.9	-143	-7.8	-111		
SD30	-17.5	-145	-17.5	-145	-16.8	-141	-16.7	-140
SD31	-10.5	-116	-13.9	-132	-10.9	-120	-10.8	-120
SD32	-10.6	-118	-14.6	-134	-10.8	-120	-9.9	-118
SD33	-6.9	-98	-13.5	-130	-7.1	-106	-7.8	-107
SD34	-11.6	-115	-13.5	-126	-11.8	-119	-11.3	-118
SD35	-7.5	-99	-10.9	-116	-7.7	-105	7.5	-101
SD36	-8.8	-104	-12.6	-124	-8.8	-110	-8.9	-108
SD37	-9.4	-110	-13.3	-129	-10.0	-116	-9.6	-113
SD38	-14.7	-131	-18.2	-149	-15.2	-136	-14.0	-129
SD39	-17.4	-140	-18.0	-147	-15.1	-135	-17.6	-129
SD40	-13.3	-127	-16.8	-143	-13.3	-130	-11.8	-118
SD41	-16.5	-137	-17.7	-144	-15.2	-134	-16.7	-138
Great Slave Lake	-17.4	-141	-17.9	-144	-18.1	-146	-18.1	-145
Slave River	-17.6	-142	-17.7	-144	-18.1	-146	-18.1	-145

Lake name	15-May-05		22-Jul-05		22-Sep-05	
	$\delta^{18}\text{O}$	$\delta^2\text{H}$	$\delta^{18}\text{O}$	$\delta^2\text{H}$	$\delta^{18}\text{O}$	$\delta^2\text{H}$
SD1	-18.9	-153.7	-15.6	-139.9	-14.5	-132
SD2	-18.8	-152.3	-14.3	-131.8	-13.6	-126
SD3	-18.8	-153	-14.8	-133.9	-14.7	-131
SD4	-18.5	-151.1	-13.3	-127.6	-14.1	-129
SD5	-19.0	-154	-15.8	-142.1	-14.7	-134
SD6	-18.3	-151.6	-14.4	-134.5	-13.5	-128
SD7	-14.3	-131.1	-12.2	-122.4	-12.5	-122
SD8	-17.8	-148.6	-14.4	-132.1	-13.4	-128
SD9	-18.9	-152.3	-15.0	-135.5	-15.0	-133
SD10	-17.1	-146.1	-15.1	-134.9	-14.5	-133
SD11	-14.4	-136.4	-12.6	-126.7	-12.4	-126
SD12	-13.0	-132	-7.1	-101.5	-9.2	-110
SD13	-13.1	-128	-10.5	-113.3	-11.0	-116
SD14	-12.6	-127.3	-9.7	-112.8	-9.9	-113
SD15	-13.5	-131.1	-11.3	-118.3	-11.1	-119
SD16	-13.6	-131.9	-12.5	-126.9	-12.2	-125
SD17	-17.4	-148.4	-13.3	-127.6	-12.8	-125
SD18	-18.2	-152.1	-13.9	-131.2	-13.2	-127
SD19	-16.4	-147.5	-10.5	-119.4	-10.8	-117
SD20	-12.6	-121.6	-10.4	-114.5	-10.5	-115
SD21	-14.8	-133.3	-10.8	-118.5	-10.8	-117
SD22	-13.2	-130.1	-10.5	-116.6	-10.2	-113
SD23	-13.7	-135.6	-8.0	-111.2	-9.4	-114
SD24	-14.3	-135	-10.2	-114.7	-10.4	-117
SD25	-13.4	-131.9	-11.3	-122.8	-10.2	-116
SD26	-14.0	-136.3	-9.7	-115.9	-9.5	-113
SD27	-14.6	-140.1	-7.6	-106.7	-9.4	-113
SD28	-18.5	-151.8	-15.5	-133.5	-14.8	-131
SD29	-18.8	-154.9	-13.4	-129	-12.0	-123
SD30	-18.4	-150.5	-17.5	-144.4	-17.1	-140
SD31	-13.0	-128.5	-11.0	-122.1	-10.9	-120
SD32	-18.6	-149.5	-14.2	-135.4	-12.9	-128
SD33	-13.3	-132.2	-7.8	-108.7	-9.1	-109
SD34	-13.1	-122.4	-11.1	-116.7	-11.0	-115
SD35	-10.6	-118.4	-7.8	-102.9	-8.31	-106
SD36	-11.7	-124.1	-8.4	-107.7	-9.275	-109
SD37	-12.7	-129.2	-9.1	-114.5	-9.42	-113
SD38	-18.4	-151.5	-14.8	-134.2	-14.88	-131
SD39	-18.1	-148.4	-16.4	-137.9	-16.68	-137
SD40	-18.7	-152.7	-14.6	-135.6	-13.84	-130
SD41	-18.3	-148.7	-15.8	-135.9	-16.61	-138
Great Slave Lake	-19.0	-148.4	-17.6	-142.6	-16.8	-138
Slave River	-18.6	-147.9	-18.1	-143.9	-16.79	-138

Table B 2. Total suspended sediment results (expressed in g/L) for SRD study lakes, the Slave River and Great Slave Lake, collected in spring 2003-2005.

	23-May-03	31-May-04	15-May-05
SD1	0.030	0.010	0.020
SD2	0.100	0.010	0.035
SD3	0.013	0.006	0.027
SD4	0.030	0.005	0.027
SD5	0.038	0.008	0.047
SD6	0.013	0.005	0.006
SD7	0.014	0.003	0.003
SD8	0.001	0.003	0.012
SD9	0.022	0.006	0.014
SD10	0.052	0.016	0.005
SD11	0.001	0.000	0.001
SD12		0.005	0.015
SD13	0.002	0.009	0.009
SD14		0.008	0.001
SD15	0.002	0.001	0.002
SD16	0.001	0.017	0.001
SD17	0.005	0.010	0.010
SD18	0.003	0.012	0.007
SD19	0.005	0.003	0.005
SD20	0.003	0.005	0.005
SD21	0.001	0.006	0.002
SD22	0.001	0.002	0.004
SD23	0.001	0.004	0.002
SD24	0.001	0.004	0.001
SD25	0.001	0.004	0.002
SD26	0.000	0.003	0.001
SD27		0.001	0.003
SD28	0.012	0.058	0.013
SD29	0.011	0.011	0.019
SD30	0.098	0.004	0.067
SD31	0.002	0.005	0.005
SD32	0.003	0.004	0.018
SD33	0.002	0.009	0.006
SD34	0.004	0.002	0.001
SD35	0.003	0.002	0.005
SD36	0.002	0.008	0.005
SD37	0.002	0.010	0.004
SD38	0.045	0.005	0.004
SD39	0.019	0.010	0.022
SD40	0.029	0.007	0.018
SD41		0.007	0.003
Great Slave Lake	0.016	0.051	0.353
Slave River	0.315	0.037	0.263